ELECTROCHEMICAL RECYCLING OF SODIUM BOROHYDRIDE FOR

HYDROGEN STORAGE: PHYSICOCHEMICAL PROPERTIES OF SODIUM

METABORATE SOLUTIONS.

by

Caroline R. Cloutier

B. A. Sc., The University of Ottawa, 1999

A THESIS SUBMITTED IN PARTIAL FULFILMENT OF THE REQUIREMENTS
FOR THE DEGREE OF

MASTER OF APPLIED SCIENCE

in

THE FACULTY OF GRADUATE STUDIES

(Materials Engineering)

THE UNIVERSITY OF BRITISH COLUMBIA

July 2006

ABSTRACT

The large-scale adoption of a "hydrogen economy" is hindered by the lack of a practical storage method and concerns associated with its safe handling. Chemical hydrides have the potential to address these concerns. Sodium borohydride (sodium tetrahydroborate, $NaBH_4$), is the most attractive chemical hydride for H_2 generation and storage in automotive fuel cell applications but recycling from sodium metaborate ($NaBO_2$) is difficult and costly. An electrochemical regeneration process could represent an economically feasible and environmentally friendly solution.

In this thesis, the properties of diluted $NaBO_2$ aqueous solutions and concentrated $NaBO_2$ alkaline aqueous solutions that are necessary for the development of electrochemical recycling methods have been studied. The conductivity and viscosity of dilute aqueous solutions of $NaBO_2$ were measured as a function of concentration at 25°C. Also, the solubility, pH, density, conductivity and viscosity of the filtrate of saturated aqueous $NaBO_2$ solutions containing varying weight percentages (1, 2, 3, 5, 7.5 and 10 wt%) of alkali hydroxides (NaOH, KOH and LiOH) were evaluated at 25°C. Selected experiments were repeated at 50 and 75°C to investigate the effect of temperature on the $NaBO_2$ alkaline aqueous solution solubility and physicochemical properties. Preliminary experiments to investigate the effect of glycine ($C_2H_5NO_2$), the smallest amino acid, on the solubility and physicochemical properties of $NaBO_2$ alkaline aqueous solutions were conducted at 25°C. Furthermore, the precipitates formed in the supersaturated 10 wt% alkaline aqueous $NaBO_2$ solutions at 25°C were characterized by X-Ray Diffraction and Scanning Electron Microscopy.

The use of KOH as the electrolyte was found to be more advantageous for the H_2 storage and generation system based on $NaBO_2$ solubility and $NaBH_4$ half-life due to the pH effect. However, the addition of NaOH led to the highest ionic conductivity, and its use seems more

suitable for the electroreduction of $NaBO_2$. Further investigations on the impact of KOH and NaOH on the electroreduction of $NaBO_2$ in aqueous media have the potential to enhance the commercial viability of this H_2 generation and storage system.

TABLE OF CONTENTS

LIST OF TABLES

LIST OF FIGURES

LIST OF SYMBOLS

Symbol	Description	Units
Roman Symbols		
A	Viscosity Coefficient	$1/M^{1/2}$
b	Tafel Slope	V
B	Viscosity Coefficient	$1/M$
B	Molar Conductivity Coefficient	$S.m^2/mol.M$
B_E	Extrapolated Viscosity Coefficient	$1/M$
B_S	Viscosity Coefficient	$1/M$
C	Molar Concentration	M
D	Viscosity Coefficient	$1/M^2$
D	Molar Conductivity Coefficient	$S.m^2/mol.M^{3/2}$
D^o_i	Limiting Diffusivity of Species i	cm^2/s
dH^o	Standard Enthalpy of Formation	KJ/mol
dG^o	Standard Gibbs Free Energy of Formation	KJ/mol
dS^o	Standard Entropy of Formation	J/mol.K
E^o	Standard Cell Voltage	V
E^o_a	Standard Anode Voltage	V
E^o_c	Standard Cathode Voltage	V
E_c	Actual Cathode Voltage	V
E_{cell}	Actual Cell Voltage	V
$E_{c,e}$	Equilibrium Cathode Voltage	V
$E_{e, cell}$	Non-standard Equilibrium Cell Voltage	V
E_{vis}	Activation Energy of Viscous Flow	J/mol
F	Faraday Constant	964853.34 C/mol
H	Constant	Dimensionless
i	Current Density	A/m^2
i_o	Exchange Current Density	A/m^2
K	Molar Conductivity Coefficient	$S.m^2/mol.M^{1/2}$ or $S.m^2/mol.M^{1/3}$
K_a	Ion Pair Association Constant	$1/M$
K_B	Boltzmann Constant	J/K
K_T	Conductivity at Temperature T	S/m
Mr	Molecular Weight Ratio of $NaBH_4$ to $NaBO_2$	Dimensionless
p	Temperature Pre-exponential Factor	Dimensionless
P	Parameter	Dimensionless
R	Universal Gas Constant	J/mol.K
S	Solubility	wt%
$t_{1/2}$	Half Life	days
T	Temperature	C or K
t^o_i	Limiting Transference Number of Species i	Dimensionless
u	Mobility	$cm^2/s.V$
u^o_i	Limiting Mobility of Species i	$cm^2/s.V$
Wh	Amount of H_2 Generated	g
Ws	Amount of $NaBO_2$ Generated	g
x	Organic Additive Concentration	wt%
y	Molar Concentration Ratio	Dimensionless
y	Solute Solubility	wt%
Greek Symbols		
α	Temperature Coefficient of Conductivity	1/C
α_c	Cathodic Transfer Coefficient	Dimensionless
ΔS_{hyd}	Standard Entropy of Hydration	J/mol.K
$\Delta \Phi_{ohm}$	Ohmic Losses	V
ε_o	Dielectric Constant of Pure Solvent	Dimensionless

κ	Conductivity	S/m
η	Dynamic Viscosity	cP
η_{con}	Concentration Overpotential	V
η_s	Surface Activation Overpotential	V
η_r	Relative Viscosity	Dimensionless
η_o	Viscosity of Pure Solvent	cP
ρ_T	Density of Solution at Temperature T	kg/m^3
$\rho_{H2O,\,T}$	Density of Water at Temperature T	kg/m^3
Λ	Molar Conductivity	$S.m^2/mol$
Λ^o	Limiting Molar Conductivity	$S.m^2/mol$
λ^o_i	Limiting Molar Conductivity of Ionic Species i	$S.m^2/mol$

LIST OF ACRONYMS

AA	Atomic Absorption
B-PEMFC	Borohydride – Proton Exchange Membrane Fuel Cell
CS	Cellulose Ester
DBFC	Direct Borohydride Fuel Cell
DOE	Department of Energy
EDA	Ethylenediamine
EDTA	Ethylenediaminetetraacetic Acid
ETV	Electro-Thermal Vaporization
FCE	Fuel Cell Emulator
FCV	Fuel Cell Vehicle
FCUPS	Fuel Cell Uninterrupted Power Supply
HMPA	Hexamethylphosphoamide
HOD	Hydrogen On Demand
ICP	Induced Coupled Plasma
MS	Mass Spectrometry
PEMFC	Proton Exchange Membrane Fuel Cell
PTFE	Polytetrafluorethylene
SHE	Standard Hydrogen Electrode
SEM	Scanning Electron Microscopy
SS	Stainless Steel
XRD	X-Ray Diffraction

ACKNOWLEDGEMENT

DEDICATION

In the loving memory of my mother, Colette Chrégheur Cloutier, for providing me with unconditional love and support, and for giving me the strength, courage and determination to pursue my goals and follow my dreams.

CHAPTER I

INTRODUCTION

1.1 Motivation

It has been proposed that switching to hydrogen (H_2) for energy production could alleviate many environmental concerns related to the combustion of fossil fuels [Hart, D., (2003)]. H_2 is an excellent energy carrier which can be produced from a variety of sources such as solar, wind, biomass, hydro, and geothermal. However, there is a long way to go before the cost of H_2 production and distribution to the users will be competitive with that of gasoline. The extensive use of H_2 as a fuel in commercial transportation is delayed by difficulties in developing a practical and efficient H_2 storage method and by concerns over its utilization hazards. The slow development of a suitable H_2 storage system to start the vehicle and rapidly respond to its fuel demand greatly restrains the commercialization of Fuel Cell Vehicles (FVCs).

Among the different H_2 storage methods, chemical hydride and light metal complex hydride based H_2 generators have the potential to address these concerns. They possess the characteristics necessary to meet the design requirements of automotive fuel cell applications and do not require handling of gaseous H_2. They currently constitute the most active area of research for H_2 storage for on-board applications [Dhanesh, C. et al., (2006)]. Various chemical and light metal complex hydrides can produce H_2 via a hydrolysis reaction. Sodium borohydride (sodium tetrahydroborate, $NaBH_4$) is one of the most attractive material for this purpose, as it has a high H_2 content (10.58 wt%), based on the hydride itself and a high energy density (1.4 KWh/l), based on a 20 wt% $NaBH_4$ solution feed to a Proton Exchange Membrane Fuel Cell (PEMFC). When in alkaline solution and in contact with a catalyst, $NaBH_4$ releases H_2 and produces sodium metaborate ($NaBO_2$). $NaBH_4$ hydrogen generators are safe, clean and lightweight systems able to deliver pure H_2 to feed PEMFCs generating electricity in a FCV. The most important obstacles to the acceptance of this system as the H_2 carrier of choice for automotive fuel cells are the high production cost of $NaBH_4$ and the difficult recyclability of the $NaBH_4$ hydrolysis by-product, $NaBO_2$, back to $NaBH_4$.

1

Depending on how $NaBO_2$ is recycled, the resulting overall H_2 generation and storage system energy cycle scheme could represent an emission free and economically viable solution. Hence, the development of an efficient $NaBO_2$ recycling path is crucial to make $NaBH_4$ play a prevailing role in overcoming the growing energetic demand and environmental challenges of the future.

1.2 Objectives

This thesis contributes to the development of an efficient H_2 storage method based on $NaBH_4$ solutions. More particularly, the goal of this work is to address the current barriers hindering the use of $NaBH_4$ for H_2 generation and storage, i.e. recyclability and cost. Currently, the knowledge of the fundamental physicochemical and transport properties of the $NaBO_2$ solution is very limited and this basic information is essential to the investigation of electrochemical recycling. In this study, the physicochemical properties of various $NaBO_2$ aqueous solutions with and without alkali additive were evaluated to determine which electrolyte media would be more favourable to the H_2 generation and storage system, as well as for the electrochemical reduction of $NaBO_2$ in water. Hence, the outcome of this study constitutes an incremental improvement in the knowledge of the properties of $NaBO_2$ aqueous solutions with and without alkali additive and also establishes a platform to address some of the key issues in the area of recyclability and cost reduction. Table 1.1 summarises the specific energy, energy density and storage cost goals for on-board H_2 generation and storage set by the US Department of Energy (DOE) for the next decade.

Table 1.1: US Department of Energy Freedom Car Targets for On-Board H_2 Storage, (Modified from [Department of Energy, (2004)]).

Year/Target	2005	2010	2015	[Units]
Specific Energy	5.40	7.20	10.80	[MJ/kg]
	1.50	2.00	3.00	[kWh/kg]
Energy Density	4.30	5.40	9.70	[MJ/l]
	1.19	1.50	2.69	[kWh/l]
Storage Cost	1.70	1.10	0.60	[$/MJ]
	6.12	3.96	2.16	[$/KwH]

An efficient way to enhance the by-product solubility and recyclability could result in cost savings and protection of the environment, and consequently contribute to overcome one of the main constraint to the adoption of $NaBH_4$ as the H_2 carrier of choice for automotive fuel cell applications.

1.3 Approach

To demonstrate the uniqueness and significance of the contribution made by this thesis, pertinent background information and a thorough literature review on the relevant topics were provided. This will show the importance of the issue of $NaBO_2$ recycling, which remains to be addressed. It will also be clear the lack of knowledge of the physicochemical properties of aqueous $NaBO_2$ solutions. For this reason, the main physicochemical transport properties of dilute aqueous $NaBO_2$ solutions (conductivity and viscosity) were determined in pure water at 25°C. The $NaBO_2$ limiting molar conductivity, important transport electrochemical parameter of electrolyte solutions, was extrapolated from experimental data at very low concentrations using the established Kohlrausch empirical correlations, while the $NaBO_2$ B coefficient was evaluated from the Jones-Dole viscosity correlations.

It will be explained that increasing the solubility of $NaBO_2$ is attractive as it would improve not only the overall H_2 storage system capacity by allowing the use of more concentrated reactant solutions but also the effectiveness of the electrochemical recycling of the spent solution to $NaBH_4$. Some work has been reported on the solubility of $NaBO_2$ in aqueous solutions, but, as will be seen, very few researchers have reported solubility data for $NaBO_2$ in caustic solution. The potential replacement of sodium hydroxide (NaOH) with another stabilizing agent, such as potassium hydroxide (KOH) or lithium hydroxide (LiOH), was explored by determining the solubility, pH, conductivity, viscosity and density, of alkaline aqueous $NaBO_2$ solutions at different weight percentages for each of those hydroxides. The effect of temperature on the physicochemical properties of the solutions and the effect of the addition of an organic additive were also briefly investigated.

1.4 Overview

This thesis is divided in six chapters. Chapter II contains background information on the provenance of boron mineral and the production of $NaBH_4$. The hydrolysis reaction is described and details of the effect of various factors on the reaction are given. The storage efficiency is discussed along with the H_2 generation and storage system and its demonstrated application possibilities. A thorough literature review including relevant state of the art theory on the $NaBO_2$ solutions and precipitate characteristics is provided in Chapter III. The following Chapter indicates the materials, procedures and characterization methodologies used to carry the experimental work. In Chapter V, the results obtained are presented and thoroughly discussed. The aqueous $NaBO_2$ solution physicochemical properties are discussed prior to the alkaline aqueous $NaBO_2$ solution physicochemical properties. The effects of temperature and of the addition of an organic compound on the solution physicochemical parameters are described separately. The precipitates characteristics are also discussed in this Chapter. Finally, Chapter VI constitutes a summary of the major findings. The significance of the experimental data collected and its impact on the H_2 generation and storage system, as well as on the electrochemical recycling are presented and future work is recommended. The thesis is followed by a series of Appendices. Appendix A holds the $NaBH_4$ solution cost calculations for the DOE target range, as well as the $NaBH_4$ H_2 generation and storage system cost, gravimetric and volumetric density calculations. Appendix B contains the summary tables of the averages of the filtrate characterization measurements as well as sample of the raw data collected. Appendix C includes the most important XRD peaks for a variety of boron compounds as well as for the precipitates studied, whereas Appendix D shows additional SEM pictures of the precipitates. Parts of this thesis have been accepted for publication in two articles [Cloutier, C. R., *et al.*, (2006), Cloutier, C. R. *et al.* (2007)].

CHAPTER II

BACKGROUND

2.1 NaBH₄ Production

2.1.1 Natural Resources

The manufacturing of $NaBH_4$ uses refined minerals containing boron-oxygen compounds as the raw material. Borates are mineral ores containing boric oxides ($B(OH)_3$). There exist at least 230 types of borate minerals [Garret, D. E., (1998)]. The commercially common ones are sodium borates, borax (sodium tetraborate, $Na_2B_4O_7.10H_2O$) and kernite ($Na_2B_4O_6(OH)_2.3H_2O$), calcium borate colemanite ($Ca_2B_6O_{11}.5H_2O$) and sodium-calcium borate ulexite ($NaCaB_5O_9.8H_2O$). As they are not easily recycled, most borates are obtained from fresh sources. Similarly to oil and gas natural resources, borate deposits are found in a limited number of geographic regions. Major deposits are located in the United States, Turkey, Chile and Argentina. Minor producers include Russia, China and other countries. This geographic dependence affects the viability and sustainability of a transportation economy entirely dependant on $NaBH_4$. Nevertheless, $NaBH_4$, as a H_2 carrier, could have an impact on the energy consumption patterns in locations where deposits are present.

2.1.2 Current Production Process

A) Production Paths

$NaBH_4$ is the only boron hydride used routinely on a commercially significant scale [Kirk, R. E. *et al.*, (1992)]. Various raw materials can be used in the preparation of $NaBH_4$: boron hydrides, alkoxyboron compounds, boric oxide, metal borates and boron halides [Roy M. A., (1964)]. Methods using components

generated by the processing of boron ores as its raw material are reported below (Modified from [Martin, D. R., (1961)]).

$$
\begin{array}{c}
\text{B}_2\text{O}_3 \\
\overset{(b)}{\nearrow} \qquad \overset{(g)}{\searrow} \\
\text{Na}_2\text{B}_4\text{O}_7 \cdot 10\text{H}_2\text{O} \xrightarrow{(a)} \text{H}_3\text{BO}_3 \xrightarrow{(c)} (\text{CH}_3\text{O})_3\text{B} \xrightarrow{(d)} \text{NaBH}_4 \\
\searrow \qquad \searrow^{(f)} \qquad \uparrow^{(h)} \\
\underset{(e)}{} \qquad \text{BF}_3
\end{array}
$$

(Eq. 2.1)
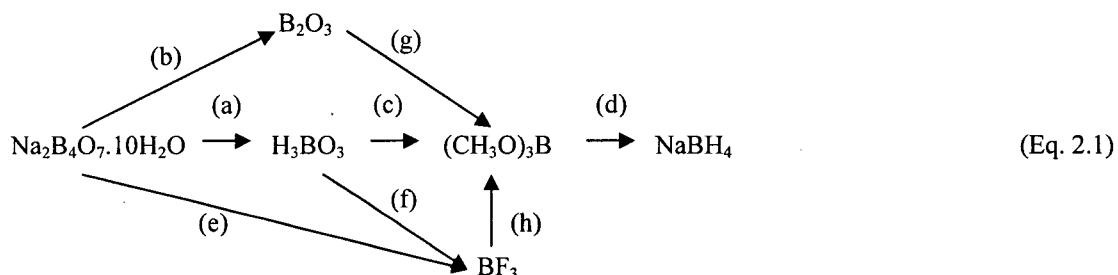
Borax ($Na_2B_4O_7 \cdot 10H_2O$) and other boron ores are converted to boric acid (H_3BO_3) by using acids (a). Boric oxide (B_2O_3) is obtained by the calcinations of boric acid (H_3BO_3) (b). Trimethoxyborane (($CH_3O)_3B$) is prepared by the esterification of boric acid (H_3BO_3) with methanol (CH_3OH) (c). Boron trifluoride (BF_3) is prepared from $Na_2B_4O_7 \cdot 10H_2O$ or H_3BO_3 by reaction with an acid in the presence of fluoride (e, f). Finally, $NaBH_4$ is obtained by a reaction of sodium and H_2 or sodium hydride with B_2O_3 (g), ($CH_3O)_3B$) (d) BF_3 (h). As it produces less greenhouse gas emissions, the production of H_2 from $NaBH_4$ synthesized from the decomposition of boron-containing compounds, such as $Na_2B_4O_7 \cdot 10H_2O$, is less harmful to the environment than the production H_2 from the processing of fossil fuel [Ay, M. *et al.*, (2005)]. However, for that to happen, the H_2 required in the $NaBH_4$ synthesis would have to originate from non-fossil fuel energy sources such as solar, wind, biomass or hydroelectricity.

B) The Schlesinger and Brown Process

Most $NaBH_4$ is produced by the Schlesinger and Brown process. It is based on the reduction of trimethoxyborane (($CH_3O)_3B$) obtained from borate ore refining. The chemical reactions involved and a general process flow diagram describing the six most important steps are provided below.

Initial borate processing: $NaBO_2 + 1/2H_2SO_4 + H_2O \rightarrow 1/2Na_2SO_4 + H_3BO_3$ (Eq. 2.2)

Preparation of boron intermediate: $H_3BO_3 + 3CH_3OH \rightarrow B(OCH_3)_3 + 3H_2O$ (Eq. 2.3)
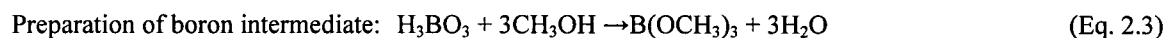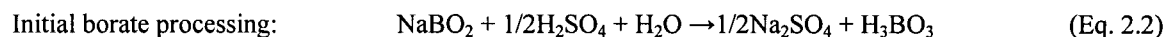
Preparation of sodium metal:	$NaCl \rightarrow Na + 1/2Cl_2$ (electrolysis)	(Eq. 2.4)
Preparation of sodium hydride:	$4Na + 2H_2 \rightarrow 4NaH$	(Eq. 2.5)
Production of $NaBH_4$:	$B(OCH_3)_3 + 4NaH \rightarrow NaBH_4 + 3NaOCH_3$	(Eq. 2.6)
Recovery of organic solvent:	$3NaOCH_3 + 3H_2O \rightarrow 3CH_3OH + 3NaOH$	(Eq. 2.7)

Overall Reaction: $\quad NaBO_2 + 4Na + 2H_2 + 1/2H_2SO_4 \rightarrow NaBH_4 + 3NaOH + 1/2Na_2SO_4$ (Eq. 2.8)
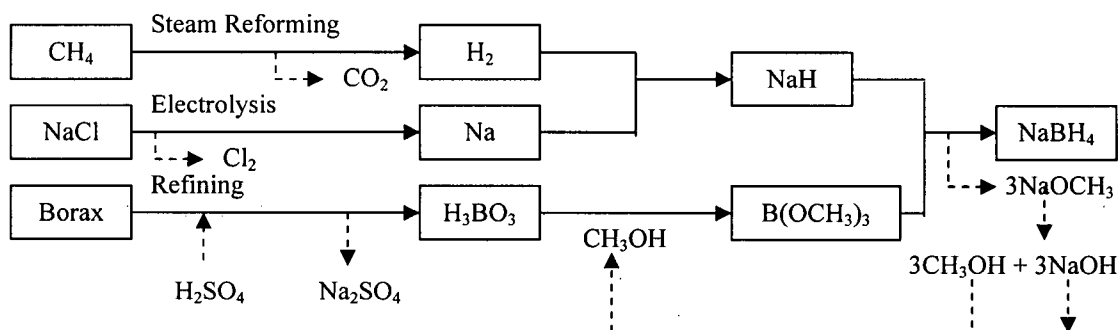
Figure 2.1: Process Flow Diagram of the Schlesinger and Brown Process (Modified from [Wu, Y. *et al.*, (2004b)]).

This method involves the use of a mineral oil suspension of sodium hydride [Ullmann, F., (2000)]. The determining reaction step is the one producing $NaBH_4$. Sodium dispersions are hydrogenated directly in the mineral oil and the oil provides a heat sink, which facilitates temperature control of the exothermic reaction with methyl borate [Amendola, S. C. *et al.*, (1999)]. The reaction is carried out in solvents such as diethylene glycol (diglyme) or tetrahydrofuran at 250-275°C. The sodium methoxide, $NaOCH_3$, can be separated from $NaBH_4$ by a series of extractions: first with amines, then with water, and finally by a counter-extraction with a solvent, such as 2-aminopropane [BCS Inc., (2002)].

The large amount of Gibbs free energy required to combine the three different elements (Na, B and H) as well as electrons and energy needed to produce $NaBH_4$ makes it difficult to make. The process includes the formation of sodium (Na) by the electrolysis of sodium chloride (NaCl). This reaction step has the highest activation energy requirements and is the most energy consuming of the entire process [Mohring, R. M. *et al.*, (2003)]. The electrolysis of Na requires 9.7 kWh per kg of Na produced [Wu, Y. *et al.*, (2004a)] and only a quarter of the sodium produced is converted to $NaBH_4$. As will be seen in Section 2.2.2 H), the energy consumption associated with the electrolysis of Na can be reduced by about 80% by

carrying out the electrolysis in a H_2-assisted molten sodium hydroxide (NaOH) media [Wu, Y. *et al.*, (2004a)]. This significant energetic improvement could reduce the production cost of $NaBH_4$, but it would not attenuate the amount of by-products (Na_2SO_4), wastes (Cl_2) and greenhouse gases (CO_2) generated by the overall Schlesinger and Brown process.

C) The Bayer Process

Bayer developed a $NaBH_4$ production batch process which is commercially viable. It uses ground borosilicate glass, elemental sodium and H_2 as per the following reaction [Ullmann, F., (2000)]:

$$(NaB_4O_7 + 7\,SiO_2) + 16Na + 8H_2 \rightarrow 4NaBH_4 + 7Na_2SiO_3 \qquad \text{(Eq. 2.9)}$$
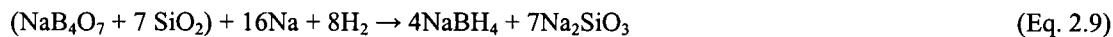
The reaction takes place at temperatures between 500 to 700 °C and at pressures between 300 and 400 kPa. However, the risks of explosion increase when the reaction temperature exceeds the decomposition temperature of $NaBH_4$ which is 400°C [Wu, Y. et al., (2004b)]. The Bayer process is operated in a batch mode. As in the case of the Schlesinger and Brown process, only one fourth of the sodium used is converted to $NaBH_4$, and elemental sodium is needed as a raw material. Also, the production of large quantities of sodium silicate by-product needs to be dealt with.

2.1.3 Economics

The intention of this section is not to do a detailed economic analysis, but to provide an overview of the economic principles of supply and demand. Some statistics regarding the current world production of borates are provided. Then the use of borates is briefly reviewed and the production cost of $NaBH_4$ is analyzed.

A) Statistics

The world's reserve base was estimated to 410,000 thousand metric tons of boron in 2004 [Lyday, P. A., (2005)]. The 2000 world apparent consumption in terms of B_2O_3 was of 461,000 metric tons while the gross weight world mine production, in various boron units (elemental boron content, gross weight boron minerals and compounds) was of 4,220,000 metric tons [Buckingham, D. A., et al. (2002)]. During the same year, the total borate production from the four California producers was reported to be 1,100,000 metric tons valued at $557US million. In 2004, the United States was one of the world's two largest producers of boron compounds and exported about half of its domestic production. All the production is concentrated in California. Exported materials competed with the ones from Turkey, the largest producer of boron ore in the world. Canada imported 42,100 metric tons of sodium borates from the US in 2000 [Lyday, P. A., (2000)]. The unit value is defined as the estimated value of boron apparent consumption in US dollars, of 1 metric ton of 100 % B_2O_3 content. The unit value was $787US per ton in 2000 [Buckingham, D. A. et al., (2002)]. Boron production remains quite low despite its desirable properties. At the 2004 consumption levels, the world resources are sufficient for the next 100 years or the foreseeable future. The world demand for boron is expected to remain strong and to grow. The most recent annual world production capacity of B_2O_3 has been cited as sufficient for forecasted requirements of borohydrides [Lyday, P. A., (2005)].

B) Borate Usage

The borosilicate glass production is the largest borate use and includes fiberglass for insulation, fabrics and reinforcement and many specialty glass products. As the boride compounds are very hard, they are used as abrasives and refractories. One of the earliest uses of borates is in the production of glazes, frits and emanels to impart color, texture, heat, chemical or wear resistance to appliances, ceramics or tiles [Garret, D. E., (1998)]. Composites of boron or boride fibers in a matrix of plastics, ceramics or metals have great strength and a high modulus of elasticity. Those advanced composites found uses in air and spacecraft applications. Boric acid, borax and pentahydrates are employed in the fabrication of fire

retardants. The mild alkalinity of borax allows it to emulsify oil and greases and reduce the surface tension of water, which aids in loosening dirt particles. It also reacts with organics to form esters and has a moderate bacterial action [Garret, D. E., (1998)]. Boric acid and sodium borates are mild antiseptics used in eyewash and some heterocyclic boron compounds inhibit tumor growth, while borax and some of its ores are efficient parasite killers. Borohydrides are well-known reducing reagents. In organic and inorganic chemistry, they are used as the sources of H⁻ or reductants. Table 2.1 summarizes the most important uses of the numerous borate ores and their related products.

Table 2.1: Partial List of Borate Uses (Modified from [Garret, D. E., (1998)]).

Abrasives	Hair creams
Adhesives	Herbicides
Alloys	Hydraulic fluids
Antiseptics	Insecticides
Bactericide	Leather tanning
Bleaches	Lubrificating oil additives
Boron filaments	Magnets
Buffering	Medical applications
Catalysts	Metallurgical applications
Cement	Metal hardening
Ceramics	Nuclear applications
Cleaning compounds	Nylon
Corrosion inhibitor	Organic synthesis
Cosmetics	Paints and pigments
Detergents	Pharmaceuticals
Disinfectants	Photography
Electrical insulation	Plastics
Electrolytic refining	Plating solutions
Electronic components	Polymer stabilisers
Electroplating	Pulp bleaching
Enamels	Purifying specialty chemicals
Enzyme stabilization	Pyrotechnics
Eye wash	Refractories
Fertilizer	Shampoos
Fiber optics	Soil sterilant
Fiber glass	Swimming pool sanitizer
Fire, flame retardants	Taxidermy
Frits	Textile finishing
Fuel additives	Textile dyes
Fuel	Transformers
Funficides	Waste treatment
Glass	Wax emulsifier
Glazes	Wire drawing
Goldsmithing	Wood preservative

C) NaBH₄ Cost

For small quantities of specialty chemical with no contract in place, the listing price of $NaBH_4$ caplets ranges between $80-$100US/kg at Rohm and Haas Company. However, the listed price of $NaBH_4$ is about $50US/kg for industrial quantities. The cost of the sodium required in the current production of $NaBH_4$ represents about 60-65% of the $NaBH_4$ cost [Wu, Y. *et al.*, (2004a)]. The inefficiencies of the current $NaBH_4$ production process render $NaBH_4$ an expensive chemical, which price greatly depends on grade, form, packaging and expected annual purchasing volume. Based on $NaBH_4$ listed prices, it was shown in Appendix A that it would cost approximately $3000-3800US (specialty chemical price) or $1900US (industrial price) to meet the 2009 US Department of Energy (DOE) of 8 kg H_2 target for 400 km [Bonhoff, K. *et al.*, (2005)]. The H_2 pre-tax cost target at the refuel pump station site has been set to $3.00US/kg for 2008 [Department of Energy, (2003)]. At the current prices of $NaBH_4$, the cost of $NaBH_4$ needed to produce 1 kg of H_2 ranges within $375-470US (specialty chemical price) or $230US (industrial price), which is significantly above the desired cost. It is clear that major costs reductions are required to attain the DOE $3.00US/gallon of gasoline equivalent (gge) target for 2009, and the $2-3.00US/gge target for 2015 [Wipke, K. *et al.*, (2006)].

While the high cost of $NaBH_4$-based solutions is not as critical in small portable Direct Borohydride Fuel Cell (DBFC) applications, it is a major obstacle to its large scale acceptance as a H_2 carrier for H_2 storage and generation in FCVs. The energy required for the manufacturing of $NaBH_4$ is significantly more then the energy required for the production of methanol [Li, Z. P. *et al.*, (2003b)] and the production cost of the $NaBH_4$ solution is approximately twenty times that of the cost of gasoline, for the same energy density. In addition, the price of H_2 generated from $NaBH_4$ is significantly higher than H_2 generated from the reforming of natural gas, and even higher than H_2 produced by electrolysis using wind generated electricity [Wee, J.-H., (2006)]. As several US and European chemical companies becomes eager to sign up to mass produce $NaBH_4$, it is possible that the price of $NaBH_4$ drops significantly in the next few years. However, until the cost of $NaBH_4$ drops by a factor of 10, technologies based on this H_2 carrier will only be economically viable for limited applications [Larminie, J. *et al.*, (2003)]. Nevertheless, currently the $NaBH_4$ manufacturing process is not only costly: it also creates a lot of wastes, which requires further

treatment, and carbon dioxide emissions. The extensive use of a $NaBH_4$ based solutions would require the disposal of large quantities of metaborate salts. A way to achieve important cost savings while reducing the quantity of waste generated would be to develop an effective method to recycle the returned spent solution of $NaBO_2$ to produce $NaBH_4$. Depending on how this is achieved, reductions in greenhouse gas emissions could be attained.

2.2 NaBH₄ Regeneration

This Section provides an overview of some of the possible ways to regenerate the borate produced from the $NaBH_4$ hydrolysis reaction. The syntheses were separated in two main categories: chemical regeneration processes and electrochemical regeneration processes. Regeneration methods falling in each category are revised in Sections 2.2.1 and 2.2.2. Based on the information available in the literature, it was not possible to determine which of the options would result in a lower $NaBH_4$ cost. For this purpose the methods described need to be thoroughly evaluated and compared using many factors, such as energy requirements, product purity, reaction yield, overall efficiency, by-product generation and environmental impact. To a minimum, one major criterion must be met: to have an energy efficient cycle, the regeneration process should not require more energy than the amount of energy released or recovered in the fuel cell system.

2.2.1 Chemical Synthesis

Aside from the Schlesinger and Brown and the Bayer processes described in the Section 2.1.2, there exist several other chemical processes to produce $NaBH_4$. Chemical regeneration approaches comprise organic based reactions, inorganic synthesis and ball milling processes. The majority of the chemical regeneration processes involve multiple chemical reaction steps which add significantly to the total manufacturing cost. Hence, even though good yields are obtained, the cost reduction of $NaBH_4$ would become increasingly difficult as the complexity and the number of chemical reaction steps increases. A list of the processes selected for discussion in this review is provided in Table 2.2. This list does not comprise

all of the possible ways to chemically produce NaBH$_4$. Other possible syntheses have been covered in a separate study [Wu, Y. et al., (2004b)].

Table 2.2: List of Possible Chemical Regeneration Synthesis.

Chemical Syntheses	References
Modified Schlesinger and Brown Process	[Amendola, S. C. et al., (2003)]
Process amendment	[Snover, J. et al., (2004)]
Three-step regeneration method	[Mohring, R. M. et al., (2003)]
Using coke or methane	[Kojima, Y. et al., (2003)]
Recycling through diborane	[Filby, E. E., (1976)]
Using a reducing agent	[Knorre, H. et al., (1968)]
Annealing methods	[Kojima, Y. et al., (2003)]
Ball milling processes	[Suda, S., (2003), Li, Z. P. et al., (2003a), Seijiro, S., (2004)]
Radiolysis Process	[Bingham, D. N. et al., (2005), Wilding, B. et al., (2004), Bingham, D. et al., (2004)]

A list of US patents pertaining to different NaBH$_4$ chemical synthesis is provided in Table 2.3, however, in this review, these patents were not individually studied in details.

Table 2.3: Chemical Synthesis Patent List.

Patent Number	Title	References
US 3379511	Production of sodium borohydride	[Knorre, H. et al., (1968)]
US 3993732	Method of recycling lithium borate to lithium borohydride through diborane	[Filby, E. E., (1976)]
WO 02062701	A process for synthesizing metal borohydrides	[Yu, Z., (2002)]
US 6524542	Processes for synthesizing borohydride compounds	[Amendola, S. C. et al., (2003)]
JP2004010446	Method for producing alkali metal boron hydride	[Seijiro, S., (2004)]
US 6706909 B1	Recycle of discharged sodium borate fuel	[Snover, J. et al., (2004)]
US 20050077170 A1	Method of forming a chemical composition	[Bingham, D. N. et al., (2005)]

A) Modified Schlesinger and Brown Process

A modification of the Schlesinger and Brown process adapted for the recycling of metaborate has been patented [Amendola, S. C. et al., (2003)]. It allows for the recycling of excess reagents and by-products

13

generated within the process to provide a greater efficiency in the production of $NaBH_4$ [Amendola, S. C. *et al.*, (2003)]. The first reaction step is carried out in a stirred tank reactor where carbon dioxide, at 30-40 atm, reacts with water and $NaBO_2$ to form a bicarbonate compound and boron oxide, which is filtrated out.

$$4NaBO_2 + 4CO_2 + 2H_2O \rightarrow 4NaHCO_3 + 2B_2O_3 \qquad \text{(Eq. 2.10)}$$
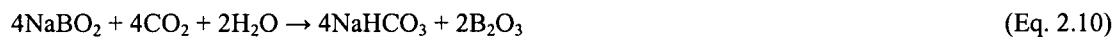
The bicarbonate is converted in sodium oxide, carbon dioxide and water by thermal decomposition at high temperatures in a rotary calciner.

$$4NaHCO_3 \rightarrow 2Na_2O + 4CO_2 + 2H_2O \qquad \text{(Eq. 2.11)}$$

Bromide is obtained by converting HBr in hydrogen and bromide by passage over a metal catalyst at temperatures of 100-500°C in a fluidized bed reactor.

$$12HBr \rightarrow 6H_2 + 6Br_2 \qquad \text{(Eq. 2.12)}$$
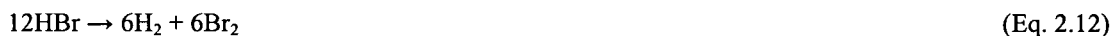
In another stirred tank reactor, boron oxide reacts with carbon and a halide compound to obtain a boron halide, boron bromide, and carbon monoxide:

$$2B_2O_3 + 6C + 6Br_2 \rightarrow 4BBr_3 + 6CO \qquad \text{(Eq. 2.13)}$$

H_2 is obtained along with carbon dioxide from the reaction of carbon monoxide and water in a shift reactor.

$$6CO + 6H_2O \rightarrow 6H_2 + 6CO_2 \qquad \text{(Eq. 2.14)}$$

The boron halide reacts with H_2 to form diborane and a halide in an autoclave:

$$4BBr_3 + 12H_2 \rightarrow 2B_2H_6 + 12HBr \qquad \text{(Eq. 2.15)}$$

Finally, sodium oxide reacts with diborane to produce $NaBH_4$, $NaBO_2$ and carbon dioxide:

$$2Na_2O + 2B_2H_6 \rightarrow 3NaBH_4 + NaBO_2 \hspace{4cm} \text{(Eq. 2.16)}$$

The process can be carried in a closed loop cycle where borate, carbon and water need to be supplied, while $NaBH_4$ and carbon dioxide are produced. The process overall reaction is:

$$3NaBO_2 + 6C + 6H_2O \rightarrow 3NBH_4 + 6 CO_2 \hspace{3cm} \text{(Eq. 2.17)}$$

As the overall equation is endothermic, so energy needs to be supplied to generate $NaBH_4$. The overall energetic requirement for the process is evaluated to be about 17551 kJ and the overall efficiency is estimated to 65 % [Amendola, S.C. et al., (2003)]. It has to be noted that natural gas reforming is used to produce H_2, which releases important amount of CO_2. Furthermore, carbon needs to be obtained from coke or methane. Thus, the environmental impacts associated with this process need to be accounted for.

B) Modified Schlesinger and Brown Process: Amendment

To improve the recovery of boron from a mixture of alkali metal borate and alkali metal hydroxide discharged from a H_2 generation system, an amendment to the modified Schlesinger and Brown process was proposed [Snover, J. et al., (2004)]. In this process, Eq. 2.10 is replaced by a reaction of carbon dioxide and lower alcohol to form trialkyl borate ($B(OR)_3$), alkali bicarbonate and water.

$$NaBO_2 + NaOH + 2CO_2 + 3CH_3OH \rightarrow B(OCH_3)_3 + 2NaHCO_3 + H_2O \hspace{1cm} \text{(Eq. 2.18)}$$
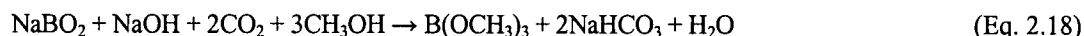
The reactor is pressurized with carbon dioxide at 15-35 atm for 1-10 hours [Snover, J. et al., (2004)]. The sodium bicarbonate formed is heated to produce sodium carbonate as in Eq. 2.11. The trialkyl borate is isolated from the reaction by distillation and then reacts with water to form boric acid as per the equilibrium:

$$B(OH)_3 + 3CH_3OH \leftrightarrow B(OCH_3)_3 + 3H_2O \qquad \text{(Eq. 2.19)}$$

In order to favour the equilibrium towards the formation of trialkyl borate, excess alcohol is required and water has to be removed. The non-reacted alcohol is recycled in the process. Due to their ability of absorbing water as it forms, the addition of solid porous water-adsorbing materials, such as alumina pellets and molecular sieves, to the reaction mixture improved the yield of trialkyl borate by 50 % [Snover, J. *et al.*, (2004)]. The trialkyl borate is then converted to alkali·borohydride by reacting with sodium hydride as in the conventional Schlesinger and Brown process described earlier. Alternatively, it could possibly be used in the three-step regeneration process described below.

C) Three-Step Regeneration

A somewhat simpler three-step regeneration process was proposed [Mohring, R. M. *et al.*, (2003)]. Figure 2.2 summarises the overall synthesis reactions.
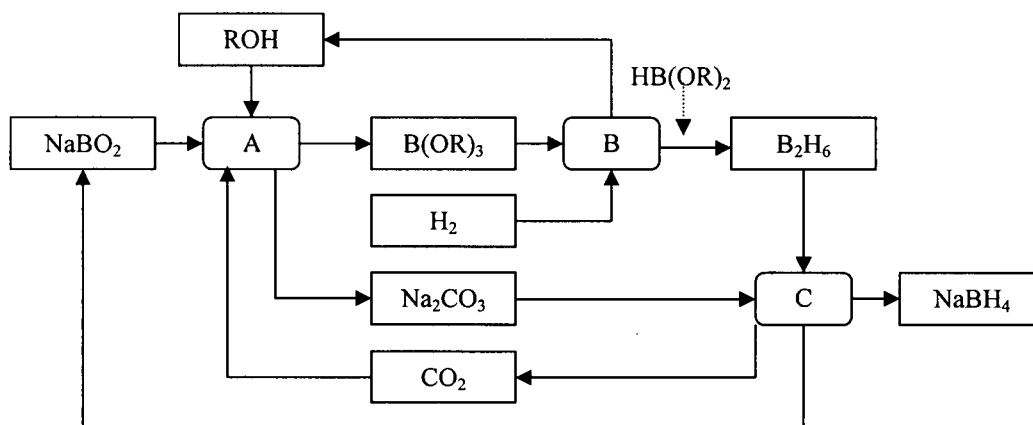
Figure 2.2: Schematic Diagram of the Three-Step NaBH$_4$ Regeneration Process (Modified from [Mohring, R. M. *et al.*, (2003)]).

The first step is a reaction (A) involving borate salts under reflux in alcohol under a CO$_2$ atmosphere to produce a trialkyl borate, B(OR)$_3$. The reaction by-product, Na$_2$CO$_3$, is reused in reaction (C) to form NaBH$_4$ from B$_2$H$_6$. The most important reaction step (B) is the one where HB(OR)$_2$ is synthesized from

B(OR)$_3$. This reaction is endothermic and requires temperatures above 500°C. It is known that dialkoxy borane, HB(OR)$_2$, disproportionate to form borane, hence, difficulties in obtaining good reaction (b) yields were anticipated. No yields were reported for reaction (b) [Mohring, R. M. *et al.*, (2003)]. Reaction (c) is described as follows:

$$2B_2H_6 + 2Na_2CO_3 \rightarrow 3NaBH_4 + NaBO_2 + 2CO_2 \qquad \text{(Eq. 2.20)}$$

$$B_2H_6 + 6H_2O \rightarrow 2B(OH)_3 + 6H_2 \qquad \text{(Eq. 2.21)}$$
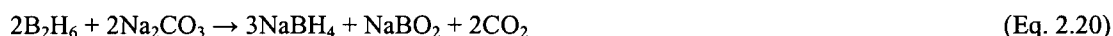
The yields for this reaction were reported to be as low as 6 to 25 %. Higher $NaCO_3$ concentrations and greater $NaCO_3$ to B_2H_6 ratios somewhat improved the yields [Mohring, R. M. *et al.*, (2003)]. The use of a ball milling technique, an increase of the B_2H_6 pressure in the reactor and the addition of diglyme to the ball milling process, all contributed to improve the dissolution of $NaBH_4$, which enhances the exposure of the reactant surface for more reaction. Even after using all those improvements, the maximum yield obtained was 75 % [Mohring, R. M. *et al.*, (2003)]. Based on the fact that the yields are low and that carbon dioxide is a reaction by-product, it is obvious that the process is not economically viable and environmentally advantageous.

D) Using Coke or Methane

The use of a classical chemical reaction, modified for the composition of the recovered $NaBO_2$, was proposed to regenerate $NaBH_4$. It was demonstrated that $NaBO_2$ can be recycled back to $NaBH_4$ using coke or methane, which are less expensive reducing agents. During synthesis, H_2 is produced from methane via a decomposition reaction at 850-950°C [Kojima, Y. *et al.*, (2003)]. The overall regeneration reaction combined with the H_2 generation reaction gives the overall reaction for the system.

Methane decomposition: $2CH_4 \rightarrow 2C + 4H_2$ (Eq. 2.22)

Regeneration: $NaBO_2 + 2CH_4 + 2H_2O \rightarrow NaBH_4 + 2CO_2 + 4H_2$ (Eq. 2.23)
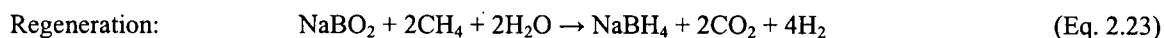
When using coke, the reaction is described as:

Regeneration: $NaBO_2 + 2C + 2H_2O \rightarrow NaBH_4 + 2CO_2$ (Eq. 2.24)
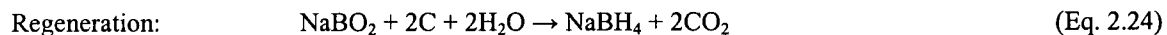
Two moles of methane are required to produce eight moles of H_2, whereas two moles of coke are needed to produce four moles of H_2. The cheapest and most energy efficient reducing agent would be coke (coal) or petroleum product [Kojima, Y. et al., (2003)]. However, in both cases, the overall regeneration would produce two moles of CO_2, which conflicts with the fundamental objective of clean energy and the main reason for using H_2.

E) Recycling Through Diborane

A method for the recycling of lithium borate to lithium borohydride was patented [Filby, E.E., (1976)]. In this synthesis, the borate reacts with hydrogen chloride and water to produce boric acid and lithium chloride, which are then converted to borohydride through a diborane intermediate. The preferred diborane synthesis is:

$2BCl_3 + 6H_2 \rightarrow B_2H_6 + 6HCl$ (Eq. 2.25)

The diborane intermediate can be reacted with a lithium species, such as lithium hydride, to produce lithium borohydride. The multi-step process overall reaction would be as follows:

$2LiBO_2 + 3C + 7H_2 + 5/2O_2 \rightarrow 2LiBH_4 + 3H_2O + 3CO_2$ (Eq. 2.26)
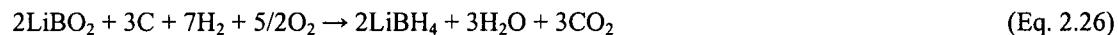
This reaction is very similar to Eq. 2.24, but in non-aqueous media. The chemical reaction steps involved in the process are relatively well known and the chemical separations are not difficult [Filby, E. E., (1976)]. The process involves the electrolysis of lithium chloride to form chlorine and lithium. If transposed to the production of $NaBH_4$, this reaction step would be equivalent to the electrolysis used in the Schlesinger and

Brown process described earlier. This is highly energy consuming. As per the overall synthesis reaction, three molecules of CO_2 are produced for every two moles of $NaBO_2$ recycled. Thus, the environmental impacts of this process are significant.

F) Reduction of $NaBO_2$ with H_2

A process for the production of $NaBH_4$ by treating $NaBO_2$ with a reducing agent in the presence of H_2 at 500°C and under atmospheric pressures up to 10 atm was patented [Knorre, H. et al., (1968)]. The reaction is described as follows:

$$NaBO_2 + Na_2O + 2H_2 + Si \rightarrow NaBH_4 + Na_2SiO_3 \qquad \text{(Eq. 2.27)}$$

The reaction is exothermic and the desired temperature range between 420 to 500°C [Knorre, H. et al., (1968)]. A $NaBH_4$ yield of 93 % with respect to $NaBO_2$ has been claimed. The reaction yield is increased when excess reducing agent is added. Adding sodium oxide to the mixture activates the exothermic reaction and allows it to be carried at milder pressures. Pure $NaBH_4$ can be extracted from the reaction product with various organic solvents. The reaction can also be carried with reductants such as carbon black and calcined charcoal.

G) Methods Using Metal Hydrides

a) Annealing

The Toyota research group has developed an annealing technique which uses alkaline-metal based hydride such as LiH, NaH, CaH_2 and MgH_2. $NaBH_4$ can be synthesized at 350-750°C by annealing $NaBO_2$ and MgH_2 or Mg_2Si under H_2 pressure ranging from 0.1 to 7 MPa [Kojima, Y. et al., (2003)]. The reaction of $NaBO_2$ with MgH_2 to produce $NaBH_4$ is as follows:

$$NaBO_2 + 2MgH_2 \rightarrow NaBH_4 + 2MgO \qquad \text{(Eq. 2.28)}$$

This reaction is spontaneous ($\triangle G° = -270$ KJ/mol $NaBH_4$). $NaBH_4$ yields up to 97-98 % were obtained at 550°C and 7 MPa, independently of the annealing time. The melting point of $NaBH_4$ and the thermal decomposition of MgH_2 played an important role in the yield of $NaBH_4$ [Kojima, Y. *et al.*, (2003)]. This method could represent an effective amendment to the Bayer process described in Section 2.1.2 C), as the use of Mg as a reducing metal would be less expensive than using Si [Wu, Y. *et al.*, (2004b)].

A similar annealing generation method to convert $NaBO_2$ and produce $NaBH_4$ with Mg_2Si under high H_2 pressure has been investigated by the same research group. The reactions are as follows:

$$NaBO_2 + 2Mg + Si + 2H_2 \rightarrow NaBH_4 + Mg_2Si + 2H_2 \qquad \text{(Eq. 2.29)}$$
$$NaBO_2 + Mg_2Si + 2H_2 \rightarrow NaBH_4 + 2MgO + Si \qquad \text{(Eq. 2.30)}$$
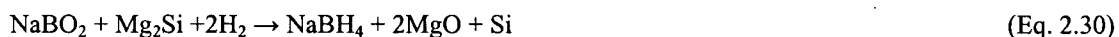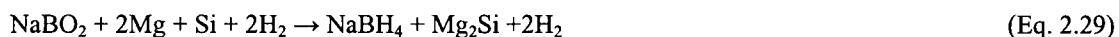
The reaction is spontaneous but yields less $NaBH_4$ then the reaction with MgH_2 [Kojima, Y. *et al.*, (2003)]. To render the annealing method practical, the process of regenerating the hydride used as the H_2 donor has to be cost-effective and the energy consumption has to be minimized.

b) Ball Milling

In a mechano-chemical process, collision energy is converted to chemical energy. A ball milling technique has been utilized in the reaction of $NaBO_2$ with MgH_2 to produce $NaBH_4$, as in Eq. 2.28 described above [Suda, S., (2003)]. Using this method, very high yields of $NaBH_4$ can be obtained at ambient conditions in limited time. The yields can be further increased by increasing temperature and pressure, but is independent of the reaction time. The addition of NaOH to the $NaBO_2$ solution further improves the reaction yield [Suda, S., (2003)].

Another academic research group investigated the formation of $NaBH_4$ through the reaction of hydrated borax and magnesium hydride with ball-milling at room temperature [Li, Z. P. *et al.*, (2003a)]. It was found that sodium compounds have to be provided to compensate for the reactant Na insufficiency and

promote the formation of $NaBH_4$. Na_2CO_3 was the most effective additive and lead to the following reaction:

$$8MgH_2 + Na_2B_4O_7 + Na_2CO_3 \rightarrow 4NaBH_4 + 8MgO + CO_2 \qquad \text{(Eq. 2.31)}$$
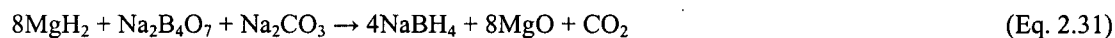
The maximum reaction yield was of 78 %. Excess addition of MgH_2 improved the borohydride yield. However, the yield decreased when more MgH_2 was added after the $NaBH_4$ yield reached a maximum value [Li, Z. P. et al., (2003a)].

The same method for manufacturing $NaBH_4$ using $NaBO_2$ and magnesium hydride as the raw materials, was patented to include the formation of MgH_2 [Seijiro, S., (2004)]. The process requires four reaction steps. First, a hydrogen halide, such as HCl, reacts with an alkaline earth metal oxide, such as MgO, to produce an alkaline earth metal halide, like $MgCl_2$. Secondly, the alkaline earth metal halide is electrolysed to an alkaline earth metal (Mg) and a halogen (Cl_2). In the third step, Mg is hydrogenated by H_2 to obtain an alkaline earth metal hydride (MgH_2). Here again, the hydrogenation can be carried at milder conditions when mechanical energy is induced by a ball-milling process where MgH_2 reacts with $NaBO_2$, to generate MgO and $NaBH_4$. In this case, a $NaBH_4$ yield of 45 % was claimed based on $NaBO_2$ [Seijiro, S., (2004)].

H) Radiolysis Process

Radiolysis is being investigated as a potential route for off-board borate regeneration [Wilding, B. et al., (2004)]. In this method, radioactive waste is used as the photolytic energy source. It provides the ionizing potential required to modify the chemical bonds of $NaBO_2$ and permit chemical reconfiguration to the desired compound [Bingham, D. N. et al., (2005)]. The photon reacts with water and/or borate causing a change in the electronic structure, which creates a molecular radical. At high concentration, the radicals collide with the neutral molecules and form a stable borohydride configuration [Wilding, B. et al., (2004)]. With efficient control in place, it was possible to produce stable borohydrides. A H_2 conversion efficiency of 53 % was calculated based on the analytical conversion of energy adsorbed [Bingham, D. et al., (2004)].

21

This process seems to be economical as it reuses radioactive waste materials, which would otherwise require processing and storage at great cost. However, the borate radiochemistry mechanisms and reactions are not well understood at this time and need to be further investigated.

2.2.2 Electrochemical Synthesis

Most electrochemical syntheses are simple as they require one reaction step. The use of an electrolytic cell for reducing $NaBO_2$ would only require the input of electrical energy. Based on the review of the chemical synthesis in the previous Section, it is clear that the use of electrochemical techniques has the potential of significantly reducing the capital and energy costs compared to chemical processes. Hence, electrochemical regeneration methods are the most likely to result in $NaBH_4$ cost reduction [Wu, Y. *et al.*, (2004b)]. Table 2.4 gives a list of possible electrochemical $NaBH_4$ regeneration synthesis from $NaBO_2$.

Table 2.4: List of Possible Electrochemical Regeneration Synthesis.

Electrochemical Syntheses	References
Electroreduction:	
Direct electroreduction	[Cooper, H. B. H., (1973), Sharifian, H., (1990), Hale, C. H., (1990), Amendola, S. C., (2002)]
Indirect electroreduction	[Cooper, H. B. H., (1973), Gyenge, E. L. *et al.*, (1998)]
Electroreduction of borate ester	[Gyenge, E. L. *et al.*, (1998)]
Electroreduction in Molten NaOH	[Wu, Y., (2004)]
H_2 assisted electrolysis:	
Molten NaOH	[Xu, J. *et al.*, (2004)]
Borate in salt melt	[Wu, Y. *et al.*, (2004a), Xu, J. *et al.*, (2004)]
Aqueous alkaline $NaBH_4$ solutions	[Mikio, K., (2003)]
Electrosyntheses:	
Methathesis	[Huff, G. F. *et al.*, (1958)]
Simulating conventional process	[Linkous, C. A., (2003-4)]

Table 2.5 is a list of patents regarding various electrochemical synthesis of $NaBH_4$. According to the first five patents listed in Table 2.5, electrochemical cells can be used to generate $NaBO_2$ by the electrochemical reduction of $NaBO_2$ in aqueous media in yields ranging from 20 to 80%. Considering the number of recent patents pertaining to the electrochemical synthesis of $NaBH_4$, it can be said that there is

an increase interest towards the recycling of $NaBO_2$ and the development of electrochemical $NaBH_4$ production processes.

Table 2.5: Electrochemical Borohydride Synthesis Patent List.

Patent Number	Title	References
US 3734842	Electrolytic process for the production of alkali metal borohydrides	[Cooper, H. B. H., (1973)]
US 4904357	Production of quartenary ammonium and quartenary phosphonium borohydride	[Sharifian, H., (1990)]
US 4931154	Production of metal borohydrides and organic onium borohydrides	[Hale, C. H., (1990)]
US 6497973	Electroconversion cell	[Amendola, S. C., (2002)]
CN 1396307A	Process for preparing boron hydride by electrolytic method	[Sun, Y. *et al.*, (2003)]
JP 2003247088	Method and apparatus for manufacturing boron hydride compound	[Mikio, K., (2003)]
US 20040011662 A1	Hydrogen-assisted electrolysis processes	[Xu, J. *et al.*, (2004)]
US 2855353	Electrolytic method for the preparation of metal borohydrides	[Huff, G. F. *et al.*, (1958)]

The patents above can be divided in three main categories: direct electroreduction (US patents 3734842, 4904357, 4931154, 6497973 and CN 1396307A), H_2 assisted electrolysis (JP patent 2003247088, US patent 20040011662 A1) and electro-synthesis (US patent 2855353). Each type of electrochemical synthesis is discussed separately in the following Sections. Only electrochemical methods allow the direct reprocessing of $NaBO_2$ to $NaBH_4$. Electrochemical regeneration processes require less energy, are emission free and are most likely to result in significant cost reduction over the Schlesinger and Brown process.

A) Direct Electroreduction

The most convenient way to regenerate $NaBH_4$ would be to use an aqueous media. The direct borate electroreduction can be described as the electrolysis of an aqueous $NaBO_2$ solution where $NaBO_2$ is directly reduced to form $NaBH_4$. The theoretical cathodic reduction of the $NaBO_2$ to $NaBH_4$ in alkaline aqueous media is as follows:

Cathode: $BO_2^- + 6H_2O + 8e^- \rightarrow BH_4^- + 8OH^-$ (Eq. 2.33)
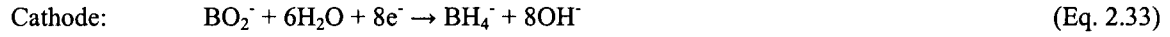
$E^o_c = -1.24$ V vs. SHE

Since the electroreduction takes place in an alkaline media, oxygen (O_2) evolves at the anode from the hydroxide ion. The release of O_2 from an aqueous basic solution at the anode is given by:

Anode: $8OH^- \rightarrow 4H_2O + 2O_2 + 8e^-$ (Eq. 2.34)

$E^o_a = 0.4$ V (pH=14) vs. SHE

This leads to the following overall cell electrochemical reaction and standard equilibrium cell voltage for the electroreduction cell:

Overall: $BO_2^- + 2H_2O \rightarrow BH_4^- + 2O_2$ (Eq. 2.35)

$$E^o_{cell} = E^o_c - E^o_a = -1.24 - 0.4(pH = 14) = -1.64V$$

The non-standard equilibrium potential, $E_{e, cell}$, is given by the Nernst equation:

$$E_{e,cell} = E^o_{cell} - RT\!/\!8F \cdot \ln\left(\frac{[BH_4^-] \cdot (P_{O_2})^2}{[BO_2^-]} \right)$$ (Eq. 2.36)

The actual cell voltage takes into account the electrode surface activation overpotentials (η_{S_a} and η_{S_c}), the concentration overpotentials (η_{con_a} and η_{con_c}) and ohmic losses ($\Delta\Phi_{ohm}$) into account. When assuming that the open circuit voltage is approximately equal to the equilibrium cell potential, the actual cell voltage is given by:

$$E_{cell} = E_{e,cell} - \eta_{S_a} + \eta_{S_c} - \eta_{con_a} + \eta_{con_c} - \Delta\Phi_{ohm}$$ (Eq. 2.37)

To shift the reaction equilibrium to the right and favor the generation of $NaBH_4$, it is desired to make E_{cell} more positive and closer to the equilibrium cell potential by minimizing the overpotentials and the ohmic drop. When pure kinetic control is assumed, the mass transfer effects and the ohmic drop can be neglected.

B) Kinetic Considerations

At the low cathodic voltage of Eq. 2.33, the release of H_2 from water is more favorable. Hence, the H_2 evolution reaction competes with the $NaBO_2$ reduction:

$$2H_2O + 2e^- \rightarrow H_2 + 2OH^-$$ (Eq. 2.38)

$$E_c^o = -0.83V \left(pH = 14 \right) vs.SHE$$

As Eq. 2.38 is likely to proceed at the cathode instead of Eq. 2.33, the electrochemical cell is not likely to generate significant amounts of $NaBH_4$. Energy is wasted as the total current is split between both reactions. Hence, a significant concern is that it takes less energy to reduce the solvent than to reduce $NaBO_2$.

To minimize the electrocatalytic H_2 evolution and favor the direct electrochemical reduction of $NaBO_2$ to $NaBH_4$, a large H_2 evolution overpotential is needed at the cathode. The H_2 overpotential (η_{S_c}) is the difference between the cathode potential produced by the H_2 evolution reaction (E_c) and the equilibrium potential for that same reaction ($E_{c,e}$). Large overpotentials can be obtained by selecting a cathode material which has a low catalytic affinity towards the H_2 evolution reaction. For Eq. 2.38, the cathodic current corresponds to the following expression based on the Tafel equation:

$$i = -i_{o,c} \exp\left(\frac{-2.3\eta_{S_c}}{b} \right)$$ (Eq. 2.39)

This expression can not be used directly for electrochemical reactions involving the transfer of more then two electrons. The exchange current density, $i_{o,c}$, depends on the electrolyte, temperature and pressure and is linked to the electrode material properties. When a simplified electrode kinetic model is used, the cathodic transfer coefficient, (α_c), is found in the denominator of the Tafel slope (b) expression.

$$b = \frac{2.3 \cdot RT}{\alpha_c \cdot F}$$ (Eq. 2.40)

Electrode materials leading to small Tafel slope (b) values and large exchange current density ($i_{o,c}$) values will result in a low surface activation overpotential (η_{S_c}). Hence, in this case, a large H_2 overpotential can be obtained by selecting an electrode material which gives a large b value and a small i_o value for Eq. 2.38. Table 2.6 lists the exchange current densities and Tafel slopes for the H_2 evolution reaction using various materials.

Table 2.6: Exchange Current Densities (i_o) and Tafel Slopes for the H_2 Evolution Reaction at Various Materials in Basic Solutions at Room Temperature., *313K [Gouper, A.M. *et al.*, (1990)].

Material	Concentration OH⁻ [M]	i_o [A/cm^2]	Tafel slope [mV]
Ag	1	3.2×10^{-7}	120
C	40%*	2.9×10^{-5}	148
Cu	0.1	1×10^{-7}	120
Cd	6	4×0^{-7}	160
Cr	6	1×10^{-7}	120
Fe	01	1.6×10^{-6}	120
Hg	0.1	3×10^{-15}	120
Ni	0.5	7.9×10^{-7}	96
Pb	0.5	3.2×10^{-7}	130
P	0.1	6.7×10^{-5}	114
Ir	0.1	5.5×10^{-4}	125
Sn	6	3.2×10^{-7}	150
Ti	6	1×10^{-6}	140
Zn	6	4×10^{-7}	210

Materials with high H_2 overpotentials are Hg, Pb, Cd, Zn, Sn, C, Cu, as well as steels. In addition, Ag, Ni and Fe are also worth considering in alkaline solutions [Gouper, A.M. *et al.*, (1990)]. Cost and availability often favours Ni or stainless steels (SS). Unfortunately, experiments have shown that materials with high H_2 overpotential are not effective to transfer electrons and H_2 to a boron center [Wu, Y. *et al.*, (2004b)].

Luckily there exist other measures to increase the H_2 evolution overpotential. For example, important overpotentials can be obtained in the presence of certain additives. When exceeding a certain concentration, the additive molecules cover the active surface of the electrode. The H atoms have no empty metal surface to adsorb on the cathode surface and the H_2 evolution reaction is minimized. The potential of the H_2 ion at the electrode increases, and thus, the H_2 evolution overpotential increases. A hydride layer forms on the cathode material surface, and the ability of H_2 to adsorb in the cathode metal increases. Some additives, such as thiourea (CH_4N_2S) and selenium dioxides (SeO_2), are catalytic poisons to the H_2 recombination reaction [Szklarska-Smialowska, S. et al., (1963)]. A systematic study of the direct electroreduction of $NaBO_2$ has been conducted in the presence of additives, such as quaternary ammonium compounds and thiourea, in order to further restrain the electrocatalytic H_2 evolution [Gyenge, E. L. et al., (1998)]. Even with those extra measures in place, the production of detectable amounts of $NaBH_4$ by the direct electrochemical reduction of borates was not achieved.

The counter electrode O_2 evolution reaction can be maximized by using an anode material resulting in a low O_2 overpotential. In other words, a material leading to small b value and a high i_o value for Eq. 2.34 would be more favorable. Materials suitable for the O_2 evolution are nickel or nickel-plated mild steel. Many coatings have been reported to have the ability of reducing the oxygen overpotential. They include metal oxides, spinels and perovskites [Gouper, A. M. et al., (1990)].

C) Patent Review

US patent 3734842 describes an electrolytic process for the reduction of alkali metal borohydrides [Cooper, H. B. H., (1973)]. An alkaline aqueous solution of $NaBO_2$ is supplied to the cathode compartment of an electrolytic cell. To ensure proper conductivity a catholyte solution of 0.1 to 5 wt% $NaBO_2$ concentration is recommended. The maximum concentration of the catholyte is limited by the solubility of $NaBO_2$ at the cell operating conditions. An aqueous solution of NaOH constitutes the electrolyte in the anode compartment [Cooper, H. B. H., (1973)]. A cationic selective membrane separates the anode and cathode compartments. This implies that the Na^+ ions are responsible for the transport through the membrane. The cell electrochemical reactions, Eq 2.33 to 2.35, can be written as:

Cathode:	$NaBO_2 + 8Na^+ + 6H_2O + 8e^- \rightarrow NaBH_4 + 8NaOH$	(Eq. 2.41)
Anode:	$8NaOH \rightarrow 2O_2 + 4H_2O + 8Na^+ + 8e^-$	(Eq. 2.42)
	$8NaOH \rightarrow 8Na^+ + 8OH^-$	
	$8OH^- \rightarrow 2O_2 + 4H_2O + 8e^-$	
Overall:	$BO_2^- + 2H_2O \rightarrow BH_4^- + 2O_2$	(Eq. 2.43)
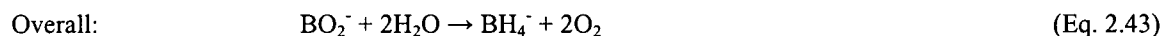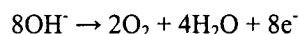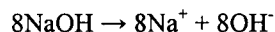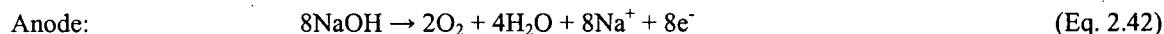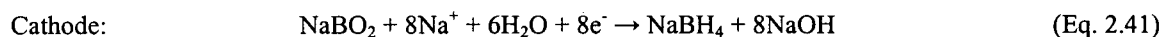
The overall cell electrochemical reaction remains the same as for Eq. 2.35. The reduction of borate ions to borohydride ions occurs in the cathode compartment to produce alkali metal borohydride solution, from which the borohydride may be later separated. The oxygen generated at the anode is vented from the anode compartment. It was suggested that the electrodes be made of graphite, carbon, nickel, cobalt, silver, stainless steel, iron, nickel-plated iron, platinized titanium or tantalum, platinum, palladium, iridium and others [Cooper, H. B. H., (1973)]. It was noted that the activation of the reaction between the borate ion and H_2 generated at the cathode surface could be advantageous. Hence, it was suggested to use hydrogenation catalytic materials as the cathode. Such materials include nickel boride, nickel, Raney nickel, cobalt, cobalt boride, platinum and palladium [Cooper, H. B. H., (1973)]. It is stated that the cell can be operated at current densities ranging from 620 to 1550 A/m^2. The operating voltage of the cell had to be greater than 1.23V, which is the voltage required for the H_2O splitting. Conversions to $NaBH_4$ ranging from 20 to 80 % were claimed [Cooper, H. B. H., (1973)].

US patent 4904357, extends the application of the electrolysis cell described in the earlier patent 3734842 to the production of quaternary ammonium and phosphonium borohydrides by the reduction of the corresponding ammonium or phosphonium boron oxide compounds [Sharifian, H., (1990)]. Various boron oxide compounds, such as perborates, tetraborates and metaborates, can be used as reactants in the process. Boron oxide concentrations ranging between 1 and 40 wt% are recommended in the aqueous catholyte solution, while concentration of salt ranging between 3 and 40 wt% are recommended in the anolyte [Sharifian, H., (1990)]. An electrolysis experiment was carried for two hours at a current density of 500 A/m^2, with an anolyte composed of 25 wt% tetramethylammonium hydroxide, a catholyte composed of 7 wt% tetramethylammonium, platinum cathode and anode, and nickel boride particles in the catholyte

compartment. A current efficiency of 50 % was achieved for the synthesis of tetramethyl ammonium borohydride. In a similar experiment using nickel powder in the catholyte compartment this time, a conversion efficiency of 45 % was reached. When no catalysts were present in the catholyte compartment, the efficiency was as low as 8 % [Sharifian, H., (1990)].

US patent 4931154 describes an electrolysis cell for the production of metal borohydrides and organic onium borohydrides [Hale, C. H., (1990)]. The process is said to be particularly useful for reducing borate ions to borohydride ions. Like in the two previous patents described above, the aqueous catholyte solutions containing 1 to 40 wt% of borate compound and alkaline catholyte solutions are preferred to stabilize the borohydride formed. A cationic-selective membrane is used to favor the migration of cations from the anolyte to the catholyte and increase the alkalinity of the catholyte solution, and Nafion^{TR} membranes are suitable [Hale, C. H., (1990)]. Unlike the other patents reviewed so far, an aqueous acidic solution constitutes the anolyte. At the anode, water in the aqueous acidic solution is ionized. The H$^+$ generated migrates through the membrane to the catholyte solution where metaborate is reduced to borohydride. As the cation in the anolyte is a hydrogen ion, oxygen is evolved and escapes from the anolyte compartment [Hale, C. H., (1990)]. According to the patent, the direct electrochemical reduction of an alkaline aqueous solution of NaBO$_2$ to NaBH$_4$ in an electrical cell using an acidic anolyte solution is as follows:

Cathode: $BO_2^- + 6H_2O + 8e^- \rightarrow BH_4^- + 8OH^-$ (Eq. 2.44)

Anode: $4H_2O \rightarrow 8H^+ + 2O_2 + 8e^-$ (Eq. 2.45)

$(8OH^- + 8H^+ \rightarrow 8H_2O)$

Overall: $BO_2^- + 2H_2O \rightarrow BH_4^- + 2O_2$ (Eq. 2.46)

Again, the overall cell electrochemical reaction still remains the same as for Eq. 2.35. Figure 2.3 represents a schematic diagram of electrolytic cell for the direct electroreduction of NaBO$_2$ to form NaBH$_4$.
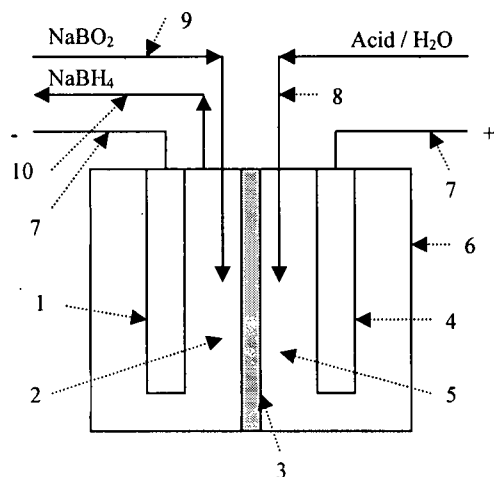
Figure 2.3: Schematic of Electrolytic Cell for the Direct Reduction of Borates to Borohydrides: 1) Cathode, 2) Catholyte, 3) Membrane, 4) Anode, 5) Anolyte, 6) Electric Cell, 7) Wire, 8) Aqueous Acid Solution, 9) Borate Aqueous Solution, 10) Borohydride Withdrawal Line, (Modified from [Hale, C. H., (1990)]).

Passing a current through the cell reduces the borate ions to borohydride ions in the cathode compartment. The borohydride can be later separated from the alkali metal borohydride solution produced. During the electrolysis, the liquid in the cell is kept at temperatures of 50°C or lower [Hale, C. H., (1990)]. The electrolytic cell can be operated in a batch or continuous way. For this acidic anolyte electrolytic cell, anodes with non-passivable and catalytic films are recommended. As the oxygen reduction reaction is slow, good catalysts such as metallic noble metals such as platinum, iridium, rhodium or their alloys, as well as mixtures of electroconductive oxides with at least one oxide being a noble metal are recommended. Suggested cathode materials included nickel, iron, stainless steel, nickel plated titanium and platinum. The cathode material can be coated or dispersed on a metal or inert substrate [Hale, C. H., (1990)]. An electrolysis experiment was carried in a cell with a 10 wt% $NaBO_2$ solution in aqueous 1 M sodium hydroxide as the catholyte and an aqueous solution of 2 M sulfuric acid as the anolyte. By carrying the electrolysis at a current density of 50 mA/cm^2 for two hours, a current efficiency of 20 % for the synthesis of $NaBO_2$ was achieved when using a platinum anode and a nickel cathode [Hale, C. H., (1990)].

US patent 6497973 claims an electroconversion cell, which has the ability to function in one or several modes [Amendola, S. C., (2002)]. This system is constituted of two electrochemical cells: one cell consuming borohydride ions to produce electricity and one cell which electrically generate borohydride ions from the borate. The cells may be separated or the same cell can be used for both processes. The

carrier may be an aqueous or non aqueous solution, but if a non-aqueous solution is used, a solubility or conductivity enhancer is needed [Amendola, S. C., (2002)]. Recharging the cell obviously assumes that it is possible to synthesize borohydride by the direct electroreduction of borates. In this patent the electrode material selection for the cathode is erroneously explained. It is said that a material with an overpotential equal to or greater than the difference in voltages between Eq. 2.33 and 2.38 are needed (1.24 - 0.8277 = 0.41 V) to minimizing Eq. 2.38 as much as possible [Amendola, S. C., (2002)]. This voltage difference was incorrectly attributed to the hydrogen overpotential for Eq. 2.38. As explained earlier, the overpotential desired is not equal to the difference of potential between those two reactions and is a function of the current exchange density and the transfer coefficient. According to the patent, the optimal cathode would be a small electrode with high current density and would be coated with a soft metal alloy [Amendola, S. C., (2002)]. It was said that soft materials have a tendency to have high H_2 overpotentials. For example, it is said that mercury, due to its E^o = -2.7 V, would allow Eq. 2.38 to proceed at high efficiency. Other soft metals judged appropriate included bismuth, lead, tin, thallium, cadmium, gallium and indium. Tellurium restrains the ability of an electrode material to generate H_2 gas and can be included in the metal [Amendola, S. C., (2002)]. Also, according to this patent, the optimal anode would have a high surface area and low current density like an electrode coated with gold or iridium oxide. Recommended anode materials for low oxygen overpotentials are gold, iridium oxide, manganese dioxide and others [Amendola, S. C., (2002)].

The Chinese patent application CN1396307 describes an electrochemical process to generate $NaBH_4$ from $NaBO_2$ [Sun, Y. et al., (2003)]. In this patent, the electroreduction of $NaBO_2$ in aqueous solution at more than 30 wt% efficiency was claimed [Wu, Y. et al., (2004b)].

D) Reproducibility

The $NaBO_2$ direct electrolysis yields claimed in the patents described above remain to be ascertained. The laboratory reproduction the direct electrochemical reduction of $NaBO_2$ did not produce any detectable amounts of $NaBH_4$ [Gyenge, E. L. et al., (1998), Suda, S., (2003)]. Hence, it is highly probable that the BH_4^- ion was not produced in significant amounts because, as explained earlier, it can not avoid the

thermodynamically favorable conversion to BO_2^-. If that is the case, the efficiency of the direct electrochemical production of $NaBH_4$ in aqueous solution is too low to be practical in industrial applications [Yu, Z., (2002)].

Furthermore, it was reported that there might be erroneously high concentrations of BH_4^- in some solutions of other reductants formed during the electrolysis according to the commonly used iodate detection method [Mirkin, M. V. *et al.*, (1991), Gyenge, E. L. *et al.*, (1998)]. More accurate, reliable and selective detection methods are needed to validate the results obtained. Using more robust methods, such as a voltammetric detection method [Mirkin, V. M. *et al.*, (1991)], and the novel phosphotungstic acid reduction analytical method [Gyenge, E. L. *et al.*, (1998)], no $NaBH_4$ was detected after the direct electroreduction of $NaBO_2$ alkaline aqueous solutions. Consequently, a square wave sweep voltammetric method having a low detection limit of 3 x 10^{-5} M has been developed to study the formation of borohydrides [Celikkan, H. *et al.*, (2005)]. Logically, this leads to the conclusion that water is not a suitable solvent to carry the direct electroreduction of $NaBO_2$.

E) Indirect Electroreduction

The cathode and anode reactions for the indirect electrochemical generation of $NaBO_2$ in aqueous alkaline media are as follows:

Cathode reaction:	$2H_2O + 2e^- \rightarrow H_2 + 2OH^-$	(Eq. 2.47)
	$BO_2^- + 4H_2 \rightarrow BH_4^- + 2H_2O$	
Anode reaction:	$2OH^- \rightarrow H_2O + 1/2O_2 + 2e^-$	(Eq. 2.48)
Overall cell reaction:	$H_2O \rightarrow 1/2O_2 + H_2$	(Eq. 2.49)
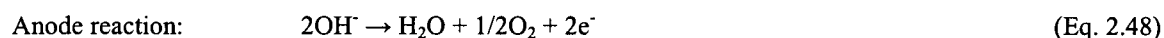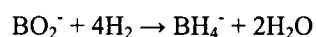
$$E^o_{cell} = E^o_c - E^o_a = -0.83 - (0.4) = -1.23V$$

In this case, the H_2 evolution reaction is used at the cathode. As it leads to a different overall reaction than in the case of the direct electroreduction of $NaBO_2$, this process can be described as an electrochemical hydrogenation. Based on the cell standard potential, it can be showed that this electroreduction process

requires a quantity of energy lower than that needed for the direct electroreduction process. This electroreduction process is said indirect as it aims at promoting the anode reaction to produce H_2 and make it react with the metaborate on the cathode material. The principle is similar to that of the H_2 assisted electrolysis process which will be described in a later Section. Hydrogenation catalysts, such as Ni, Raney-Ni, NiB, palladium or zinc, are recommended cathode materials [Cooper, H. B. H., (1973)]. In this case, the hydrogenation catalyst role is to promote the H_2 evolution reaction, and to affect the adsorption and dissociation of H_2 at the electrode surface. Experiments showed that the use of Raney-Ni was not successful as it catalyzes the H_2 evolution reaction but does not catalyse the reaction of BO_2^- and H_2 [Gyenge, E. L. et al., (1998)]. This was not the case when using NiB as the cathode material. Nevertheless, experiments demonstrated that this process did not generate any detectable quantities of $NaBH_4$ [Gyenge, E. L. et al., (1998)].

Another research group attempted to explain why the cathodic electroreduction of the borate ion of Eq. 2.33 follows an indirect reduction process [Wei, X.-Y. et al., (2003)]. The negatively charge borate ion has difficulties to approach the cathode. According to their findings, a possible scenario would be that the water molecules release an electron and produce H_2 at the cathode, which in turns reduces BO_2^- to BH_4^-. Hence, the mechanism for the reduction of $NaBO_2$ would be controlled by the absorption of H_2 on the cathode. If this was the case, Ni would be a good cathode material as it strongly absorbs H_2. This also reemphasizes the importance of selecting a medium favourable to electron transfer. Another finding was that the imposition of a positive pulse on the cathode forced the anion to absorb directly on the cathode surface and rendered the electroreduction, as per Eq. 2.33, a direct process [Wei, X.-Y. et al., (2003)].

F) Electroreduction of Borate Ester

The electroreduction of borate ester in organic media on graphite and aluminum cathodes has also been investigated [Gyenge, E. L. et al., (1998)]. This rigorous reduction based on solvated electrons was performed using a hexamethylphosphoramide (HMPA)-ethanol mixture or ehtylenediamine (EDA) as the catholyte, and with lithium salts as supporting electrolyte. No $NaBH_4$ was detected in these experiments.

G) Electroreduction in Molten Hydroxide Media

As part of the US DOE Hydrogen Program, a research group discovered a stable molten hydroxide system in which $NaBO_2$ might be directly reduced to $NaBH_4$. The apparent electrolytic activity of $NaBO_2$ in hydroxide melt was observed. The addition of $NaBO_2$ to a hydroxide melt caused significant changes in the cyclic voltammograms, but the reduction wave remains unidentified at this point [Wu, Y., (2004)].

H) Hydrogen Assisted Electrolysis

Using H_2 gas at the anode lowers the overpotential on the anodic side of an electrolytic cell, and lowers the overall cell voltage required during the electroreduction process [Xu, J. *et al.*, (2004)]. Hence, the use of H_2 gas lowers the cell voltage, resulting in an improved regeneration efficiency of borate or sodium electroreduction processes [Wu, Y., (2003b)]. Consequently, the H_2 assisted electrolysis for the regeneration of $NaBH_4$ represents a lower cost alternative to electrochemical processes generating O_2 at the anode. The resulting energy efficient improvement could lower the production cost of $NaBH_4$. Three different types of H_2 assisted electrolysis process are discussed in this Section: the electrolysis of molten NaOH, the electrolysis of borate in salt melt, and the electrolysis of aqueous alkaline borate solutions.

a) Molten NaOH Electrolysis

The electrolytic reduction of sodium hydroxide, NaOH, to sodium metal, Na, can be performed by the H_2 assisted molten NaOH electrolysis. The electrochemical reactions for the conventional sodium electrolysis and for the H_2 assisted molten NaOH electrolysis are described below [Xu, J. *et al.*, (2004)]. Note that the cathode sodium reaction is the same in both cases.

Conventional sodium electrolysis:

Cathode:	$Na^+ + e^- \rightarrow Na$	(Eq. 2.50)
Anode:	$Cl^- + e^- \rightarrow \frac{1}{2} Cl_2$	(Eq. 2.51)
Overall:	$Na^+ + \frac{1}{2} Cl_2 \rightarrow Na + Cl^-$	(Eq. 2.52)

$$E^o_{cell} = E^o_c - E^o_a = -2.71 - 1.36 = -4.07 V$$

Hydrogen assisted molten NaOH electrolysis:

Cathode:	$2Na^+ + 2e^- \rightarrow 2Na$	(Eq. 2.53)
Anode:	$2OH^- + H_2 \rightarrow 2H_2O + 2e^-$	(Eq. 2.54)
Overall:	$2Na^+ + 2H_2O \rightarrow 2Na + 2OH^- + H_2$	(Eq. 2.55)
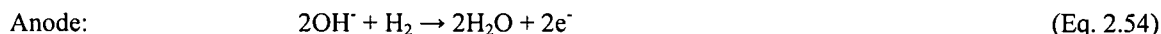
$$E^o_{cell} = E^o_c - E^o_a = -2.71 - (-0.83) = -1.88V$$

The standard cell potential of the H_2 assisted molten NaOH electrolysis is 53.76 % less then that for the conventional sodium electrolysis. A lower voltage results in cost savings. This process could be directly integrated in the currently used Schlesinger and Brown process described in Section 2.1.2 B) to improve the efficiency of Na production. Figure 2.4 represents a schematic diagram of electrolytic cell with H_2 at the anode for the electrolysis of sodium hydroxide in molten NaOH.
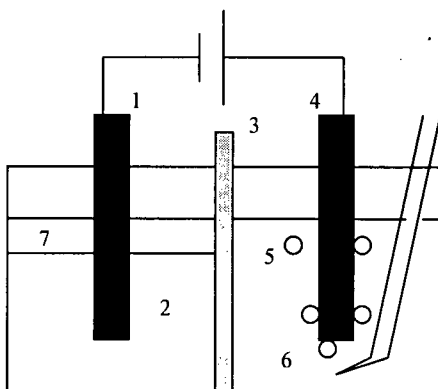
Figure 2.4: Hydrogen Electrolytic Synthesis of NaOH in Salt Melt 1) Cathode, 2) Catholyte, 3) Membrane, 4) Anode, 5) Anolyte, 6) Hydrogen sparger, 7) Molten sodium, (Modified from [Xu, J. *et al.*, (2004)]).

H_2 is supplied at the anode compartment where it oxidizes to protons, which then react with hydroxide and produce water. In the cathodic compartment, the molten sodium hydroxide medium is reduced to produce metallic sodium. Molten NaOH is present in both cell compartments, which are separated by a membrane. Since the cathode compartment has to be free of water, the membrane has to be impermeable to water and water vapor produced during the reaction, but permeable to alkali metal cations [Xu, J. *et al.*, (2004)]. Cation exchange ceramics, such as sodium beta alumina, are said to be appropriate membrane materials. The cathode material has to be inert at high temperatures for this reaction, such as nickel, copper and

stainless steel. The anode is a H_2 diffusion electrode with a high specific surface area, like nickel or supported noble metals. The reaction is carried at 300°C and above to maintain the anolyte and catholyte in the molten state. The sodium produced by electrolysis in the cathode compartment floats on top of the catholyte as a molten layer. It can be continuously or intermittently removed, while the molten NaOH feed can be continuously or intermittently supplied to the cell [Xu, J. *et al.*, (2004)]. Operating voltages ranging from 1.46 to 6 V are used to carry the electrochemical reaction [Xu, J. *et al.*, (2004)]. The cell voltage necessary to convert the alkali metal oxide to reduced metal is about 1.46 V at 350°C while the cell voltage needed to convert the alkali metal hydroxide to alkali metal in the absence of H_2 gas at the same temperature is of 2.44 V.

b) H_2 Assisted Molten Salt Electroreduction of Borate

The successes obtained in the sodium H_2 assisted electrolysis were transferred to the reduction of $NaBO_2$ for the production of $NaBH_4$. It has been shown that borates are more active in a molten hydroxide melt than in water. Therefore, it might be preferable to carry the H_2 assisted borate electrolysis in a molten hydroxide melt. The alkaline solvent provides stability and solubility for the borate reactants and borohydride products. It was demonstrated that $NaBH_4$ is stable in a mixed melt containing NaOH and KOH. At the eutectic point of NaOH and KOH, the melting point of the solids is below 190°C. At 200°C, $NaBH_4$ hydrolysis was minimal [Wu, Y. *et al.*, (2004a)]. The H_2 assisted electrochemical reaction, the H_2 used at the cathode and the electrolyte present in a molten state provides the H_2 required for forming $NaBO_2$, which would not readily be produced without H_2. While H_2 is passed in the cathode compartment, the borate is electrochemically reduced to borohydride, according to the same electrochemical reactions as for the indirect electrochemical reduction process, Eq. 2.47 to 2.49. Figure 2.5 represents a schematic diagram of electrolytic cell with H_2 at the anode and cathode for the synthesis of $NaBH_4$ from hydroxide melt containing $NaBO_2$ [Xu, J. *et al.*, (2004)].
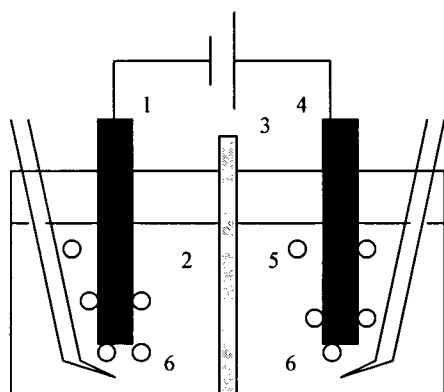
Figure 2.5: Hydrogen Electrolytic Synthesis of NaBH₄ in Salt Melt 1) Cathode, 2) Catholyte, 3) Membrane, 4) Anode, 5) Anolyte, 6) Hydrogen sparger (Modified from [Xu, J. *et al.*, (2004)]).

As shown in Fig. 2.5, H_2 is passed in the anodic and cathodic compartments from an outside source. The cathodic compartment contains alkali metal borate dissolved in a molten ionic salt and the anodic compartment contains a molten solution of sodium hydroxide with or without ionic salt dissolved in it. Water has to be removed from the system to avoid its electrolysis and the back-electrolysis reaction of borohydrides to borates. Carrying this process in a molten anolyte and catholyte which contains no water is the best way to ensure the cathodic compartment is free of water [Xu, J. *et al.*, (2004)]. The borohydride is formed in the cathodic compartment and water is formed in the anodic compartment. The electrolytic cell membrane's is only permeable to alkali metal ions and not permeable to other ions, water or water vapor. As for the sodium electrolysis process, a cation-exchange ceramic membrane made of sodium beta alumina is suitable. The reaction is carried at temperatures ranging from 100 to 500°C depending on the catholyte and anolyte melting points [Xu, J. *et al.*, (2004)]. Here again, the catholyte can be continuously or intermittently processed to remove the alkali metal borohydride produced. The residual alkali metal hydroxide is recycled to the anode, while the alkali metal borate is fed to the cathode compartment. The water vapor forming at the anode is carried away by the non-reacted H_2 leaving the anode chamber. Alternatively, an alkali metal oxide, such as sodium oxide, can be used to convert the remaining water vapors to NaOH, and prevent them from entering the cathode chamber [Xu, J. *et al.*, (2004)]. Theoretical calculations showed that from a 5 g of NaOH/NaBO₂ mixture containing 10 wt% NaBO₂, a current of 1000 mAh can generate 0.18 g of NaBH₄ at 100 % efficiency [Xu, J. *et al.*, (2004)]. This electrochemical

process has the potential of replacing the current $NaBH_4$ production method. However, in an industrial setting, the external H_2 needed in this process would most likely be obtained from natural gas reforming.

c) Aqueous Alkaline Borate Solutions

A H_2 assisted direct electroreduction process to produce borohydride from metaborate in alkaline aqueous solution was patented [Mikio, K., (2003)]. In this process, an aqueous alkaline solution of metaborate is electroreduced in an electrolytic cell, supplied with H_2 gas only in the anode compartment. The ion exchange membrane is an anion conductive diaphragm. The cathodic oxidation reaction is the same as Eq. 2.33, while the anodic reaction can be either the oxygen evolution reaction, Eq. 2.34, or the H_2 reduction reaction, Eq. 2.38. The gas, the electrolyte and the electrode then form a three-phase interface [Mikio, K., (2003)]. When the anode reaction is the H_2 reduction reaction, an anode material having a small H_2 overvoltage is desired and a gas diffusion electrode is preferable for the anode. Recommended anode materials with low H_2 overvoltage include palladium, platinum, ruthenium, osmium, iridium, rhodium, gold, cobalt, silver, nickel, tungsten, iron, copper, titanium and carbon. Among those, materials having also a high O_2 overvoltage, such as palladium, gold and silver, are preferable [Mikio, K., (2003)]. Cathode materials with a large H_2 overvoltage, such as tantalum, indium, zinc, lead or carbon, are recommended. On the other hand, when the anode reaction is the O_2 reduction reaction, it is recommended to use cathode materials with large H_2 overpotentials such as indium, zinc, lead, and carbon, and anode materials with small O_2 overpotentials, such as nickel, cobalt, platinum, and iron. With a gas diffusion anode, a tantalum cathode, an aqueous solution of $NaBO_2$ in 6 M NaOH as the catholyte and an aqueous solution of 6 M NaOH as the anolyte, BH_4^- was generated at 80 % current efficiency when a current of 1 V was imposed on the cell and supplying the anode with 2 MPa H_2 gas [Mikio, K., (2003)].

I) Methathesis

This electrosynthesis process for the preparation of borohydrides utilizes a methathetic reaction between a metal halide and a borohydride [Huff, G.F. et al., (1958)]. It is an electrochemical displacement

of one metal by another metal. The anode metal selected has to correspond to the metal of the desired borohydride. For example, when $NaBH_4$ is electrolysed using a magnesium anode and a mercury cathode in an ionizing non-aqueous solvent, the following reactions occur:

Anode: $Mg \rightarrow Mg^{2+} + 2e^-$ (Eq. 2.56)

Cathode: $Na^+ + e^- + Hg \rightarrow Na(Hg)$ (Eq. 2.57)

Overall: $Mg + 2Na^+ + Hg \rightarrow Mg^{2+} + 2Na(Hg)$ (Eq. 2.58)
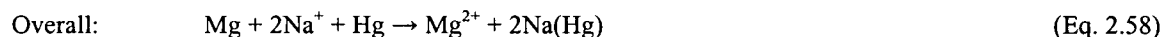
The sodium cations are replaced with magnesium cations and magnesium borohydride precipitates. Reaction yields of 98 % were obtained [Huff, G. F. *et al.*, (1958)].

J) Simulating Conventional Synthesis

The Florida Solar Energy Center, Hydrogen R&D Division at the University of Florida has a project targeting stationary H_2 generation systems based on $NaBH_4$ for NASA [Linkous, C. A., (2003-4)]. Their research is focused on the development of an electrochemical process, simulating the conventional Schlesinger and Brown synthesis in which $NaBH_4$ is formed from the reaction between alkali metal hydride and trimethoxyborate, $B(OCH_3)_3$. The following reactions have been postulated:

Anode $2H_2 \rightarrow 4H^+ + 4e^-$ (Eq. 2.59)

                $4H^+ + BO_2^- + 3CH_3O^- \rightarrow B(OCH_3)_3 + 2H_2O$ (Eq. 2.60)

Cathode $2H_2 + 4e^- \rightarrow 4H^-(s) B(OCH_3)_3 + 4H^-(s) \rightarrow BH_4^- + 3CH_3O^-$ (Eq. 2.61)

Overall $4H_2 + BO_2^- \rightarrow BH_4^- + 2H_2O$ (Eq. 2.62)
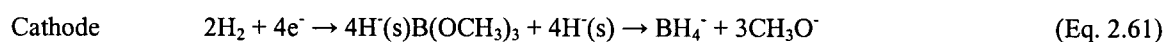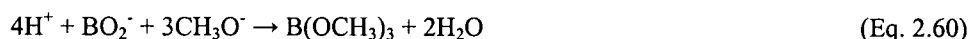
The anode reaction would consist of H_2 oxidation to form H^+, which would then be used to convert BO_2^- to trimethoxyborate. At the cathode, H_2 would be reduced to hydride ion (H^-), which then displaces the methoxide ion, generating BH_4^-. Noble metal catalysts active towards the electrooxidation of H_2, such as Pt and Pd, will be used to demonstrate the electrochemical hydriding of the trimethoxyborate intermediate

39

[Linkous, C. A., (2003-4)]. Preliminary experiments were conducted to identify proper electrode materials for the anodic and cathodic reactions, but no published papers regarding this work are available yet.

2.2.3 Infrastructure

According to the life cycles proposed by various research groups, [MERIT, Ltd., (1986), Levy, A. *et al.*, (1960), Jacques, S. *et al.*, (2004)], a scheme analogous to the current gasoline distribution infrastructure could be used to dispense $NaBH_4$ solution. The electrochemical regeneration of $NaBO_2$ to $NaBH_4$ would be carried out off-board. $NaBH_4$ fuelling infrastructure is depicted in Fig. 2.6.

Hydroelectric Power Plant or Nuclear Power Plant

$NaBH_4$ Fuelling Station

Spent fuel Spent fuel Spent fuel H_2 Fuel Cell Vehicles

Fresh fuel Fresh fuel Fresh fuel

Electrochemical Recycling
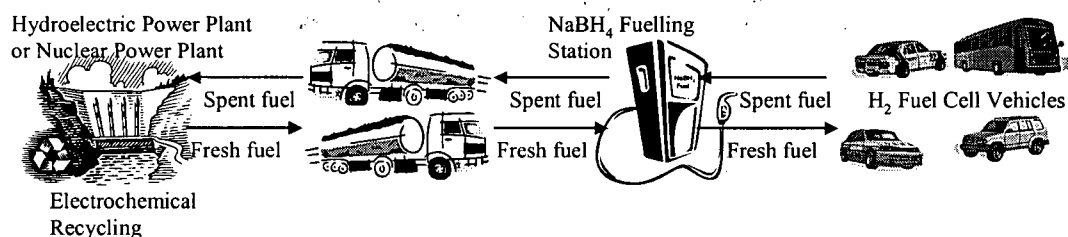
Figure 2.6: $NaBH_4$ Fuel Infrastructure Schematic Diagram (Modified from [MERIT, Ltd., (1986)]).

Once H_2 is produced, the $NaBO_2$ slurry must be removed from the vehicle while fresh $NaBH_4$ solution is added. Refuelling could be done within a few minutes. The recovered spent solution would then be transported to an industrial recycling facility for regeneration. Moreover, if an electrochemical regeneration process is used, it could be combined with load levelling operations with hydroelectric or nuclear power plants. Then, the electricity produced during off-peak electricity demand hours would be sufficient to supply the energy necessary to electrochemically regenerate $NaBH_4$. However, the energy required for the large-scale electrochemical regeneration of borohydride is difficult to evaluate with accuracy at this time [Jacques, S. *et al.*, (1970)]. The electricity provided could also come from other renewables such as wind, tide and solar energy sources.

2.3 NaBH₄ H₂ Generation and Storage System Efficiency

Among the currently known chemical hydrides, $NaBH_4$ seems to be the most suitable compound for H_2 storage as it releases more H_2 at lower reaction temperatures and has a higher H_2 density than other chemical hydrides. Even though $NaBH_4$ alkaline aqueous solutions have a lower gravimetric capacity then gasoline, when it is used to feed a PEMFC, it has the potential to exceed the volumetric capacity of gasoline used in an engine. As it will be seen in this Section, the H_2 storage efficiency of $NaBH_4$ renders it competitive for H_2 generation.

2.3.1 Gravimetric Capacity

The $NaBH_4$ hydrolysis reaction is very efficient on a weight basis. $NaBH_4$ has a theoretical H_2 content of 10.58 wt% based on the compound itself. Table 2.7 compares the theoretical H_2 content of various chemical hydrides.

Table 2.7: H_2 Content of Various Chemical Hydrides.

Name	Formula	Formula H_2 [wt%]
Sodium borohydride	$NaBH_4$	10.6
Lithium borohydride	$LiBH_4$	18.2
Lithium hydride	LiH	13
Magnesium hydride	MgH_2	7.6
Sodium Aluminum hydride	$NaAlH_4$	7.4

During the hydrolysis of this compound, water becomes another source of H_2. The extra water added has to be considered as a reactant and must be taken into account in the H_2 generation percentage. Out of the four moles of H_2 produced, half comes from $NaBH_4$ and half comes from H_2O [Amendola, S. C. *et al.*, 2000a)]. Thus, the hydrolysis using excess H_2O leads to superior storage capacity than the total amount of H_2 stored in the $NaBH_4$ itself [Jacques, S. *et al.*, (1970)]. If 1 mole of $NaBH_4$ (37.8g) produces 4 moles of H_2 (8.00g), a theoretical storage density of about 21.2 wt% H_2 based on the weight of $NaBH_4$ could be obtained. The theoretical specific gravimetric energy density of 30.55 kWh/kg was calculated in Appendix

A for 200 g of NaBH$_4$, assuming 4 moles of H$_2$ are generated per mole of NaBO$_2$. The gravimetric density has been reported for various NaBH$_4$ concentrations [Mohring, R. M. et al., (2003)]. The actual maximum H$_2$ storage capacity has been measured to be 6.7 wt% for a solution containing about 34.5 wt% NaBH$_4$ and 3.3 wt% NaOH at 25°C [Hua, D. et al., (2003)]. The DOE system gravimetric energy targets for 2010 and 2015 are of 6 wt% (2 kWh/kg) H$_2$ and 9 wt% (3 kWh/kg) H$_2$ respectively [Department of Energy, (2004)]. It appears that the NaBH$_4$ H$_2$ generation and storage system could reach 21.2 wt% and exceed the DOE FreedomCAR goals when water produced by the PEMFC is recycled back to the stored NaBH$_4$ slurry. However, this decreases to 12 wt% when calculated based on the resulting NaBO$_2$ [Davis, B. et al., (2005)]. If the by-product hydration level and the quantity of alkaline additive would be taken into account, it is very likely that the system storage gravimetric energy density would be too low to meet the DOE targets.

The balance of plant (BOP) also has a significant impact on the storage system capacity. For a 25 wt% NaBH$_4$ solution, the gravimetric storage density of the system drops of about 53 % when a BOP of 40 wt% is assumed [Mohring, R. M. et al., (2003)]. Similarly, assuming a storage system BOP taking up 20 % of the size of the tank, the volumetric storage density of a 25 wt% NaBH$_4$ solution decreases of about 16 %.

2.3.2 Volumetric Capacity

In theory, a litre of 30 wt% NaBH$_4$ solution yields about 67 g of H$_2$. Assuming the ideal gas law, this is equivalent to 744.5 L of H$_2$, which is an excellent system volumetric capacity. The volume of NaBH$_4$ solution of different concentrations required to store varying amounts of H$_2$ was reported [Mohring, R. M. et al., (2003)]. As the NaBH$_4$ solution concentration increases, more H$_2$ is stored in a given volume. When combined with a proton exchange membrane fuel cell (PEMFC, at 60 % efficiency), the NaBH$_4$ solutions have the potential to exceed the volumetric energy density of gasoline being burned in an internal combustion engine (ICE, at 30 % efficiency) [Davis, B. et al., (2005)]. Furthermore, it was calculated in Appendix A that the theoretical volumetric energy density contained in a 20 wt% NaBH$_4$ 0.2 M NaOH solution generating H$_2$ to feed a PEMFC is about 1.4 kWh/L of solution. This exceeds the energy density of a PEMFC feed with H$_2$ at 200 atm and 25°C, which is about 0.54 kWh/L of H$_2$. The DOE FreedomCAR system energy density targets are of 1.5 kWh/L (0.045 kg/L) for 2010 and of 2.7 kWh/L (0.081 kg/L) for

2015 [Department of Energy, (2004)]. It is important to note that these are system targets and that the material energy density must be greater in order to meet the system requirements.

Table 2.8 compares $NaBH_4$ volumetric storage ability with that of other borohydrides. The values are representing the volume (L) required to store 1 kg of H_2. The additional equipment required to contain the hydride and generate the H_2 was not taken into account in those volumetric calculations.

Table 2.8: Volume Required for the Storage of 1 kg of H_2 from Different Borohydrides.

Name	Formula	Volume to Store 1 kg H_2 [l]
Sodium borohydride (30 wt%)	$NaBH_4 + H_2O$	15
Sodium borohydride	$NaBH_4$	9.5
Lithium borohydride	$LiBH_4$	8.1
Aluminum borohydride	$Al(BH_4)_3$	11

The volumetric capacity of $NaBH_4$ is only slightly lower then some other hydrides, but it is still very competitive has it possessed other advantageous characteristics that other hydrides do not possess. Of the available hydrides, $NaBH_4$ has one of the lowest heat of reaction per mol of H_2 produced. It is stable compared to other hydrides so its hydrolysis is less violent and easier to control, while its handling is unproblematic. Furthermore, $NaBH_4$ has a simple structure and is relatively easy to use.

2.3.3 Fuel Comparison

Figure 2.7 gives a comparison of the theoretical volumetric and gravimetric energy densities of various fuels and H_2 carriers.
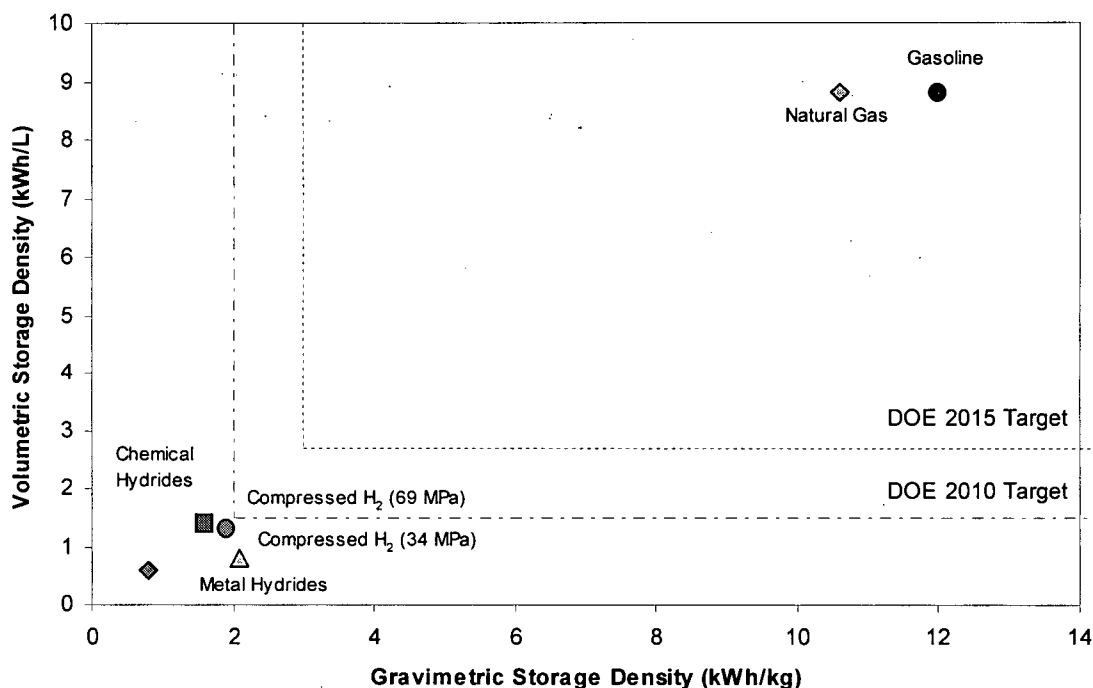
Figure 2.7: Comparison of the Gravimetric and Volumetric Energy Densities of Various Fuels and H_2 Carriers (Modified from [Chandra, D. et al., (2006)]).

The theoretical storage system gravimetric and volumetric energy densities are very different than the actual values and the weight and volume of the equipment needed to generate the H_2 has a significant impact on the storage system gravimetric and volumetric capacities. For example, a storage system with a volume of 2 L and a weight of 2 kg, holding 1 L of solution composed of 30 wt% $NaBH_4$, and 3 wt% NaOH, would have a storage efficiency of 3.35 wt% H_2 and a specific gravimetric energy density of 1.34 kWh/kg [Larminie, A. et al., (2003)]. Optimization of the solution composition and integration of the storage system water and heat utilisation is needed to maximize the actual system specific and volumetric energy densities. Hence, it is clear that significant improvements in actual storage efficiencies are still required to attain the DOE energy density targets.

2.4 Hydrolysis of NaBH₄ for H₂ Generation and Storage

A description of the non-volatile and non-flammable $NaBH_4$ solution hydrolysis reaction is provided in this Section. The overall performance of the $NaBH_4$ storage system is affected by numerous parameters,

including pH, catalyst material and catalyst loading, temperature, $NaBH_4$ concentration, electrolyte concentration, and steam. The individual impact of these parameters is reviewed separately in the following sections.

2.4.1 Hydrolysis

The chemical reaction of a hydride with water to produce H_2 gas is defined as hydrolysis. The hydrolysis of $NaBH_4$ at atmospheric pressure is described as follows.

$$NaBH_4\,(aq) + 4H_2O\,(l) \rightarrow 4H_2\,(g) + NaOH\,(aq) + H_3BO_3\,(aq) \qquad \text{(Eq. 2.63)}$$

$$NaOH\,(aq) + H_3BO_3\,(aq) \rightarrow NaBO_2.2H_2O\,(aq) \qquad \text{(Eq. 2.64)}$$

Overall: $\quad NaBH_4\,(aq) + 4H_2O\,(l) \rightarrow 4H_2\,(g) + NaBO_2.2H_2O\,(aq) \qquad \text{(Eq. 2.65)}$
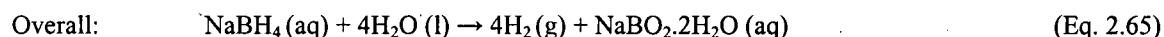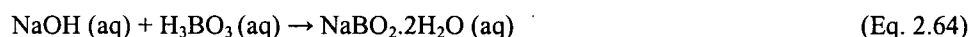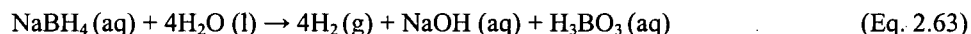
As per Eq. 2.63, the production of sodium hydroxide (NaOH) creates an increase in pH. In Eq. 2.64, boric acid (H_3BO_3), which is a weak electrolyte, reacts further to generate a hydrous metaborate salt, $NaBO_2.2H_2O$, which is the predominant species. As Eq. 2.64 is slower, the solution becomes increasingly alkaline as the overall reaction progresses [Schlesinger, H. I. et al., (1953)]. Since $NaBH_4$ exists as a complex ion in solution, the aqueous reactions are more realistic [Suda, S., (2003)].

In the early studies, the hydrolysis is reported to obey first order kinetics with respect to $NaBH_4$ concentration at a constant pH [(Brown, J. B., (1957), Levy, A. et al., (1960), Davis, R. E. et al., (1962)]] and to obey first order kinetics with respect to H^+ ion [(Brown, J. B., (1957), Davis, R. E. et al., (1962)]. In a buffered media, the hydrolysis followed pseudo-first order kinetics [Kaufman, C. M. et al., (1985)]. Pseudo-first order kinetic models are typically used to find second order reaction by dividing the effective first order constant by the concentration of the reactant in excess. More recently, it is reported that the hydrolysis reaction follows zero-order kinetics with respect to $NaBH_4$ concentration when using Ru or Ni based catalysts [Amendola, S. C. et al., (2000b), Hua D. et al., (2003), Pinto, A. M. F. R. et al., (2006)].

The $NaBH_4$ hydrolysis reactions are not easily reversible, yet, recyclability is a DOE H_2 storage system requirement. After hydrolysis, the recovered solution contains crystalline $NaBO_2$, and sodium hydroxide

(NaOH) dissolved in water. The NaBO₂ by-product is a basic hydrated solid, which looks like a paste. It possesses a low solubility limit. Hence, its formation inhibits the heat and mass transfer properties of the reaction medium, the H_2 generation reaction rate, and eventually results in clogging the hydrolysis reactor. Hence, the solubility limit of $NaBO_2$ constitutes an important challenge that needs to be addressed to optimize the H_2 storage and generation system.

The overall reaction is exothermic and liberates 75 kJ/mole of H_2 formed at 25°C [Amendola, S. C. *et al.*, (2000)]. The enthalpy of reaction, $\triangle H$, was reported to be about –218 kJ/mole [Larminie, J. *et al.*, (2003), Wee, J.-H., (2006)] at unknown conditions. Using data reported in the literature [Dean, J. A., (1999), Li, J. *et al.*, (2000)], at standard conditions, the enthalpy of formation of BO_2^- (aq) ($\triangle H^o$) and the Gibbs energy of formation of BO_2^- (aq) ($\triangle G^o$) were calculated to be -248.87 kJ/mole and -318.93 kJ/mole respectively. Hence, the reaction is very energetically favourable and no energy input is required to produce H_2. The hydrolysis of $NaBH_4$ liberates a determined amount of H_2 at ambient temperature and pressure with no side reactions or hazardous by-product. At ambient conditions and in alkaline media, the solution is stable. The H_2 generation rate is affected by many factors. As it is shown in Sections 2.2.2, 2.2.3, and 2.2.4, the hydrolysis of $NaBH_4$ can be accelerated by the addition of an acid, by a catalyst and by an increase in temperature.

2.4.2 Effect of pH

A) pH Equilibria of Borates

In aqueous solution, boron is in the negatively charged borate ion or un-dissociated boric acid form, depending on the concentration and pH of the solution. For example, the pH of borax solution increases with increasing concentration and decreases with increasing temperature [Kirk, R. E. *et al.*, (1992)]. Over the entire pH range, there are four borate compounds which can be formed in aqueous solution: boric acid, sodium pentaborate, sodium tetraborate, sodium metaborate. The addition of NaOH to a boric acid solution increases the pH and sodium pentaborate is formed. It has a comparably higher solubility than boric acid. At pH ranging from 7 to 10, sodium tetraborate, which has a lower solubility, is formed. At pH greater

then 10, sodium metaborate ($NaBO_2$), which has the lowest solubility, is formed. Thereby, it is the prevalent compound present in the highly alkaline solutions which are investigated in this study. However, traces of other polyborates, such as tetraborates and pentaborates, can also be present. The borate species generally stable in aqueous solutions are the othoboric acid ($B(OH)_3$), the monoborate ion ($B(OH)_4^-$), the triborate ion ($B_3O_3(OH)_4^-$) and the polyborate ion ($B_4O_5(OH)_4^{-2}$).

Boron compounds can exist in the form of mononuclear boric acid, a very weak acid, in water. In the free state, two boric acids exist: metaboric (HBO_2) and orthoboric ($B(OH)_3$). At specific conditions, both can be hydrated or dehydrated to form the other. For example, in a dilute aqueous solution, boric acid exists as orthoboric acid H_3BO_3 or $B(OH)_3$ at pH lower then 7. Thus, the metaboric acid is rapidly converted to orthoboric by hydration under acidic conditions [Jigong, L. *et al.*, (1999)]. Hence, depending on temperature, concentration and pH, boric acid weakly dissociates to form monoborates and polyborates in solution. For instance, boron occurs as a dissociated borate ion, $B(OH)_4^-$, at pH greater than 9 [Jigong, L. *et al.*, (1999)]. In aqueous solutions, boric acid reacts with strong bases and produce $B(OH)_4^-$ according to the following equilibrium reaction:

$$B(OH)_3 + NaOH \leftrightarrow B(OH)_4^- + Na^+ . \qquad \text{(Eq. 2.66)}$$

In concentrated solutions, boron condenses and polymeric ions are formed. The prevalent polyborate is the trimeric hydroxyborate [Jigong, L. *et al.*, (1999)]:

$$2B(OH)_3 + B(OH)_4^- \leftrightarrow B_3O_3(OH)_4^- + 3H_2O. \qquad \text{(Eq. 2.67)}$$

Numerous studies were carried to determine which ions are present in borate solutions, giving a sense of the system complexity. For example, the polyborates most likely to be found in concentrated solutions in the pH range from 7 to 9 were the focus of an entire study [Jigong, L. *et al.*, (1999)]. It has been reported that various alkali polyborate species are likely to be formed in concentrated alkali borate aqueous solutions [Momii, R. K., (1967), Hampton, D. S. Jr. *et al.*, (1972), Mesmer, R. E., (1972), Covington, A. K. *et al.*, (1973), Salentine, C. G., (1983), Botello, J. C. *et al.*, (2003)].

B) Effect of pH on the NaBH₄ Solution Stability

Acid, such as hydrochloric acid (HCl), can be added to decrease the pH and, thus, improve the $NaBH_4$ hydrolysis reaction rate. Generally, stronger acids produce greater H_2 generation. However, boric oxide, which is derived from a weak acid, was found to be as effective [Schlesinger, H. I. et al., (1953)]. For convenience, ideally, the acid accelerator should be able to be safely mixed and compressed with the solid $NaBH_4$ to form pellets. Also, it was determined that the H_2 generation rate depends on the pH and not on the type of acid added. Thus, it is possible to accelerate the hydrolysis by adding an acid and terminate it by adding a base, such as NaOH. It was noted that, since at stoichiometric water addition efficient wetting is difficult to obtain, excess water is required to maximize the contact between $NaBH_4$ and the acid solution. Otherwise, some $NaBH_4$ remains unreacted and the reaction yield remained low [Schlesinger, H. I. et al., (1953)].

It was established that the rate of hydrolysis of the BH_4^- ion at a specific pH within the 12 to 14 range is independent of the nature of cation present. At lower pH values, the rate of hydrolysis dependency on the buffer system used was uncertain. However, it was confirmed that the alkali stabilization effect results from the suppression of the hydrolysis equilibrium of $NaBH_4$ [Weiren, R. et al., (1998)]. The rate of hydrolysis of $NaBH_4$ solutions in water depends on the pH and temperature of the solution. The solution half-life ($t_{1/2}$) was found to empirically correspond to the following expression [Kreevoy, M. M. et al., (1979)]:

$$\log(t_{1/2}) = pH - (0.034T - 1.92),$$
(Eq. 2.68)

where $t_{1/2}$ is in minutes and the temperature, T, is in K. Hence, a high alkali concentration extends the $NaBH_4$ solution half-life at a given temperature. The stability of KBH_4 in alkaline solutions was previously investigated and compared to that reported for $NaBH_4$ [Brown, B. B., (1957)].

C) Effect of Electrolyte Concentration on the NaBH₄ Hydrolysis

As seen in the last Section, the pH, has a direct impact on the H_2 generation rate from the $NaBH_4$ hydrolysis. Decreasing the concentration of NaOH increased the H_2 generation rate when using a Ru-based catalyst [Amendola, S. C. et al., (2000a)]. As the OH^- ion strongly complex the water molecules, high NaOH concentrations reduced the activity of water. Low concentrations of NaOH lead to higher H_2 generation rates and leave more by-product in solution, which directly improves the H_2 storage system efficiency. However, in another study using a Pt-LiCoO₂ catalyst, it was found that the H_2 generation rate was independent of the NaOH concentration [Kojima Y. et al., (2004a)]. Contradictorily, the H_2 generation rate increased with higher NaOH concentration when using a Ni based catalysts [Hua, D. et al., (2003), Pinto, A. M. F. R. et al., (2006)]. Those dissimilar results were attributed to different reaction mechanisms involved depending on the catalyst used. It was stipulated that, with Ni based catalyst, the OH^- ions are involved in complex surface reactions. This effect compensated for the reduced water activity and lower by-product solubility at high NaOH concentrations. Whichever the catalyst is, one fact remains the same: as the reaction progresses, the quantity of NaBO₂ produced eventually exceeds its solubility limit in the alkaline aqueous solution, resulting in precipitation on the catalyst surface and prevention of further H_2 evolution [Hua, D. et al., (2003), Pinto, A. M. F. R. et al., (2006)].

To date, there seems to be no consensus on the optimum hydroxide concentration needed to carry out the catalytic hydrolysis reaction Eq. 2.65. A 0.01 M concentration of NaOH has been considered sufficient to prevent the NaBH₄ decomposition, but dilute enough to cause negligible NaBO₂ and NaBH₄ solubility changes [Stockmayer, W. H. et al., (1955)]. Even though small amounts of alkali are sufficient to obtain a stable NaBH₄ solution at room temperature, alkali concentrations ranging from 4 to 25 wt% (about 1 to 6 M) were used to study this H_2 storage and generation system. NaOH is predominantly chosen to stabilize the solution as it is more readily available and affordable than other hydroxides.

2.4.3 Effect of Catalysts

As acid reagents are not desirable, catalysts are preferred to control the hydrolysis reaction. They are required in smaller quantities then acid accelerators and are as effective. Also, they do not directly alter the pH of the solution. With catalysts, the reaction proceeds at a more constant rate until completion. As in the case of acid accelerators, excess water improves the H_2 yield. This is because the reaction by-product is hydrated. Various catalysts were proposed for accelerating the $NaBH_4$ hydrolysis. A summary table of the catalyst studied for the $NaBH_4$ hydrolysis since 2000 is presented in the literature [Wee, J.-H., (2006)]. Some of the most important catalysts are discussed in more details in this Section.

A) Noble Metal Catalysts

Although expensive materials, noble metals such as platinum (Pt) and ruthenium (Ru) are excellent catalysts for the $NaBH_4$ hydrolysis. To limit the amount of noble metal used and improve the effective surface area, the noble metal is typically mounted on a bead support. Some of the supported Pt and Ru catalysts are discussed in this Section.

a) Supported Platinum

Carbon supported platinum catalysts (Pt/C), synthesised by an impregnation method, were adopted to the hydrolysis of $NaBH_4$ solutions [Wu, C. *et al.*, (2004)]. By comparing different carbon supports, it was found that the specific area of the support did not affect the H_2 generation performance. Increased Pt loading enhanced the H_2 generation rates and efficiencies. Unfortunately, the temperature under which the experiments were conducted was not reported. Higher Pt utilization was obtained with small particle size and uniform particle size distributions. The catalyst active area and adsorbability was enhanced with large quantities of micropores. The Pt/C catalyst showed good H_2 generation rates and the H_2 generation efficiencies were near 100 % after 20 minutes [Wu, C. *et al.*, (2004)].

b) Supported Ruthenium

By the investigation of various metal salts, it was concluded that Ru and rhodium (Rh) salts rapidly liberate H_2 from $NaBH_4$ solutions. However, Ru is less expensive and responds faster than metallic Rh. In comparison, studies showed that Co and Pt catalysts only have a modest H_2 generation rate [Amendola, S. C. et al., (2000a)]. High surface area Ru, supported on anion exchange resin beads, was investigated. Ion exchange beads have high stability in strong alkaline solutions [Amendola, S. C. et al., (2000a)]. Anionic resins gave better results than cationic resins as catalyst support [Amendola, S. C. et al., (2000b)]. The volume of H_2 generated by Ru catalyzed $NaBH_4$ hydrolysis increased linearly with time. It was deduced that BH_4^- was adsorbed on the Ru catalyst surface. The activation energy for Ru catalyzed hydrolysis of $NaBH_4$ was calculated to be 47 kJ/mol [Kojima, Y. et al., (2002)]. This value compares favourably with other reported activation energies found for $NaBH_4$ hydrolysis catalyzed with other metals, which are summarized in Table 2.9.

Table 2.9: Comparison of Some Catalyst Activity (Modified from [Kaufman, C. M. et al., (1985), Amendola, S. C. et al., (2000a)].

Metal	Activation Energy [kJ/mol]
Ru	47
Co	75
Ni	71
Raney Ni	63

From a systematic study using different loadings of a Ru catalyst and varied reactant concentrations, it was determined that the hydrolysis was limited by the reaction at the catalyst surface [Richardson, B. S. et al., (2005)]. Also, using a Ru catalyst supported on ion exchange resin IRA 400, it was found that the H_2 generation curve was divided in four distinct stages [Xia, Z. T. et al., (2005)]. First, the activity of the catalyst increased and the H_2 generation is improved. Secondly, as the $NaBH_4$ concentration decreased, the H_2 generation went down. Thirdly, the catalyst particles were pulverized by the formation of $NaBO_2$. This increased the available catalyst surface and favoured the hydrolysis reaction. Finally, as the concentration of $NaBH_4$ decreased and that of $NaBO_2$ increased, the H_2 generation kept decreasing. Therefore, it seems

like $NaBO_2$ is beneficial for the catalyzed H_2 evolution. In addition, it was noted that Ru on alumina was unstable in aqueous alkaline $NaBH_4$ solution, but that Ru on metal titanium (Ti) was stable [Gervasio, D. *et al.*, (2005)].

B) Non-Precious Transition Metal Catalysts

Among different transition metal salts, it was determined that, on a qualitative basis, the best hydrolysis catalyst accelerators were Ni salts, and that, on a quantitative molar basis, Ni and Co salts had higher catalytic efficiencies than monoprotic salts [Kaufman, C. M. *et al.*, (1985)]. For example, after 10 minutes of reaction time at 21.4°C, 1 mol % of Ni generated 0.13 mol/dm^3 of $NaBH_4$ while 1 mol % of Co generated 0.11 mol/dm^3 of $NaBH_4$. Under the same conditions, 4 mol % of Ni generated 0.17 mol/dm^3 of $NaBH_4$ while 4 mol % of Co generated 0.14 mol/dm^3 of $NaBH_4$. Each of these salts is discussed separately. Other types of transition metal catalysts, including filamentary Ni mixed Co, metal hydrides and metal-metal oxides are also reviewed.

a) Cobalt Boride

Among the chloride salts of Mn, Fe, Co, Ni and Cu, Co, which were studied as catalysts for the hydrolysis of $NaBH_4$ solutions, Co resulted in the highest H_2 generation rate [Schlesinger, H. I. et al., (1953)]. All of these chloride metal salts promptly formed dark suspensions of boride precipitates. These precipitates had noticeable catalytic action, especially in the case of Co. It was deduced that the active catalyst was the precipitate formed, a cobalt boride, Co_2B [Schlesinger, H. I. *et al.*, (1953)]. This was confirmed by some researchers [Levy, A. *et al.*, (1960)] but contradicted by others, as the formation of metal borides in aqueous solution is not thermodynamically favourable [Kaufman, C. M. *et al.*, (1985)]. Differences were found in the mechanisms and rate of the reduction of various metal salts. It seems that the catalysis is partly caused by the generation of protons during the metal salt reduction. Hence, in the presence of metal salts, the hydrolysis would be catalyzed by the metal salt and by the acid generated at the same time [Kaufman, C. M. *et al.*, (1985)]. Although the chloride metal salt catalysts are active, the

dissolved metal ions tend to contaminate the aqueous spent $NaBO_2$ solution [Zhang, Q. *et al.*, (2006)]. In a recent study, it was determined that Co-B catalysts have an activity for the hydrolysis of $NaBH_4$ similar to that of Ru catalysts and that an increase in hydroxide ions concentration positively affected the activation of the Co-B catalyst [Jeong, S. U. *et al.*, (2005)].

b) Nickel Boride

Heat treated nickel boride catalyst, Ni_xB (x = 4, 5), is easily prepared and inexpensive compared to noble metal catalysts. It is highly stable and enhances the H_2 generation from $NaBH_4$ solutions. The heat treatment conditions were found to significantly affect the catalyst activity [Hua, D. *et al.*, (2003)]. The H_2 generation rate of the Ni_xB catalyzed hydrolysis of $NaBH_4$ in NaOH was compared with that of Ru/C catalyst. In the case of Ni_xB rate of hydrolysis increased with increasing NaOH concentration, whereas in the case of Ru/C, the rate of hydrolysis decreased with increasing NaOH concentration [Hua, D. *et al.*, (2003)].

Typically, it is assumed that the $NaBH_4$ hydrolysis takes place by the reaction of borohydride ions with protons dissociated from water and that, in alkaline solution, the slow self-hydrolysis is due to the reduction of proton concentration. According to this hypothesis, the hydroxide ions would inhibit the catalyzed BH_4^- hydrolysis and greater NaOH concentration would reduce water activity and lower the solubility of the by-product $NaBO_2$. Interestingly, this explanation, which is valid in the case of Ru/C, does not hold for the Ni_xB catalyzed $NaBH_4$ hydrolysis. The accelerating effect of higher NaOH concentration on the Ni_xB catalyzed $NaBH_4$ hydrolysis was attributed to the fact that this reaction follows a different surface mechanism than Ru/C [Hua, D. *et al.*, (2003)]. It was observed that, when using Ni_xB, water is stoichiometrically consumed and gives rise to an equivalent NaOH concentration during the hydrolysis. The hydrolysis accelerating effect caused by the rise of NaOH concentration observed with Ni_xB catalyst might be able to compensate for the H_2O concentration decrease and the accumulation of $NaBO_2$ over time. This would be very beneficial to the long term operational efficiency of the H_2 generation system. The activation energy using Ni_xB was calculated to be 38 kJ/mole in 10 wt% NaOH and 1.5 wt% $NaBH_4$, which is lower then the values reported for lower NaOH and greater $NaBH_4$ concentrations [Hua, D. *et al.*,

(2003)]. It is also quite low compared to the reported values for other metal catalysts listed in Table 2.6. This implies that it would require less energy to activate the NaBH$_4$ hydrolysis reaction with NixB catalysts. Interestingly, it was recently discovered that a Ni powder based catalyst exhibited enhanced hydrolysis activity after being recovered from previous use by washing, filtrating and drying [Pinto, A. M. F. R. et al., (2006)].

c) Filamentary Nickel Mixed Cobalt

The filamentary Ni mixed Co catalyzed hydrolysis of NaBH$_4$ had a short response time and maintained the maximum H$_2$ generation rates for extended time periods due to its large surface area. Filamentary Ni is easy to handle and is inexpensive. It was found that the hydrophilic properties of stylene-butadiene-rubber make it an effective catalyst binder. The cyclic properties of the Ni mixed Co catalyst on the hydrolysis of NaBH$_4$ in alkaline solution were also studied. The H$_2$ generation decreased overtime as a film was formed on the catalyst surface. About 76 % of the initial H$_2$ generation remained after 200 cycles [Kim, J.-H. et al., (2004b)]. It is suspected that the precipitation of NaBO$_2$ deteriorated the catalyst. With cycling, the hydrated NaBO$_2$ stacked upon the pasted catalyst and the catalyst surface oxidizes and eventually degrades. In addition, the catalyst agglomerated over cycling and its surface area decreased [Kim, J.-H. et al., (2004b)].

d) Metal Hydrides

In general, metal hydrides catalysts result in inferior hydrogenation rates due to their mediocre kinetic properties. However, it was found that it is not the case for Mg$_2$Ni, a high-temperature hydriding alloy, as the hydride phase of Mg$_2$Ni is different from that of other metal hydrides. The hydride phase gradually forms from the surface towards the center of the particle [Suda, S. et al., (2001)]. A fluorination treatment, called the F-treatment, was investigated. It removes oxides to form fluoride and create hydride layers at the surface of the granular particles. The fluoride layer exhibits high affinity to proton uptakes. The F-treatment generates larger specific area then untreated particles. The hydride layer acted as the active site

for hydrolysis [Suda, S. *et al.*, (2001)]. The kinetics of various fluorinated catalysts was compared. The experiments showed that the catalytic hydrolysis of F-treated Mg_2Ni and F-treated Mg_2NiH_4 was superior to that of the untreated catalysts in both cases.

e) Metal-Metal Oxide

Compared to other metals and metal oxides, $Pt-LiCoO_2$ was found to be a good catalyst for the hydrolysis of $NaBH_4$ solutions. The supercritical CO_2 method generated superior catalysts then the conventional impregnation method [Kojima, Y. *et al.*, (2002)]. The catalyst activity increased with the surface area of the Pt metal. The H_2 generation rate of $Pt-LiCoO_2$ increased with time, while that of a reaction with a Ru catalyst remained constant [Kojima, Y. *et al.*, (2002)]. $Pt-LiCoO_2$ produced 100 % of the theoretical amount of H_2 using excess water [Kojima, Y. *et al.*, (2004a)]. Nanosized $Pt-LiCoO_2$ also resulted in a superior catalytic activity than a mixture of Pt and $LiCoO_2$ when applied to the hydrolysis of $LiBH_4$ [Kojima, Y. *et al.*, (2006)]. Furthermore, when using a $PtRu-LiCoO_2$ supported catalyst, instead of $Pt-LiCoO_2$ or $Ru-LiCoO_2$, the catalyst efficiency was doubled for concentration of $NaBH_4$ up to 10 wt% [Krishnan, P. *et al.*, (2005)].

C) Organic Catalysts

Organic pigments consisting of carbon and other non-metals were found to be effective catalysts to control the rate of H_2 evolution from $NaBH_4$ [Linkous, C. A. *et al.*, (2003-4)]. These compounds have been used as photocatalysts for water decomposition. The organic pigments investigated were fused hetero-aromatics, which possess distinctive molecular and electronic structures. Their structure is constituted of extended fused aromatic system with one or more hetero-atoms affiliated with the pi-electron cloud [Linkous, C. A. *et al.*, (2003-4)]. The hetero-atoms lower the energy of the first excited state energy level, making it predisposed to reduction. The H_2 generation from $NaBH_4$ solutions of the various pigments was evaluated using buffered $NaBH_4$ solutions. Constant pigment catalyst loadings, 100 mg, were compared with an equivalent weight of cobalt powder. Pyranthrenedione, indanthrene Gold Orange and perylene

dime pigments were as good or better catalysts than the conventional cobalt powder. Pyranthrenedione increased the rate of H_2 generation from buffered $NaBH_4$ solutions 6.5 times more then that without catalyst.

D) Catalyst Comparison

Different researchers used diverse solute concentrations to perform their experiment. Missing information regarding the experimental conditions, such as catalyst loading used, temperature, volume of solution, makes an overall catalyst comparison difficult based on the currently available data. Nevertheless, Table 2.10 attempts to compare the various catalysts reviewed in this section.

Noble metals (Pt, Ru) are among the suitable catalysts, but other less expensive materials, such as Ni, are effective [Linkous, C. A. *et al.*, (2003-4)]. Fabrication, treatment and ease of handling should be considered as they impact on the catalyst cost. Since the hydrolysis reaction rate is limited by catalyst surface area, more research needs to be done to enhance the catalyst specific surface area and optimize the catalyst loadings. Lower catalyst loadings would reduce the system cost. The effect of NaOH concentration on the NixB catalyst activity should be further examined. Research on catalyst durability has been limited. The catalysts long-term degradation behaviour due to by-product coating has to be studied in more detail. In addition, the catalyst performance at elevated pressures and temperatures, its chemical stability in hot caustic environment and its mechanical resistance to the formation of the bulky $NaBO_2$ hydrated molecules needs further investigation.

Table 2.10: Catalysts for NaBH$_4$ Hydrolysis.

Catalyst	Chemical Formula	Catalyst/Support (Amount [g], Loading [wt%])	H$_2$ generated after 5 min [l]	T [°C]	Composition [wt% NaBH$_4$, wt% NaOH]	Reference
Supported Platinum	Pt/C	0.1 g - 5 wt%	2	-	10, 5	[Wu, C. et al., (2004)]
Supported Ruthenium	Ru/C	0.5 g - 2 wt%	0.5	-	20, 1	[Richardson, B. S. et al., (2005)]
	Ru/IRA 400	0.02 g - 5 wt%	0.0075	25	10, 10	[Xia, Z. T. et al., (2005)]
Cobalt Boride	CoB	0.05 g	1.6	25	20,10	[Jeong, S.U. et al., (2005)]
Nickel Boride	NixB	0.1 g	0.1	30	1.5, 10	[Hua, D. et al., (2003)]
Filamentary Ni mixed Co	Ni-Co	1 g - 20 wt%	0.425	30	10, 0.01 M KOH	[Kim, J.-H. et al., (2004a)]
Metal-Metal Oxide	Pt-LiCoO$_2$	0.239 g, 10 wt%	0.1	25	5, 5	[Krishnan, P. et al., (2005)]
	PtRu-LiCoO$_2$	0.125 g, 10 wt%	0.25	25	5, 5	
Fluorinated Metal Hydrides	F-Mg$_2$NiH$_4$	1.91 m^2/g surface area	0.83	-	50 g/L NaBH$_4$, 10	[Suda, S. et al., (2001)]
Organic	Pyranthrenedione	0.1 g	0.055	-	pH buffer at 11	[Linkous, C. A. et al., (2003-4)]

2.4.4 Effect of Temperature

To maximize the H_2 storage system energy density, it is important to minimize the size of the H_2 storage tank needed to instantaneously deliver H_2 to the fuel cell and the reactor start-up speed is directly affected by the hydrolysis temperature rise [Zhang, Q. et al., (2006)]. The temperature at which the hydrolysis is carried has a direct impact on the H_2 generation rate. The H_2 generation rate increases dramatically with temperature [Amendola, S. C. *et al.*, (2000a), Pinto, A. M. F. R., *et al.*, (2006)]. This is partly due to the increase in self-hydrolysis at high temperatures. Thus, from a reaction kinetics point of view, it is favourable to run the hydrolysis reactor at high temperatures. However, as explained in Section 2.3.2 B), high temperatures have a negative impact on the $NaBH_4$ solution stability. When the vehicle is shutdown the $NaBH_4$ solution will gradually cool down, but some self-hydrolysis will occur. Hence, a storage tank will be needed to store the small quantity of H_2 produced during the system shutdown.

Since the hydrolysis of $NaBH_4$ is exothermic, no preheating is needed and no heat sources are necessary to sustain the hydrolysis reaction. Thus, the hydrolysis reactors can be operated auto-thermally [Zhang, Q. *et al.*, (2006)]. For a peak H_2 generation rate of 2.5 g/s, derived for a vehicle with 68 kW net power and 24 % overall efficiency, the storage system must be designed to reject about 93 kW of heat. To maximize the cooling efficiency, it would be preferable to have a high reaction temperature to allow for a greater difference between ambient and rejection temperatures. Thus, for cooling efficiency purposes, it would be beneficial to carry the hydrolysis with steam rather than liquid H_2O, as it will be discussed in Section 2.4.6. However, the H_2 may require cooling as the PEMFC have a limit on the allowable reactant inlet temperature, typically about 80°C. Cooling the H_2 before delivery to the fuel cell has the added benefit of increasing the relative humidity of the H_2. The excess water provided for the hydrolysis cools the system and slows the reaction. If the reaction occurs too rapidly, the reaction vessel can become very warm due to the large amount of heat generated.

2.4.5 NaBH$_4$ Concentration

The range of a FCV depends on the amount of H$_2$ stored on-board and for a NaBH$_4$ H$_2$ storage system, the range is determined by the initial mass fraction of NaBH$_4$ in the solution. The NaBH$_4$ solution concentration and the mass of the solution carried on-board would then fix the FCV range. Another key design consideration for a FCV is weight which is directly affected by the NaBH$_4$ storage system mass. Increasing the initial mass fraction of NaBH$_4$ will increase the mass of the solution, assuming that no fuel cell produced water is available for reuse in the hydrolysis of NaBH$_4$. If the fuel cell produced water was reused, the mass of the storage system would be lower as less water would initially need to be stored on board. Thus, to minimize the mass of H$_2$O to be carried on board, the initial concentration of NaBH$_4$ in the solution should be as large as practical. However, increasing the mass fraction of NaBH$_4$ can have a negative impact on the H$_2$ generation rate.

Low concentrations of NaBH$_4$ typically result in greater H$_2$ generation rates [Amendola, S. C. *et al.*, (2000a), Pinto, A. M. F. R. *et al.*, (2006)]. At 25°C and using a Ru catalyst, the H$_2$ generation rate was maximized in the range of 5-15 wt% NaBH$_4$ [Amendola, S. C. *et al.*, (2000a)]. This is partly because at low NaBH$_4$ concentration, the low solution viscosity reduces the mass transport losses and allows more NaBH$_4$ and water to contact the catalyst surface. Another reason is that at high NaBH$_4$ concentrations, while the reaction proceeds, the NaBO$_2$ by-product will eventually exceeds its solubility limit, precipitates on the catalyst surface and slow down the hydrolysis reaction [Amendola, S. C. *et al*, (2000a), Pinto, A. M. F. R. *et al.*, (2006)]. It was reported that hydrolysis reactors were susceptible to clogging at NaBH$_4$ concentrations above 25 wt% [Richardson, B. S. *et al.*, (2005)]. Hence, decreasing the mass fraction of NaBH$_4$ positively impacts the H$_2$ generation rate. High initial H$_2$ generation rates are crucial to quickly respond to the H$_2$ demand for FCV acceleration.

2.4.6 Steam Hydrolysis of NaBH$_4$

Instead of using liquid water or water vapour at ambient temperature, H$_2$ could be produced by hydrolysis with steam at high temperature. At these conditions, no acid addition or catalysts are necessary,

but excess steam is preferable to improve the reaction yield [Aiello, R. *et al.*, (1999)]. It was found that the yield depended strongly on temperature and, to a lesser extent, on the steam flow rate. At 110°C, close to 100 % of the theoretical yield was obtained for the hydrolysis of $NaBH_4$. Interestingly, the highest H_2 yields were obtained at the lowest temperature. At higher temperatures, the hydrated borate by-product released its hydration water and formed a solid layer on the unreacted hydride, inhibiting the reaction rate [Aiello, R., *et al.* (1999)]. The fastest rate of H_2 generation from 1 g $NaBH_4$ was obtained at 110°C and a flow rate of 0.1 ml steam/min. However, only 88 % of the theoretical yield was reached. On the other hand, the hydrolysis of 1 g $NaBH_4$ at 110°C and 0.035 ml steam/min took place at a slower rate but a yield of 99 % was reached. The differences in the rates of H_2 generation were attributed to mass transfer constraints [Aiello, R., *et al.* (1999)]. It was estimated that the exothermic hydrolysis reaction could provide the heat of vaporization necessary for steam generation, but a heat source would be required to start the reaction. It was proposed to use the excess heat to generate additional H_2 from the endothermic dehydrogenation of a metal hydride.

2.5 NaBH₄ Applications

2.5.1 NaBH₄ Hydrolysis Reactors

The main engineering component for the $NaBH_4$ H_2 generator use in combination with a PEMFC (B-PEMFC) system is a hydrolysis reactor. Generators using these solutions can take several forms. Some ionic hydrides generators were previously designed to generate H_2 for a large range of applications, while various small-scale reactors were developed for laboratory chemical hydride testing purposes. A selected variety of these reactors is reviewed in this Section.

A) Kipp Generator

The Kipp generator basically consists of a column of hydride inverted in water as shown in Fig. 2.8. Water enters the bottom of the column and reacts with the hydride. The H_2 generated during the reaction

rises to the top of the column, where it is removed through a control valve. The pressure exerted by the H_2 over the water column controls the reaction rate [Linden, D., (1984)].
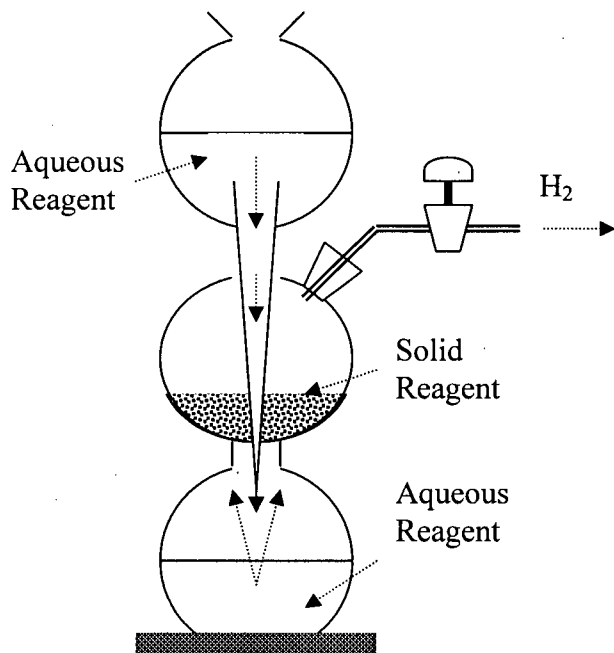
Figure 2.8: Schematic Diagram of a Kipp Generator (Modified from [Mattson, B., (2005)]).

It was shown that the Kipp generator concept can be adapted to the catalyzed hydrolysis of $NaBH_4$ solution [Amendola, S. C. et al., (2000a)]. In that case, the column contained a catalyst. The $NaBH_4$ solution, pushed by differential pressure, enters the column bottom where it reacts with the catalyst. H_2 is delivered to the fuel cell as needed. When no H_2 is required, the pressure builds up in the generator, forcing the solution away from the catalyst, ending the reaction. Only simple controls are required to ensure safe operation of this low cost and compact reactor. However, in order to keep control over the reaction, the column must remain in the upright position [Linden, D., (1984)]. Otherwise, a small pump has to be added to meter the $NaBH_4$ solution flowing to the tubular catalyst bed and make the reactor functionality independent of its orientation [Amendola, S. C. et al., (2000a)]. This reactor design exhibits a very rapid response to the fuel cell H_2 demand.

B) Remote Fuel-Cell Power Source

The US Army Mobility Equipment Research and Development Command developed a high energy density, refuelable metal hydride fuel-cell system for remote, equipment operating at the 1 to 50 W level for long periods of unattended operation [Linden, D., (1984)]. No auxiliary equipment is required. Figure 2.9 represents a schematic diagram of the generator.
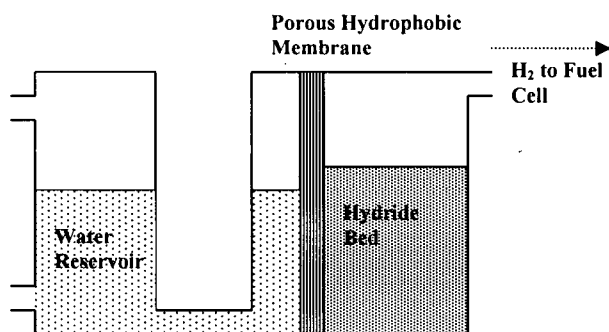
Figure 2.9: Schematic of Remote Hydride System (Modified from [Linden, D., (1984)]).

In this system, the water flows from the reservoir to the water chamber adjacent to a porous hydrophobic membrane. The water vapour diffuses through the membrane, and reacts with the hydride to release H_2. The H_2 flows out of the chamber and feeds a fuel cell [Linden, D., (1984)]. At no load, no H_2 is consumed. The pressure in the reaction chamber builds-up and the water is forced out of the chamber and to the reservoir, which hinders the generation of H_2. As H_2 is consumed from the fuel cell, the water level will self-adjust and H_2 will be produced as required [Linden, D., (1984)].

C) Solid Hydride and Liquid Water or Water Vapour

In the solid hydride and liquid water laboratory test scale reactor, the hydride is contained in a cylindrical basket made of fine nickel mesh. A schematic diagram of the liquid water reactor is shown in Figure 2.10 (a). Water is feed from the reactor bottom using a syringe. The reactor is simply a thick wall bottle sealed with a cap which is fixed with a clamp. The water flows up through the basket, where it contacts the

hydride. The H_2 produced flows out to a water trap collector and measuring system [Kong, V. C. Y. *et al.*, (1999)].
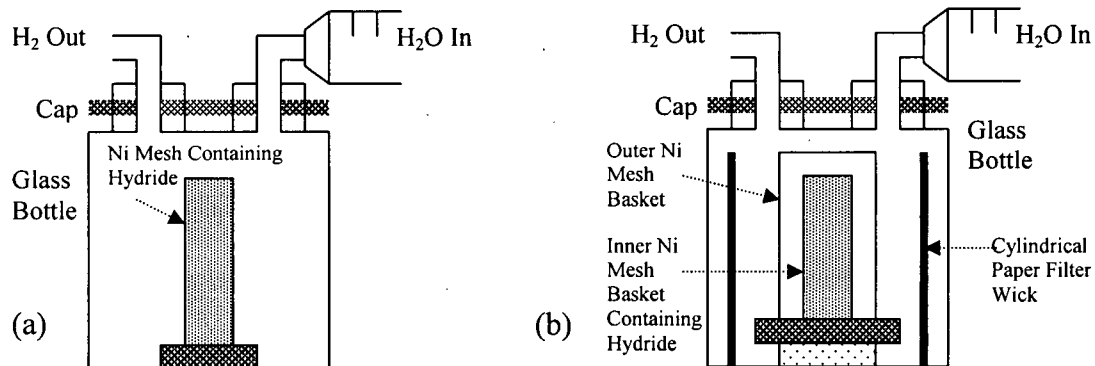
Figure 2.10: Schematic of Hydride Reactor (a) with Liquid Water, (b) with Water Vapor (Modified from [Kong, V. C. Y. *et al.*, (1999)]).

A solid hydride and water vapour reactor can be seen in Figure 2.10 (b), this experimental reactor is very similar to the solid hydride and liquid water reactor described above, except that, for reaction with vapour, the hydride basket is elevated on a platform to ensure liquid water does not directly contact the hydride. Excess water is added to the reactor bottom. Also, an additional mesh cylinder is added around the inner cylinder to contain the hydroxide reaction product, which passes through the inner mesh basket [Kong, V. C. Y. *et al.*, (1999)]. Wetted water filter can be placed around the inside wall of the bottle to act as a wick in order to facilitate water evaporation. Like in the previous reactor, the H_2 produced is collected and measured in a water trap.

D) Solid Hydride and Steam

The hydrolysis reaction with steam requires a more complex reactor design with additional control in place as shown in Figure 2.11.
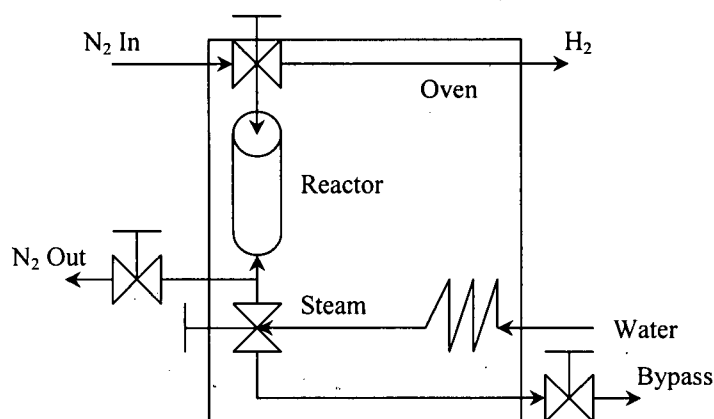
Figure 2.11: Schematic of Steam Hydrolysis Reactor System (Modified from [Linden, D., (1984)]).

A programmable syringe pump feeds a steady rate of water to the reactor. To achieve nearly isothermal operation, the reaction system needs to be enclosed in a mechanical convection oven. The solid hydride is added on a mesh, covered with glass wool, fitted to the bottom of the reactor. To ensure that no steam contacts the hydride prior to reaction, the reactor needs to be purged with nitrogen while the oven and the water are heated. The water from the preheating coil bypasses the reactor until constant steam production was obtained. The N_2 purge is stopped when the steam reaches the desired temperature. Then the syringe pump is reset and restarted to deliver the water rate needed. Finally, the reaction bypass valve is opened to allow steam to enter the reactor and contact the hydride [Linden, D., (1984)].

E) Catalytic Reactors

The catalytic hydrolysis reactors are all based on the same fundamental principle: the solution is brought in contact with a suitable catalyst to release H_2 and the H_2 generation stops when the solution is removed from the catalyst. The catalyst can be either dipped in the $NaBH_4$ solution or the $NaBH_4$ solution can be injected on the catalyst. An example of a catalytic reactor where the $NaBH_4$ solution is pumped to the hydrolysis reactor is shown in Figure 2.12.
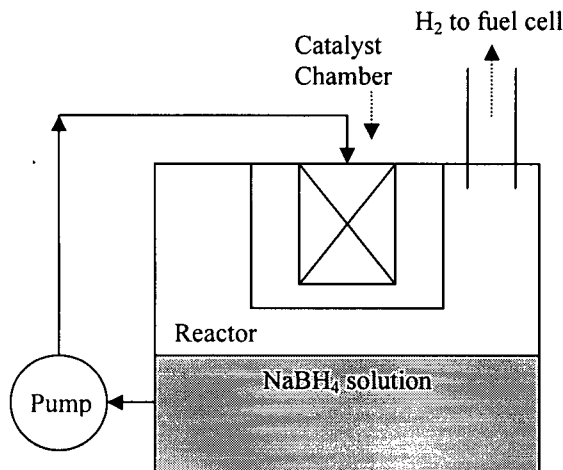
Figure 2.12: Reactor for Releasing H_2 from an Alkaline Aqueous Solution of $NaBH_4$ (Modified from [Larminie, J. *et al.*, (2003)]).

The rate of the H_2 generation is controlled via the stabilized aqueous $NaBH_4$ solution pumping rate. The pump motor is switched on/off by a controller, which senses the H_2 pressure. The solution flows through the reactor so that the catalyst is continuously in contact with fresh solution [Larminie, J. *et al.*, (2003)].

A similar strategy developed by NASA is to add solid $NaBH_4$ tablets to an alkaline aqueous solution. As shown in Figure 2.13, the catalyst's surface is exposed to the solution to accelerate the reaction as required [Linkous, C. A. *et al.*, (2004)].
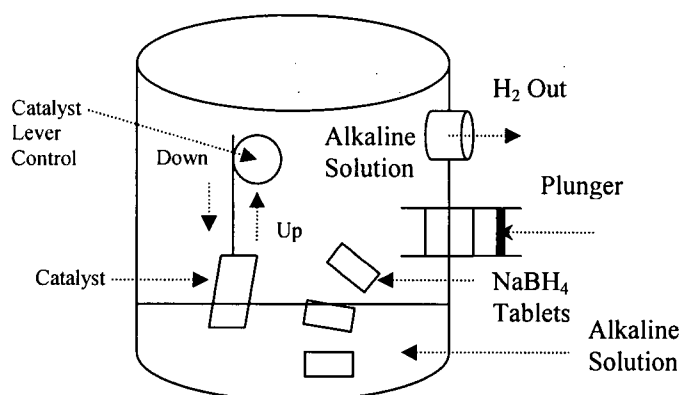
Figure 2.13: Schematic of a H_2 Generation Vessel with Catalytic Control of Evolution Rate (Modified from [Linkous, C. A. *et al.*, (2004)]).

A 10 kW scale H_2 generator composed of a storage tank for $NaBH_4$ solution, a pump, a by-product storage tank, a separator and a hydride reactor which contained a honeycomb monolith coated with catalyst

has been built and tested [Kojima, Y. *et al.*, (2004b)]. A controlled hydride solution rate was pumped to the bottom of the reactor and flowed upward through the channel. When contacting the honeycomb monolith, the solution generated H_2 gas and $NaBO_2$ and the temperature increased. The H_2 gas and the $NaBO_2$ solution were separated by a separator, which also acted as a small storage buffer for H_2 gas [Kojima, Y. *et al.*, (2004b)].

2.4.2 B-PEMFC Systems

To date, the B-PEMFC system has been evaluated by few researchers, and the integrated system performance and technical feasibility has been scarcely documented. Possible B-PEMFC applications include portable fuel cells, fuel cell Uninterrupted Power Supply (FCUPS) and emergency power sources [Mohring, R. M. *et al.*, (2003)], whereas the present study focuses on automotive related applications.

A) Hydrogen on Demand™

Hydrogen on Demand™ (HOD) is a proprietary B-PEMFC system developed by Millennium Cell Inc. which relies on the catalytic hydrolysis of $NaBH_4$. It can supply H_2 pure enough to feed directly the PEMFC without the need for purification, compression or liquefaction. A schematic diagram of the system is provided in Figure 2.14. In this system, heat and water management are of great importance. The H_2 generation and storage system comprises two storage tanks for $NaBH_4$ and $NaBO_2$ respectively, a pump, a catalyst chamber reactor, a liquid/gas separator, and a heat exchanger. The $NaBH_4$ aqueous alkaline solution is kept in a light plastic tank at ambient conditions. The release of H_2 from the $NaBH_4$ solution occurs by pumping the fluid mixture through a tubular reactor containing a proprietary catalyst. The heat supplied by the exothermic reaction partially humidifies the H_2 gas by evaporating water, which is beneficial to the PEMFC membrane. The H_2 produced contains less than 0.5 ppm of CO, and no NO_x or SO_x [Mohring, R. M. *et al.*, (2003)].
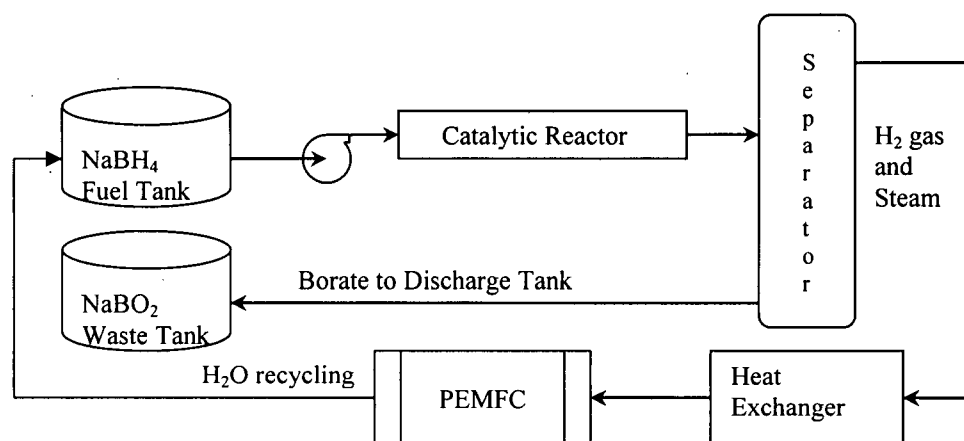
Figure 2.14: Schematic Diagram of the Hydrogen on Demand™ System (Modified from [Mohring, R. M. *et al.*, (2003)]).

The H_2 is cooled down in a heat exchanger before being directly fed to a PEMFC or to a H_2 internal combustion engine. The rate of H_2 generation is controlled by pumping a desired amount of $NaBH_4$ solution in the catalyst reaction chamber. Stopping the flow of $NaBH_4$ solution to the catalyst chamber brings the H_2 production to an end. Water generated from the PEMFC can be recycled back to the solution storage tank. The Hydrogen on Demand™ system is claimed to have a volumetric storage of about 63 g H_2/L using a 30 wt% $NaBH_4$ solution. This value is comparable and equivalent to 71 g H_2/L for liquid H_2 and about 39 g H_2/L for H_2 gas pressurized at 68.93 MPa [Mohring, R. M. *et al.*, (2003)].

2.4.3 Vehicle Prototype

There exist opportunities for the integration of a $NaBH_4$ storage system in a FCV that are unachievable with either liquid or pressurized H_2 storage systems. Among other things, the $NaBH_4$ solution tank geometry is flexible, the H_2 pressure and flow rate can be easily regulated by feedback control, and refuelling with fresh $NaBH_4$ solution is rapid, simple and can be done at any time. The $NaBH_4$ H_2 generation system was evaluated with a fuel cell emulator (FCE) to test its performance under true vehicle operating conditions without the need of a real fuel cell [Mohring, R. M. *et al.*, (2003)]. It was found that the system was capable of responding to the H_2 demand for the application. A vehicle prototype taking advantage of the B-PEMFC technology was developed and is reviewed in this Section.

A) B-PEMFC Vehicle

In 2001, Daimler Chrysler built a Town and Country Natrium® minivan prototype which incorporated a H_2 storage system that produces H_2 from the hydrolysis of $NaBH_4$. The manufacturer claimed that the vehicle has a range of 500 km and can accelerate from 0 to 100 km/h in 16 seconds. As shown in Figure 2.15, Daimler-Chrysler's prototype vehicle power train fits under the vehicle floor and is very compact. It is significantly more space-efficient way than using compressed H_2 as the H_2 storage system and do not take room away from the passenger and storage compartments [Daimler Chrysler, (2002)]. The acceleration and power demands require a maximum H_2 flow rate of about 1000 slpm. The storage system is designed to produce sufficient H_2 to satisfy the real time demand from the $NaBH_4$ stored on-board. Millennium Cell Inc. developed the $NaBH_4$ catalyst system for the Daimler Chrysler Natrium® vehicle. The response curve of the vehicle's storage system was found to be closely identical to the response curve of a pressurized H_2 gas storage system.
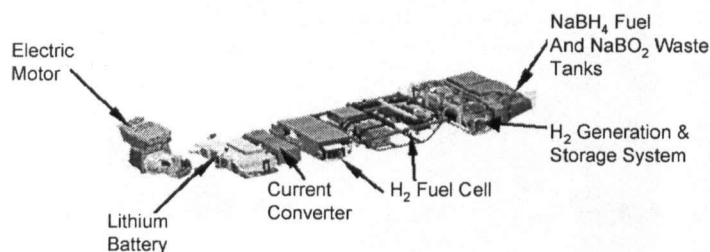
Figure 2.15: Daimler Chrysler Natrium Vehicle Power Train (Modified from [Wu, Y., (2003a)]).

CHAPTER III

PHYSICOCHEMICAL PROPERTIES OF NaBO₂

Although the thermodynamic properties of $NaBH_4$ and $NaBO_2$ have been investigated by a number of researchers through the years, the transport properties of $NaBO_2$ alkaline and non-alkaline aqueous solutions were not systematically determined. In this Chapter, the literature on the determination of the physicochemical properties of aqueous $NaBO_2$ solutions with and without alkali additive and on the characterization of the precipitates formed from those solutions is reviewed.

3.1 NaBO₂ Solution Characteristics

The alkaline waste solution (i.e. containing $NaBO_2$) solubility and physicochemical properties such as viscosity and conductivity, affect the H_2 generation and storage system as well as the electrochemical recyclability of the by-product. For this reason, it is important to determine and analyze the solubility and physicochemical transport properties of the borate ion in aqueous solutions (1:1 electrolyte). In this section, the relevant electrolyte theory, $NaBO_2$ solubility and physicochemical properties, as well as the expected effects of temperature and of organic additives on the solution properties are reviewed.

3.1.1 Solubility

A) NaBO₂ Solubility

No solubility studies were found specifically on the $NaBO_2$-H_2O-MOH system, where M represents Na, K or Li. The solubility of mixed alkali borate systems, including combinations of sodium pentaborates and diborate, ammonium pentaborate, tetraborate and diborate, and potassium pentaborate and diborate in water at 20, 30 and 40°C, was studied. It was found that the maximum solubility was controlled by the

mixture's pH [Roathnaum, H. P. *et al.*, (1936)]. The solubility of the binary salt-water $NaBO_2$-H_2O system was reported by Urusova and Valyashko at elevated temperatures up to 400°C [Urusova, M. A. *et al.*, (1993)]. The salt solubility continuously increased with temperature up to the melting point. The solubility of $NaBO_2$ was determined to be 61.9 wt% at 245°C and exceeded 67 wt% at 350°C. The most relevant solubility isotherms for the system under investigation are found in reviews of the ternary system of sodium oxide - boric oxide – water (Na_2O-B_2O_3-H_2O). This system was studied over the temperature range of 0 and 100°C [Blasdale, W. C. *et al.* (1938)]. Previous work was reviewed in an attempt to correct discrepancies reported in the early literature [Nies, N. P. *et al.*, (1967)]. Since the ensemble of the isotherms reported was not always homogeneous among the various publications, the entire system was once more re-investigated from -30 to 100°C [Kocher, J. *et al.*, (1970)]. It was suspected that the ternary system solubility values determined so far were inflated due to the presence of silica and carbonate, which increase the apparent solubility [Mellor, J. W., (1980)].

Based on those studies, there exist three known $NaBO_2$ hydrates: a tetrahydrate (1:1:8, $Na_2O.B_2O_3.8H_2O$, $NaBO_2.4H_2O$), a dihydrate (1:1:4, $Na_2O.B_2O_3.4H_2O$, $NaO_2.2H_2O$) and hemihydrate (1:1:1, $Na_2O.B_2O_3.H_2O$, $NaBO_2.0.5H_2O$). The transition temperature to the dihydrate occurs around 54°C, while the transition temperature to the hemihydrate is around 105°C [Blasdale, W. C., *et al.* (1938), Nies, N. P. *et al.*, (1967)]. Hence, at 25°C, the stable hydrate is $NaBO_2.4H_2O$ in saturated aqueous solutions. This was also confirmed in a crystallographic study of the $NaBO_2$-H_2O system [Menzel, H. *et al.*, (1943)]. The solubility of saturated $NaBO_2$ in water at 25°C was reported at around 22 wt% in terms of anhydrous solids [Blasdale, W. C., *et al.* (1938), Nies, N. P. *et al.*, (1967)]. It was visually determined that in water at 25°C, the solubility of $NaBO_2$ is 28g/100g of water, while that of $NaBH_4$ is about 52 to 55g/100g of water [Kojima, Y., *et al.*, (2002), Kojima, Y. *et al.*, (2004b)]. For comparison, those values were converted to weight percentages by calculating the amount of solute per 100 g of saturated solution. These values are equivalent to about 22 wt% and 36 wt% respectively. The solubility of $NaBO_2$ was measured at various NaOH wt% in water at 25°C [Amendola, S. C. *et al.*, (2000a)]. It was observed that the solubility of $NaBO_2$ decreased as the NaOH content increased, but no values were reported. The solubility of $NaBO_2$ in a 10 wt% NaOH solution was reported as 2.16 mol/l (14.2 wt%) at 25°C [Suda, S., (2003)] while the solubility of $NaBH_4$ in the same solution was reported to be 550 g/l (55 wt%) at 25°C [Suda, S. *et al.*,

(2001)]. To keep $NaBO_2$ in solution, the maximum composition of $NaBH_4$ has to be less than 16g/100 g of water (13.8 wt%) at 25°C [Kojima, Y. *et al.*, (2002)] or 26 wt% at 60°C [Kojima, Y. *et al.*, (2004b)]. Even if there is limited information on the solubility of aqueous alkaline $NaBO_2$ available in the literature, the published solubility data compiled is sufficient to undertake a comparative study and form the basis to carry out further experiments.

B) NaBH₄ Solubility

As previously explained, when no alkali stabilizers are present in an oversaturated $NaBH_4$ aqueous solution, the dissolved $NaBH_4$ will react with water at a certain reaction rate and this will trigger $NaBH_4$ dissolution. No data was found to compare the $NaBH_4$ rate of dissolution to its hydrolysis rate. However, it might be possible to measure the total boron content of the solution, i.e. that of $NaBH_4$ and the $NaBO_2$ resulting from the hydrolysis reaction. On the other hand, if an alkaline additive is used to stabilize the $NaBH_4$ aqueous solution and hinder the hydrolysis reaction, then, the $NaBH_4$ solubility measured may not be representative of the solubility of $NaBH_4$ in water. As seen in Section 2.4.2, the addition of alkali stabilizers greatly affects the solubility of $NaBO_2$ in water. Table 3.1 shows the $NaBH_4$ solubility values reported in the literature for various solvents. In water at 25°C, the solubility of $NaBH_4$ is almost two times greater than that of $NaBO_2$.

Table 3.1: NaBH₄ solubility in Various Solvents.

Solvent	Temperature [°C]	Solubility [wt%]	Reference
Water	25	55	[Lide, D. R., (2005-6)]
Dimethylformamide	25	18	[Dean, J. A., (1999)]
Methanol	20	16.4	[Dean, J. A., (1999)]

C) Effect of Temperature on the Solubility of NaBO₂

Table 3.2 shows the solubility of $NaBO_2$ in aqueous solution at 25, 50 and 75°C, as well as at the transition temperature. It is clear that the solubility of $NaBO_2$ increases as the temperature increase.

Table 3.2: Solubility of $NaBO_2$ in Water at Selected Temperatures.

Reference	Temperature [°C]	$NaBO_2$ [wt%]	$NaBO_2.2H_2O$ [wt%]
[Blasdale, W. C. et al. (1938)]	25.0	22.00	30.45
	50.0	35.02	54.20
	54.0	37.85	58.58
	75.0	43.80	67.78
[Nies, N. P. et al., (1967)]	25.0	21.60	33.43
	50.0	34.10	42.77
	53.6	36.90	57.11
	75.0	42.20	65.31
[US Borax]	25.0	21.58	33.40
	50.0	34.12	52.80
	53.6	36.90	57.10
	75.0	42.20	65.30

It can be observed that a transition temperature exists at about 54°C. Below the transition temperature, $NaBO_2.4H_2O$ is known to be the stable compound. At the transition temperature, $NaBO_2.4H_2O$ coexists along with $NaBO_2.2H_2O$. At temperature above the transition temperature, $NaBO_2.2H_2O$ becomes the stable compound. The hydration level of the solute impacts on the physico-chemical properties of the solution. Above the transition temperatures less water is needed to hydrate the hydrolysis by-product. The hydration level of the $NaBO_2$ by-product affects the mass and heat transport properties of the solution and influences the theoretical gravimetric energy density of the H_2 storage and generation system. Hence, it would be preferable to operate the H_2 generation system at a temperature above the transition temperature to favour the formation of a less hydrated form of $NaBO_2$.

3.1.2 Single 1:1 Electrolyte Theory

Many publications pertaining to the theories of aqueous single 1:1 electrolyte solutions are available [Erdey-Gruz, T., (1974), Horvath, A. L., (1985)]. The equations resulting from those theories include a number of simplifying assumptions which more or less affect the properties of the solution as concentration changes.

A) Conductivity

The solution molar conductivity (Λ) is related to the solution specific conductivity (κ) and the molar concentration of solute (C) as per:

$$\Lambda = \frac{\kappa}{C},$$

(Eq. 3.1)

where κ is in S/m, C in mol/m^3 and Λ in S.m^2/mol. At infinite dilution, the ions are far apart and do not influence each other. The solute limiting molar conductivity can be determined by extrapolating Λ to infinite dilution according to the Kohlrausch's law for strong electrolytes given by:

$$\Lambda = \Lambda^o - KC^{\frac{1}{2}},$$

(Eq. 3.2)

where Λ^o is the limiting conductivity and K is a constant. Using this equation, it is possible to obtain the limiting value of conductivity with an accuracy of 0.1% from conductivity data in highly diluted solutions (≤ 0.0001 M) [Erdey-Gruz, T., (1974)]. The validity of the square root law was brought to a wider concentration range by the addition of another term:

$$\Lambda = \Lambda^o - KC^{\frac{1}{2}} - BC.$$

(Eq. 3.3)

The addition of a third term further extended the equation's validity to concentration as high as 0.1 M:

$$\Lambda = \Lambda^o - KC^{\frac{1}{2}} - BC - DC^{\frac{3}{2}}.$$

(Eq. 3.4)

In more concentrated solution of strong electrolytes, the cube-root law is more appropriate:

$$\Lambda = \Lambda^o - KC^{\frac{1}{3}}.$$ (Eq. 3.5)

Kohlrausch's law of independent ion migration states that the solution limiting conductivity is the sum of the limiting molar conductivities (λ^o) of ionic species (i) in the solution. For the dissociation of the 1:1 electrolyte AB, z_+ and z_- are unity and the following relationships can be obtained:

$$A_{v_+} \cdot B_{v_-} \leftrightarrow v_+ \cdot A^{Z_+} \cdot v_- \cdot B^{Z_-}$$

$$\Lambda^o = \Sigma v_i \lambda_i^o.$$ (Eq. 3.6)

A value of 50.11 S.cm^2/mol was reported for limiting ionic molar conductivity of Na$^+$ [Dean, J. A. (1999)]. Applying the Nernst-Einstein relation at infinite dilution to a simple 1:1 electrolyte system where z_i is unity gives:

$$\lambda_i^o = F u_i^o = \frac{F^2 D_i^o}{RT},$$ (Eq. 3.7)

where F is the Faraday constant, R the universal gas constant and T the temperature. Knowing the limiting molar conductivity for one ion renders it possible to calculate the limiting mobility (u_i^o) and the limiting diffusivity (D_i^o) of the same ion.

Also, in a binary electrolyte, the sum of the cation and anion transference numbers is equal to one. Therefore, it is possible to calculate the ionic limiting transference numbers (t_i^o) based on the limiting value of the ionic molar conductivities as:

$$\lambda_i^o = t_i^o \Lambda^o.$$ (Eq. 3.8)

The Debye-Huckel-Onsager theory provides an expression for evaluating the theoretical value of the constant K:

$$K = A + B\Lambda^o.$$

For a binary salt electrolyte solution at 25°C, A = 60.21 $1/M^{1/2}$ and B = 2.289x10^{-5} S.m^2/mol.$M^{1/2}$ [Horvath, A. L., (1985), Snyder, K. A., (2005)]. The Onsager expression gives a theoretical explanation for the coefficients in the Kohlrausch equations and somewhat extends the concentration range [Horvath, A. L., (1985), Helmy, F. M., et al., (1987)]:

$$\Lambda = \Lambda^o - (\theta\Lambda^o + \sigma)c^{1/2}$$

(Eq. 3.10)

$$\text{where} \quad \theta = \frac{8.205 \times 10^5}{(\varepsilon_o T)^{3/2}},$$

(Eq. 3.11)

$$\sigma = \frac{82.48}{\eta_o(\varepsilon_o T)^{1/2}},$$

(Eq. 3.12)

and where ε_o is the dielectric constant of pure water (78.56), η_o is the viscosity of pure water (0.008948 P) and T is the temperature in K [Horvath, A. L., (1985)]. This equation is applicable to the alkali salts in a solvent of high dielectric constant, such as water, in which strong electrolytes are completely ionized [Helmy, F. M. et al., (1987)] and is valid over concentrations ranging from 0.001 to 2 M [Shedlovsky, T., (1938)]. Many additional equation extensions and other empirical correlations were developed to predict conductivity in low concentration binary electrolyte systems but were not applied in this investigation [Horvath, A. L., (1985), Helmy, F. M. et al., (1987)].

B) Dynamic Viscosity

For a Newtonian fluid such as water, the dynamic viscosity is the proportionality constant between the velocity gradient in the direction perpendicular to the plane on which a shear stress is applied. Hence, it represents the resistance of a fluid to deform under shear stress. Based on the study of several electrolytes at constant temperature, Jones and Dole found that the dynamic viscosity was empirically related to concentration up to 0.1-0.2 M as follows:

$$\eta_r = \frac{\eta}{\eta_o} = 1 + AC^{\frac{1}{2}} + BC , \qquad \text{(Eq. 3.13)}$$

where η_r is the relative dynamic viscosity, η is the solvent viscosity, η_o is the viscosity of the pure solvent and C is the solute molar concentration. The dynamic viscosity of the solution can be calculated from the product of the kinematic viscosity and the solution density. The coefficient A is always a positive value while coefficient B can have either signs depending on the solute and the solvent [Erdey-Gruz, T., (1974)]. Coefficient A is specific to the solvent properties and limiting conductivities of the ions. It represents the ion-ion interactions and can be calculated from the Debye-Huckel theory based on the limiting ionic molar conductivities according to [Breslau, B. R. *et al.*, (1970)]:

$$A = \frac{1.45}{\eta_o (2\varepsilon_o T)^{\frac{1}{2}}} \cdot \left(\frac{\lambda_+^o + \lambda_-^0}{4\lambda_+^o \lambda_-^o} - \frac{\lambda_+^o - \lambda_-^o}{(3 + 2^{\frac{1}{2}})\lambda_+^o \lambda_-^o (\lambda_+^o + \lambda_-^o)} \right) . \qquad \text{(Eq. 3.14)}$$

Coefficient B qualitatively represents the ion-solvent interaction and is specific to the individual ions. More precisely, the B coefficient is related to the effect of the solvated ion size, the orientation of the solvent molecules and the change in solvent structure on viscosity [Erdey-Gruz, T., (1974)]. This coefficient usually has the most important impact on the viscosity as the ion-ion interaction effect becomes significant only in very concentrated solutions [Erdey-Gruz, T., (1974)]. Coefficient B is the sum of the contributions of the individual ions constituting the solute. The Jones-Dole B[+] coefficient for Na^{+} was

reported as being 0.0863 1/M at 25°C [Horvath, A. L., (1985)]. Kaminsky extended the Jones-Dole equation by adding a quadratic term to fit viscosity measurements in concentrated aqueous systems, described as:

$$\eta_r = \frac{\eta}{\eta_o} = 1 + AC^{1/2} + BC + DC^2 , \qquad \text{(Eq. 3.15)}$$

and where the B and D parameters are interdependent [Martinus, N. *et al.*, (1977)]. Hence, the coefficient B obtained from the original Jones-Dole equation (Eq. 3.13) is different from the one obtained from the extended Jones-Dole equation (Eq. 3.15). Several other viscosity correlations to interpret experimental viscosity data of single electrolytes exist [Horvath, A. L., (1985)], but were not considered in this work.

a) Effect of Temperature on the Viscosity and Ionic Mobility

Temperature has a significant impact on the solubility and transport properties of the ions in solution. The temperature dependence of viscosity is typically expressed by the following Arrhenius relationship [Uddin, F. *et al.*, (2001)]:

$$\eta = p \cdot \exp\left[\frac{E_{vis}}{RT}\right], \qquad \text{(Eq. 3.16)}$$

where p is a pre-exponential factor, E_{vis} is an activation energy of viscous flow, T is the temperature and R is the universal gas constant. A graph of $\ln(\eta)$ as a function of 1/T should illustrate a straight line relationship. Hence, as the temperature is increase, the viscosity of the solvent typically decreases while the ionic mobilities increase.

The limiting value of the ion mobility is affected by the interaction changes between the solvent molecules and between the solvent molecules and the ions, by the mutual electrostatic interaction between

the ions, and by the changes in the degree of association or dissociation of ions [Erdey-Gruz, T., (1974)].

For a single ion in solution, the ionic mobility dependence on temperature follows a cubic equation:

$$u^o = u^o_{25^o} + a(T - 298) + b(T - 298)^2 + c(T - 298)^3 \qquad \text{(Eq. 3.17)}$$

Where u^o and u^o_{25} are the limiting values of mobility at T and 298K respectively and where a, b, and c are temperature-independent coefficients. This expression leads to a cubic dependence of the conductivity on the temperature. Hence the limiting ionic mobility values increases with increasing temperature.

b) Effect of Temperature on the B Coefficients

The extended Jones-Dole B coefficients for a single electrolyte of Eq. 3.15 depend on temperature as per the following expression [Out, D. P. J. *et al.*, (1980)]:

$$B = B_E + B_S \cdot \exp[-P(T - 273.15)]. \qquad \text{(Eq. 3.18)}$$

A value of 0.023 can be attributed to parameter P. To evaluate the coefficient B of Eq. 3.18, the values of B and D have to be extrapolated from the rearranged extended Jones-Dole correlation using a least square analysis at zero concentration:

$$B + D \cdot C = \left[\left(\frac{\eta}{\eta_o} \right) - 1 - AC^{\frac{1}{2}} \right] \div C . \qquad \text{(Eq. 3.19)}$$

The parameter B_S depends on the standard entropy of hydration (ΔS_{hyd}) and is a measure of the structure breaking/making effects [Lencka, M. M. *et al.*, (1998)]. For monovalent ions, the following relationship can be used:

$$B_s = -0.00233 \cdot \Delta S_{hyd} - 0.297 \,. \qquad \text{(Eq. 3.20)}$$

A decrease of B values with a rise in temperature indicates that the ions are structure promoters. This means that the ions ability to polarize water molecules decreases with increasing temperature due to increasing thermal motion [Afzal, M. et al., (1994)]. On the other hand, ions for which the B values increase with a rise in temperature are structure breaking and have the opposite effect.

C) Walden's Rule

According to Walden's rule, the product of the molar conductivity of an electrolyte solution, Λ (S.m^2/mol), times its dynamic viscosity, η (cP), is nearly constant for the same ions in different solvents at constant temperature as per Eq. 3.21.

$$\Lambda \cdot \eta \approx const \qquad \text{(Eq. 3.21)}$$

The Walden product is generally constant for a given electrolyte in different solvent or solvent mixtures in which ion-solvent interactions are uniform [Chowdoji Rao, K. et al., (1999)]. The Walden product is generally not constant for highly concentrated salts and solutions of small ions. Nevertheless, it indicates that a change in molar conductivity is affected by a change in the dynamic viscosity. When generalized for the NaBO$_2$ aqueous alkaline systems under consideration, Eq. 3.21 becomes:

$$\Lambda_{Na^+BO_2^-\cdot H_2O} \cdot \mu_{Na^+BO_2^-\cdot H_2O} \approx \Lambda_{Na^+BO_2^-\cdot H_2O\cdot MOH} \cdot \mu_{Na^+BO_2^-\cdot H_2O\cdot MOH} \qquad \text{(Eq. 3.22)}$$

For a 1:1 electrolyte at a given temperature, the Walden product of the viscosity and the limiting molar conductivity is equal to:

$$\Lambda_0 \cdot \eta = 0.8201 \cdot \left(\frac{1}{r_s^+} + \frac{1}{r_s^-} \right),$$ (Eq. 3.23)

where the hydrodynamic factor, $(1/r_s^+ + 1/r_s^-)^{-1}$, quantify the ions hydrodynamic radii and represent the ion interactions with the solvent and $\Lambda_0.\eta$ is in $Sm^2.Cp/mol$ [Chowdoji Rao, K., *et al.*, (1989)]. The ionic hydrodynamic radius is the apparent size of the dynamic hydrated or solvated ion based on its diffusion.

3.1.3 Physicochemical Properties

This Section reviews the physicochemical properties of $NaBO_2$ aqueous solutions and alkaline aqueous solutions which have been reported in the literature.

A) Aqueous NaBO₂ Solutions

The electrical conductivity of 1 to 20 wt% aqueous $NaBO_2$ solutions has been reported from 20 to 300°C [Maksimova, I. N. *et al.*, (1963)]. Over these aqueous $NaBO_2$ concentrations, conductivity was expressed by the equation:

$$\kappa_2 = \kappa_1 (1 + \alpha(T_2 - T_1)),$$ (Eq. 3.24)

where κ_1 is the specific conductivity at 40°C and $T_1 = 40°C$ over temperature ranging from 20 to 200°C. The temperature coefficient of the conductivity,

$$\alpha = \left(\frac{1}{\kappa_1} \right) \left(\frac{d\kappa}{dT} \right),$$ (Eq. 3.25)

is also linked to the $NaBO_2$ concentration as per:

$$\alpha = a + bC, \tag{Eq. 3.26}$$

where C is the Na_2O concentration in wt%, and where a and b are dimensionless constants equal to 2.045×10^{-2} and 3.38×10^{-4} respectively for temperatures within 20 to 200°C. A maximum, which shifts with temperature, is present in the solubility curve at temperatures lower than 80°C. For example, at 25°C and 40°C, the maximum conductivity is located at 15 wt% and 17 wt% $NaBO_2$ respectively [Maksimova, I. N. et al., (1963)].

The density of $NaBO_2$ solutions (ρ_T) in the temperature range of 20 to 100°C, without taking account of the solution compressibility, can be calculated by [Maksimova, I. N. et al., (1963)]:

$$\rho_T = \rho_{H_2O,T} + 1.14 \times 10^{-2} \cdot C. \tag{Eq. 3.27}$$

Using Eq. 3.25 to 3.27, the molar conductivity and the specific gravity was calculated as a function of the temperature. The data reported for 5.4 wt% and 20.2 wt% $NaBO_2$ aqueous solutions is summarized in Table 3.3.

Table 3.3: Specific Gravity and Conductivity of 5.4 and 20.2 wt% $NaBO_2$ Aqueous Solutions, (Modified from [Maksimova, I. N. et al., (1963)]).

$NaBO_2$ (wt%)	5.4	20.2	5.4	20.2
Temperature [°C]	Specific Gravity		Molar Conductivity [S/m]	
25	1.0585	1.2202	39	51
50	1.0484	1.1950	64	114
75	1.0364	1.1840	91	175

The Kohlrausch correlation, Eq. 3.24, was found to be applicable to $NaBO_2$ concentrations up to 1.4 M and was used to extrapolate the limiting value of the molar conductivity of $NaBO_2$. Thus, the limiting value of the molar conductivity of the BO_2^- ion at infinite dilution was determined [Maksimova, I. N. et al., (1963)]. The values obtained are summarized in Table 3.4.

Table 3.4: Molar Conductivity at Infinite Dilution at Various Temperatures (Modified from [Maksimova, I. N. et al., (1963)]).

Temperature [°C]	Λ_o [S.m^2/mole]			
	NaBO$_2$	NaB$_5$O$_8$	NaOH	BO$_2^-$
25	78	100	250	28
75	196	200	416	80

The molar conductivity ratios calculated (λ/λ^o) were found to be independent of temperature, but decreased as the concentration increased. The ionic strength was used to calculate the corresponding activity coefficients. Table 3.5 show the reported activity coefficients and conductivity ratios obtained for different aqueous NaBO$_2$ solution concentration.

Table 3.5: Molar Conductivity Ratios at Varying NaBO$_2$ Concentrations (Modified from [Maksimova, I. N. et al., (1963)]).

Concentration [M]	Activity Coefficient	Conductivity Ratio
0.159	0.716	0.800-0.835
0.472	0.622	0.664-0.696
0.868	0.566	0.566-0.588
1.400	0.532	0.470-0.546

The viscosity B coefficients of B(OH)$_4^-$ and of NaB(OH)$_4$ were reported as 0.233 and 0.316 1/M at 25°C in dilute aqueous solutions, respectively [Corti, H. et al., (1980)]. In aqueous solutions of various metaborates, the equivalent mobility of the anion was reported to be 390000-400000 S.m^2 [Kesans, A. et al., (1955)].

B) Alkaline Aqueous NaBO$_2$ Solutions

To the author's knowledge, no experimental data on the conductivity, viscosity, pH or density of NaBO$_2$ in concentrated alkaline aqueous solutions has been reported in the literature at 25, 50 or 75°C. An investigation of the transport properties of the tetrahydroxoborate anion in alkaline aqueous media was found. The mobility of the tetrahydroxoborate anion, $u_{B(OH)_4^-}$, was calculated based on the dissociated constant of boric acid, K_a H$_3$BO$_3$ = 6.2x10^{-10} [Frei, V. et al., (1963)] as per the following equation:

$$u = u_{Na^+} \cdot C_{Na^+} + u_{B(OH)_4^-} \cdot \left(\frac{K_{aH_3BO_3} \cdot C_{B^{3+}}}{[H^+] + K_{aH_3BO_3}} \right) + u_{H^+} \cdot [H^+] + u_{OH^-} \cdot [OH^-], \qquad \text{(Eq. 3.28)}$$

where u_{Na^+}, u_{H^+} and u_{OH^-} are the ionic mobilities of Na$^+$ (45.4), H$^+$ (324.9) and OH$^-$ (181.4) respectively and C_{Na^+} and $C_{B^{3+}}$ are the concentrations of sodium hydroxide and boric acid, respectively. Using this expression, it was found that the apparent mobility of B(OH)$_4^-$ decreased with an increase of NaOH concentration as it forms undissociated complexes with Na$^+$ [Frei, V. *et al.*, (1963)].

3.1.4 Organic Additives

As mentioned in Section 2.2.2, water is not favorable to the direct electroreduction of NaBO$_2$. Other media such as molten salts, ionic liquids and anhydrous organic solvents might be more suitable. In a proper media, the electroreduction of NaBO$_2$ would occur before the electroreduction of the media itself. In aprotic organic solvents, NaBH$_4$ is known to be stable and NaBO$_2$ is soluble to varying extents. In this Section, the few hydroborate solubility studies available in the literature are reviewed to determine which organic additive would be the most capable to enhance the solubility of NaBO$_2$.

A) Amides

The amides decrease the solubility of sodium tetraborate salts. The systems are simple eutonic as no complex salts or solid solution are formed. The effect of urea, thiourea and acetamide are reviewed.

a) Urea

The potassium borate – urea - water system, KBO$_2$-N$_2$H$_4$CO-H$_2$O, was studied at 15, 25 and 40°C [Druzhinin, G. *et al.*, (1968)]. After the solution reached equilibrium, the liquid and solid phases were sampled and the solution's composition was determine using various methods. The solubility of KBO$_2$ in

pure water at 25°C is about 40 wt%. The addition of 12.8 wt% urea decreased slightly the solubility limit of KBO_2 to 37.5 wt% [Druzhinin, G. et al., (1968)]. This drop in solubility was attributed to the formation of a double compound, $KBO_2.CO(NH_2)_2$. A solubility diagram of the system sodium tetraborate-urea-water, $Na_2B_4O_7$-N_2H_4CO-H_2O, was developed at 25°C [Sadetdinov, Sh. V., (1985)]. The solubility isotherm of the tetraborate was approximated by the linear equation:

$$y = -0.0427 \cdot x + 3.12,$$
(Eq. 3.29)

where y is the $Na_2B_4O_7$ solubility in wt% and x is the wt% of urea. Alkali metal metaborates are known to form different kind of solid solutions with urea in aqueous solution [Skvortsov, V. G., (1974)]. At 15°C, the sodium metaborate – urea - water system, $NaBO_2$-$CO(NH_2)_2$-H_2O, has a eutonic solution composition of 4.99 wt% $NaBO_2$ and 46.16 wt% urea. Furthermore, the salting out effect of urea on $NaBO_2$ was accentuated as the temperature was increased.

b) Thiourea

The solubility of the sodium tetraborate-thiourea-water system, $Na_2B_4O_7$-Na_2H_4CS-H_2O, was investigated at 25°C [Sadetdinov, Sh. V., (1985)]. Thiourea additions lowered the salt solubility. The solubility isotherm of the borate was approximated by the linear equation:

$$y = -0.0688 \cdot x + 3.07,$$
(Eq. 3.30)

where y is the sodium tetraborate solubility in wt% and x is the wt% of thiourea.

c) Acetamide

The solubility of the sodium tetraborate – acetamide - water system, $Na_2B_4O_7$-CH_3CONH_2-H_2O, was determined at 25°C [Sadetdinov, Sh. V., (1985)]. The presence of acetamide decreased the solubility of the salt. The solubility isotherm of the borate was approximated by the linear equation:

$$y = -0.0423 \cdot x + 3.11,$$ (Eq. 3.31)

where y is the sodium tetraborate solubility in wt% and x is the wt% of acetamide.

B) Ammonia

Ammonia (NH_3) increases the solubility of boric acid in water as per the following relationship:

$$\log S = \log S_o + H\sqrt{C}$$ (Eq. 3.32)

where S represents the solubility in wt%, H is a dimensionless constant, and C is the salt concentration in wt%. Per linear interpolation, it was estimated that, at 25°C, K has a value of 1.1575 and log S is equal to 0.6292 [Constable, F. H. et al., (1953)]. The addition of the ammonium ion to the ternary system sodium oxide - boric oxide - water, Na_2O-B_2O_3-H_2O, enlarged the maximum solubility pH range of B_2O_3 in the solution, thereby positively affecting the solubility of the total solids present in the solution [Rothbaum, H. P. et al., (1956)]. Hence, the peak B_2O_3 solubility can be augmented by switching to the sodium oxide - ammonium oxide - boric oxide - water system, Na_2O-$(NH_4)_2O$-B_2O_3-H_2O. In this system, the Na_2O:$(NH_4)_2O$ ratio can be varied to change the pH without significantly affecting the B_2O_3 solubility. Based on this knowledge, it would be interesting to investigate the effect of ammonia additions on the solubility of $NaBO_2$ and explore the hydrolysis of ammonium borohydride, (NH_4BH_4).

C) Diethylene Glycol

$NaBH_4$ is only slightly soluble in ethylene glycol (monoglyme, $C_4H_{10}O_2$) however it is more soluble in diethylene glycol (diglyme, $C_6H_{14}O_3$) or triethylene glycol (triglyme, $C_8H_{18}O_4$) [Brown, H. C. *et al.*, (1955)]. Diethylene glycol is an organic solvent often used to remove remaining hydroborate reagents in solution after exchange reactions to improve product purity. The solubility of $NaBH_4$ in diglyme at 20°C was measured to be 2.42 wt% [Konoplev, V. N., (1988)]. At 40°C, $NaBH_4$ dissolves in diglyme to a concentration up to 3 M. The solubility decreases at higher or lower temperatures. The precipitate formed is a 1:1 solvate of diglyme and $NaBH_4$ [Brown, H. C. *et al.*, (1955)]. The solubility of lithium hydroborate ($LiBH_4$) and hydroaluminate ($LiAlH_4$) was studied in diglyme at temperatures ranging from 25 to 60°C [Mal'tseva, N. N. *et al.*, (1991)]. At 25°C, the solubility of $LiBH_4$ in diglyme was reported as 9.92 wt% and the precipitate formed was a 1:1 $LiBH_4$-diglyme compound. As temperature increased, the solubility of $LiBH_4$ increased and the solution viscosity significantly increased.

D) Glycine

The effect of glycine, $C_2H_5NO_2$, on the solubility of lithium, sodium and potassium tetraborates [Skvortsov, V. G. *et al.*, (1986a)], of lithium, sodium and potassium pentaborates [Skvortsov, V. G. *et al.*, (1986b)], and of lithium, sodium and potassium metaborates [Skvortsov, V. G. *et al.*, (1988)] was investigated in water at 25°C. The systems were all simple eutonic. The addition of glycine appears to enhance the solubility of sodium tetra- and pentaborates in water. The solubility improvement of the glycine addition was more pronounced on the tetraborates of lithium and the least on those of potassium while the solubility improvement of glycine addition was more pronounced on the pentaborates of lithium, and the least on those of potassium. The solubility of sodium pentaborate is linearly dependent on the glycine concentration as per the following expression:

$$y = 0.152 \cdot x + 11.51 \,, \qquad \text{(Eq. 3.33)}$$

where y is the sodium pentaborate solubility in wt% and x is the glycine concentration in wt% [Skvortsov, V. G. et al., (1986)]. Unexpectedly, although the medium remained alkaline, it was found that the solubility of sodium and potassium metaborates decreased in the presence of glycine, while that of lithium metaborates improved. It seems that the metaborates tend to react with glycine to produce polyborates, such as alkali metal tetraborates, and aminoacetates [Skvortsov, V. G. et al., (1988)].

The solubility of the simple eutonic ammonium tetraborate – glycine - water, $(NH_4)_2B_4O_7$-NH_2CH_2COOH-H_2O, and ammonium tetraborate – $EDTANa_2$ - water, $(NH_4)_2B_4O_7$-$C_{10}H_{14}O_8N_2Na_2.2H_2O$-$H_2O$, systems was determined at 25°C [Skvortsov, V. G. et al., (1992)]. It was found that glycine did not dehydrate the borate and that its hydration properties were weaker than that of $EDTANa_2$. The solubility of the ammonium tetraborate and of the organic component both increased. At the eutonic point, the ammonium tetraborate concentration was 15.59 wt% while its solubility in water was only 8.76 wt% [Skvortsov, V. G. et al., (1992)].

The solubility isotherms of the glycine - boric acid - water system, glycine-H_3BO_3-H_2O, were investigated at 0, 25, 50 and 70°C to determine possible interactions between the components [Eysseltova, J. et al., (1994)]. At 25°C, the solubility of boric acid in the glycine solution was correlated by the following linear equation:

$$y = 0.034 \cdot x + 5.66,$$ (Eq. 3.34)

where y is the boric acid solubility in wt% and x is the wt% of glycine in the solution. A weak interaction between glycine and boric acid was believed to exist in the low temperature range.

E) Organic Additive Comparison

Table 3.6 summarizes the effect of the addition of about 10 wt% organic compound has on the solubility of various borates. In all cases, the solubility of the borate compound is lower than in pure water.

Table 3.6: Effect of Organic Additive on the Solubility of Borate Compounds at 25°C.

Solute	Organic Additive	Organic Additive Concentration [wt%]	Solubility [wt%]
$Na_2B_4O_7$	Urea	10.00	2.69
$Na_2B_4O_7$	Thiourea	10.00	2.38
$Na_2B_4O_7$	Acetamine	10.00	2.69
H_3BO_3	Ammonia	11.00	3.20
NaB_5O_8	Glycine	10.00	13.03
H_3BO_3	Glycine	10.00	6.00
$NaBO_2$	Glycine	9.68	2.47
KBO_2	Glycine	10.66	25.10
$LiBO_2$	Glycine	10.36	2.11

3.2 Precipitate Characteristics

Accurate determination of hydrated borates by X-Ray Diffraction (XRD) is difficult as the peaks of many compounds in the hydrated borate group almost overlap with each other [Kim, J.-H. et al., (2004b)]. Bouaziz investigated the radiocrystallography of lithium and sodium borates and found similarities between the two [Bouaziz, R., (1962)]. A compilation of data on crystal morphology, XRD and fusion of $NaBO_2.2H_2O$ were made [John, K. R. C. Jr., (1951)], and a wide variety of XRD patterns and crystal pictures were reported [Menzel, H. et al., (1943)]. A large diversity in the XRD peak location and intensity exists depending on the conditions under which the crystals were prepared. The structure of the hydrolysis by-product was confirmed to be $NaBO_2.2H_2O$ by XRD, after drying the by-product solution at room temperature for 24 hours [Kojima, Y., et al., (2002)]. In another study, the intensity curve of the by-product obtained from a 25 wt% $NaBH_4$ solution was compared to that of $NaBO_2$ and $NaBO_2.2H_2O$ [Kojima, Y. et al., (2004b)]. The same research group also evaluated the by-product formed from H_2 generation at high pressure of a solution with a $H_2O/NaBH_4$ molar ratio of 2 by XRD. The by-product was allowed to evaporate at 50°C and vacuum dried at room temperature. The XRD intensity curve corresponded to amorphous $NaBO_2$ [Kojima Y. et al., (2004a)]. In the same study, the by-product generated at atmospheric pressure from a solution with a $H_2O/NaBH_4$ molar ratio of 4 was analyzed. According to the XRD pattern, its by-product was found to be $NaBO_2$ as well. Since at high pressure, only half of the water was required to carry out the hydrolysis, it was deduced that $NaBO_2.2H_2O$ transformed into amorphous $NaBO_2$ during the vacuum drying preparation step. On the other hand, the Kurcel-Merit

group mentioned that the hydrolysis by-product is $NaBO_2.4H_2O$ [Suda, S., (2003)]. Even though many boron oxides could have formed, XRD data indicated that $NaBO_2.2H_2O$ was the hydrolysis reaction product [Gervasio, D. *et al.*, (2005)]. The most important peaks of XRD pattern data of boron compounds relevant to this study can be found in Appendix C.

CHAPTER IV

EXPERIMENTAL METHODS

4.1 Materials

The Fisher Scientific alkali hydroxides used were sodium hydroxide electrolytic pellets (NaOH, S318-500, 98.1% purity), potassium hydroxide pellets (KOH, P250-500, 87.7% purity) and lithium monohydrate crystals (LiOH.H$_2$O, L127-500, 99%[+] purity). The three alkali hydroxides were used independently. Sodium metaborate 4 mol (NaBO$_2$.2H$_2$O, 99%[+] purity) from U.S. Borax Inc. was used. The hydration level of NaBO$_2$.2H$_2$O was not constant over the entire study. Solutions were prepared with deionized distilled water having an electrical ionic conductivity of 1.5 μS/m at a pH of 6.1. Glycine, (C$_2$H$_5$NO$_2$, CH$_2$NH$_2$COOH), US Pharmacopeia grade, was obtained from Fisher Scientific (G48) in the white crystalline powder form.

4.1.1 Properties

Tables 4.1 and 4.2 list the pertinent anion and cation properties, while Table 4.3 contains the thermodynamic data pertaining to the species under considerations in the system investigated. Figure 4.1 describes the molecular chain arrangement of glycine, which is a non-polar hydrophobic aliphatic.

Table 4.1: Anion Properties.

Property	B(OH)$_4^-$	BH$_4^-$	OH$^-$	Reference
Ionic radius [nm]	0.229 ± 0.019	0.205 ± 0.019	0.152 ± 0.019	[Roobottom H. K. *et al.*, (1999)]
Volume [nm^3]	0.058	0.066 ± 0.015	0.032 ± 0.008	[Jenkins, H. D. B. *et al.*, (1999)]

Table 4.2: Cation Properties.

Property (in H_2O at 25°C)	Na^+	K^+	Li^+	Reference
Ionic radius [A°]	0.98	1.33	0.68	[Antropov, L. I., (1972)]
Effective ionic radius [A°]	4	3	6	[Dean, J. A., (1999)]
Limiting ionic conductivity [$10^{-4}.m^2$.S/mol]	50.11	73.5	38.69	[Dean, J. A., (1999)]

Table 4.3: Thermodynamic Data.

Species	dG° [KJ/mol]	dH° [KJ/mol]	dS° [J/mol.K]
BO_2^-	-678.94	-772.37	-37.24
OH^-	-157.28	-230.015	-10.90
BH_4^-	114.27	48.16	110.50
Na^+	-261.88	-240.34	58.45
H_2 (g)	0	0	130.68
H_2O (l)	-237.14	-285.83	69.95
NaOH (aq)	-419.20	-469.15	48.10
KOH (aq)	-440.53	-482.37	91.60
LiOH (aq)	-451.9	-508.40	7.10
$NaBO_2$ (aq)	-940.81	-1012.49	21.80
$NaBO_2$ (c)	-920.70	-977.00	73.54
KBO_2 (aq)	-962.19	-1024.75	65.30
KBO_2 (c)	-923.40	-981.60	79.98
$LiBO_2$ (c)	-976.10	-1032.20	51.50
$NaBH_4$ (aq)	-147.61	-199.60	169.50
BO_2^-	-678.94	-772.37	-37.24
[Dean, J. A., (1999)]			
$NaBO_2.2H_2O$	-1415.20	-3228.07	
$LiBO_2.2H_2O$	-2873.80		
$B(OH)_4^-$	-1159.87	-1345.46	-622.47
Li^+		-278.48	-293.30
Na^+		-240.12	-261.89
K^+		-252.38	-283.26
[Li, J. et al., (2000)]			
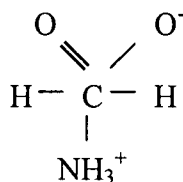
Figure 4.1: Molecular Chain Arrangement of Glycine.

4.1.2 Contamination

Table 4.4 summarizes the ICP-MS analysis of deionized distilled water used throughout this study.

Table 4.4: Deionized Distilled Water ICP-MS analysis.

Element	B	Na	K	Li
Concentration [mg/l]	3.5	8	<2	0.08

Other than the elements listed in Table 4.4, impurities present in the solutions are Ca, Cu, Fe and Zn. During the course of the experiment, a potential source of boron contamination can be attributed to the use of borosilicate glass. Hence, the use of glass was avoided whenever possible during the solution preparation and physicochemical properties determination.

4.2 Experimental Plan

Figure 4.2 represents the experimental plan followed in this study. Tests were conducted on aqueous $NaBO_2$ solutions, saturated $NaBO_2$ solutions, unsaturated $NaBO_2$ solutions and diluted $NaBO_2$ solutions containing no alkali or various wt% of alkali and organic additives at 25, 50 and 75°C. The solution preparation procedures are presented in Section 4.3. Filtration, as described in Section 4.4, was only performed when evaluating the properties of saturated solutions.
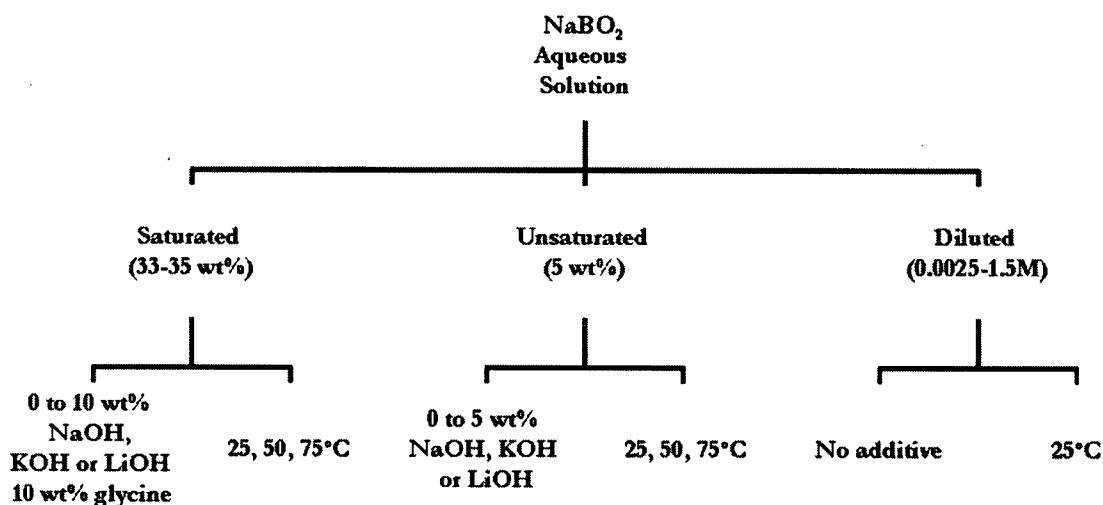
Figure 4.2: Experimental Plan Schematic Diagram.

The filtrate properties determined included solubility, conductivity, pH, viscosity and density. The precipitates were evaluated by X-Ray Diffraction and Scanning Electron Microscopy. The procedures followed for the filtrate and precipitate characterization are described in Sections 4.5 and 4.6, respectively.

4.3 Solution Preparation

Three types of solutions were prepared in this study. Dilute solutions of $NaBO_2$ in water, saturated solutions of $NaBO_2$ in water, with or without alkali additives, and finally, saturated solutions of $NaBO_2$ with an organic additive with and without alkali additives. The solution preparation procedures are described below.

4.3.1 Dilute Aqueous $NaBO_2$ Solutions

Solutions of different $NaBO_2$ concentrations were prepared by dilution. An appropriate weighted amount of $NaBO_2$ was placed in a 50 ml ±5 % graduated beaker and de-ionized water was added up to 30 or 40 ml depending on the desired concentration. The solutions were magnetically stirred for a few minutes to ensure homogeneity. An analog-controlled Cole-Parmer polystat heated circulating water bath (Model EW-12107-40) was used to keep the solutions at a constant temperature ±0.2°C.

4.3.2 Concentrated Alkaline Aqueous $NaBO_2$ Solutions

An isothermal solution saturation methodology was followed to prepare the solutions. A predetermined quantity of alkali additive (1, 2, 3, 5, 7.5 or 10 wt%) was combined in a flask containing excess sodium metaborate (32-35 wt%). A fixed de-ionized distilled water volume (55 ml) was added to the mixture. The liquid to solid ratio was made sufficient to allow efficient stirring. The water to boron weight ratio before filtration ranged from 1.83 to 1.9 in most experiments. Polytetrafluorethylene (PTFE) flasks were used to avoid potential contamination with the boron contained in borosilicate glass. The flasks were sealed with rubber stoppers with a small vent hole open to the atmosphere. This prevented pressure

build up but did not prevent water evaporation to the ambient atmosphere during the high temperature experiments. The solutions were magnetically stirred for 5 hours to accelerate the homogeneous solid dissolution and allow equilibrium to be reached. At this point, temperature, pressure and composition were assumed to be constant. The stirring time required to establish equilibrium was estimated based on the time reported for similar experimental conditions and components with similar solubilities. After reaching equilibrium, stirring was stopped and the solutions were allowed to stand for one hour to enable excess solute settling and phase separation. The heated circulating water bath mentioned above was used to keep the solutions at the desired temperature $\pm$ 0.2°C throughout the sample preparation period. Saturation of the solution was confirmed by visual observation.

4.3.3 Organic Additives

Preliminary tests were conducted using glycine as an organic additive. The procedure followed to conduct the tests with glycine was very similar to the one used to prepare the concentrated alkaline aqueous solution described above. The tests were conducted using a mixture of 5 wt% NaOH or KOH, 10 wt% glycine, and excess sodium metaborate (35 wt%) in 50 ml of de-ionized distilled water. For saturated $NaBO_2$ alkaline aqueous solutions containing glycine, the time required to establish equilibrium was much longer than for the solutions containing no organic additives. The solutions were magnetically stirred for 36-39 hours, then stirring was stopped and the solutions were allowed to settle for one hour.

4.4 Filtration

After the solution was prepared and equilibrium reached, a sample of the liquid was taken and filtered. Filtration was carried out differently, depending on the temperature at which the experiment was performed.

4.4.1 Filtration at 25°C

Filtration of the solution at 25°C was conducted in two different ways. First, preliminary solubility experiments were conducted after vacuum filtration using different types of membranes, and then by syringe filtration. Syringe filtration was adopted to conduct the bulk of the experimental work at ambient temperature.

A) Vacuum filtration

In vacuum filtration, a flask was clamped to a ring stand and a funnel was connected to it with an adaptor. A piece of filter paper was placed in the funnel and the side of the flask was then connected to the vacuum source. The paper was wetted using a small amount of solution. The water circulation bath maintained the temperature constant throughout the filtration. The vacuum was turned on to start the filtration and the funnel was pressed on to engage seal with filter adapter. The filtrate solution was poured on the filter paper. After filtration, the rubber tubing was disconnected before turning off the vacuum. The filter paper was removed and the solids were collected and dried.
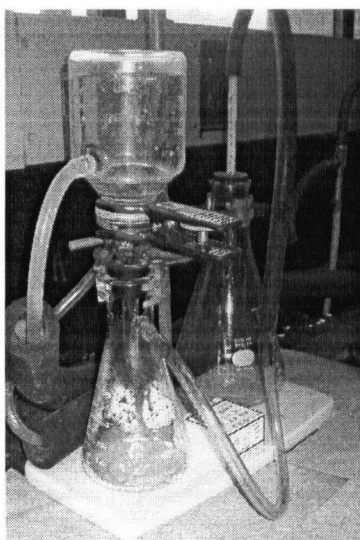
Figure 4.3: Vacuum Filtration Apparatus.

Different paper filters with pore sizes of 0.45 um were tested: cellulose ester (CS) filters and hydrophobic Teflon (PTFE) filters. The CS filter tended to leak and break under high vacuum while the hydrophobic PTFE filter would not filter until made hydrophilic by pre-wetting with acetone. Hydrophillic PTFE filters were judged too expensive for the number of experiments to be conducted.

B) Syringe Filtration

In this case, sampling was conducted using a graduated plastic syringe and plastic tube. Syringe filters, fitted with PTFE membranes with 0.45 μm diameter pores, were used to filter a clarified solution sample withdrawn from the flask. Difficulties were encountered in the withdrawal of saturated solution samples when the solution was highly viscous due to cavitation. Pushing the aqueous solution through the hydrophobic PTFE filter was very difficult. Hence, a filtration apparatus was built and designed to simplify the task. Filtration was conducted at room temperature using the stainless steel filtration apparatus assembly described in Figure 4.4, which ensured a steady filtration rate.
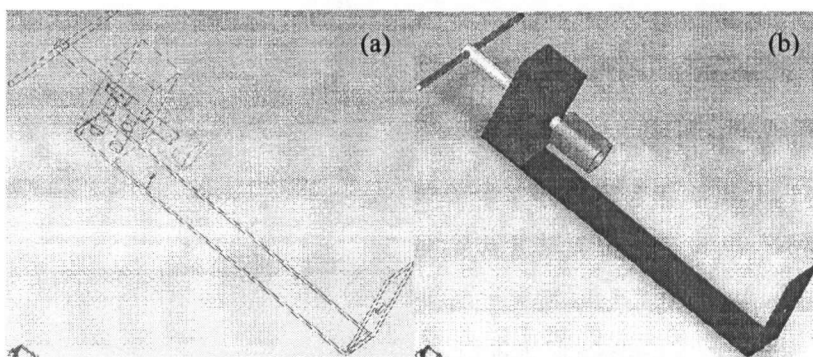
Figure 4.4: Syringe Filtration Apparatus: (a) Schematic Diagram (b) Full View.

Table 4.5 is a comparison of the $NaBO_2$ solubility results obtained in aqueous solution at $25^{\circ}C$ using different filtration techniques described in Section 4.3.1.

Table 4.5: Filtration Method Comparison.

Filtration Method	Filter Type	$NaBO_2$ Solubility in Water at 25°C [wt%]	Average Standard Deviation [%]
Vacuum	CS	30.45	1.28
Vacuum	PTFE	30.41	0.13
Syringe	PTFE	29.21	0.79

It is important to note that temperature was not controlled or maintained to 25°C during syringe filtration. It was assumed that the solubility standard deviations were caused by temperature variations estimated to be of ± 3°C, during the filtration step. In all cases, during filtrate characterization, the filtrates were kept in sealed plastic bottles maintained at 25°C with the water circulation bath described earlier.

4.4.2 Filtration at 50 and 75°C

Major difficulties were encountered when using the apparatus described above to filter the sample solutions in an oven set at the desired temperature. At higher temperatures, the syringe plastic became too soft, and the syringe shaft would fold under pressure rather than pushing the sample solution through the attached syringe filter. A SS plunger was built to use in the plastic syringe core. However, the sealing between the SS part and the soft plastic part was poor. Hence, the fluid was leaking on the side of the plunger and the liquid was not pushed through the filter. Another option was to use a simple filtering method. For the tests performed at 50 and 75°C, the equilibrium phases were decanted and filtrated by gravity using a Whatman paper filter No. 4, for course and gelatinous precipitates, placed on a preheated funnel. This process was conducted in an oven heated at a temperature slightly above the desired temperature in order to prevent recrystallization during sampling and filtration. It is important to note that the pore sizes of the paper filter were much larger than that of the syringe filters used to filter the solutions at ambient temperature.

4.5 Filtrate Characterization

At a minimum, three solutions of the same composition, i.e. MOH and $NaBO_2$ concentration, were characterized. The physicochemical properties values reported represent the average of the measurements performed on at least three solutions.

4.5.1 Solubility

There exist many methods to determine the content of boron in a liquid. The most relevant ones are reported in this Section.

A) Boron Detection Methods

In analytical methods, the solubility is directly determined by a chemical analysis of the phases in equilibrium. Typically, this is done by carrying out a titration with an acid or base and a variety of reagents, such as polyols, and a color indicator to determine the end points. The volume of acid or base used to the end-point indicates how much boron is present in the solution. The most common titration method used for the determination of boron in alkaline aqueous solution is carried out using mannitol and methyl red. The results obtained tend too be too high as interferences with carbon dioxide and silica are present. Carbon dioxide interferences can be addressed by refluxing the solution prior to titration. Other possible boron determination methods include coulometry, chromatography, potentiometry, volumetry, voltammetry, atomic absorption and mass spectrophotometry. Some references for each method are listed in Table 4.6.

Table 4.6: List of Some Boron Detection Methods.

Type	References
Analytic	[Brown, H. C., (1955), Rudie, C. N., (1979), Johnson, E. A. *et al.*, (1954), Dodd, S., (1929), Blumenthal, H., (1951), Drescher, A. *et al.*, (1998), Midgley, D., (1992), Belcher, B. *et al.*, (1970)]
Coulometric	[Kuleshova, O. D., (1985), Ross, W. J. *et al.*, (1960)]
ICP	[Wei, W. C. *et al.*, (1995)]
Potentiometric	[Norkus, P. K., (1968), Drescher, A., (1989)]
Spectrophotometric	[Sagrado, S., (1998)]
Atomic Absorption	[Andrew, H. E., (1976)]
Spectrophotometric	[Staden, J. F., (2000), Van Staden, J. F. *et al.*, (2000), Basson, W. D. *et al.*, (1969), Chaurasia, S. C., (2004), Hayes, M. R. *et al.*, (1962), Betty, K. R. *et al.*, (1986), Lopez Garcia, I. *et al.*, (1985), Sah, R. N., (1997)]
Volumetric	[Chaikin, S. W., (1953), Lyttle, D. A., (1963)]
Voltammetric	[Mirkin, M. V., (1991), Celikkan, H. *et al.*, (2005)]
Colorimetric	[Dawidowicz, A. L. *et al.*, (1989)]

B) Induced Coupled Plasma Mass Spectrometry

In this study, induced couple plasma (ICP) mass spectrometry (MS) was chosen for the quantitative determination of the filtrate boron, sodium, potassium and lithium content. The ICP-MS analysis was carried at International Plasma Laboratories Ltd. Prior to ICP-MS analysis, samples were digested to ensure solubility of any precipitate which could have formed after filtration. Minimum detection ranged from 0.01 to 2 mg/l and maximum detection was 999 or 9999 mg/l. It has been shown that the detection sensitivity for boron can be further improved with the use of mannitol as a chemical modifier in electrothermal vaporization inductively coupled plasma mass spectrometry (ETV-ICP-MS) [Wei, W. C. *et al.*, (1995)].

4.5.2 pH

A VWR Scientific digital pH meter (Model SP21), with a resolution of ±0.01 and a pH range from -2 to 19.99 was used to determine the pH at the filtrate temperature. A Corning rugged bulb combination glass electrode (Model 476560) with Ag/AgCl internals was used. After 30 minutes of standing and after an hour of standing, the changes in pH were within ±0.4 pH units. At 25°C, the average standard deviation on the pH measurements of $NaBO_2$ saturated alkaline aqueous solutions was about ± 0.2 pH units.

4.5.2.1 Glass Electrode

General purpose glass electrodes are suitable in the pH range from 1 to 10, but at other pH values special "low sodium error" electrodes which can operate at high temperatures are preferable. Standard glass electrodes measure erroneously high pH values in highly alkaline solutions (pH > 10). In those solutions, the glass membrane is not selective to the H^+ ions. At low concentration of H^+, alkali metal cations such as Li^+, Na^+, and K^+, present in large excess, tend to combine with the membrane surface, resulting in an electrode response. The potential dependence on the pH becomes non-linear. This interference phenomenon is known as the alkaline error.

A) pH Meter

The pH meter was calibrated using standard buffers at pH 4, 7 and 10 between each series of measurements. The measured pH is affected by temperature. The chemical equilibrium and the electrode properties are both affected.

$$E = E^0 - \frac{2.303RT}{F} pH$$

(Eq. 4.1)

The slope of the Nernst equation increased with temperature. The electrode did not reach thermal equilibrium spontaneously and pH fluctuations were likely to occur. Hence, temperature needed to be recorded along with the pH measurements.

4.5.3 Conductivity

The filtrate electrical conductivity measurements were made with an Orion 105A portable conductivity meter with a conductivity measurement range from 0 to 199.9 S/m ±0.5%. Measurements were normalized with a temperature adjustment of 2.5%/°C at 25°C. The average standard deviation on the conductivity

measurements for saturated solutions at 25°C was about ±4.8 S/m. For the dilute aqueous $NaBO_2$ solutions, the conductivity measurement average standard deviation was approximately ±0.05 S/m in the higher concentration range and ±0.005 S/m in the lower concentration range. At higher temperatures, more time was allowed for the conductivity measurements to be stabilized. The filtrate temperature was recorded along with the conductivity measurements which were later adjusted to the desired temperature of 50 and 75°C using a compensation factor of 2.1°C per degree. The water circulation bath, pH meter and conductivity meter set-up are shown in Fig. 4.5.
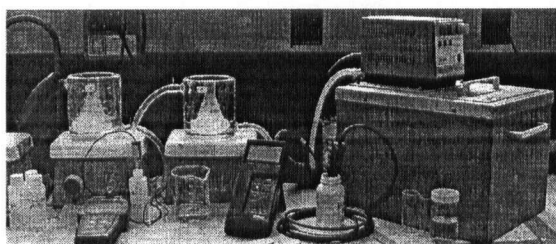
Figure 4.5: pH and Conductivity Experimental Set-up.

4.5.4 Viscosity

Cannon-Fenske routine viscometers are accurately calibrated glass tubes used to measure the kinematic viscosity of a fluid. Viscometers universal size number 75 (1.6-8 cSt), 100 (3-15 cSt), 150 (7-35 cSt) and 200 (20-100 cSt) were used to determine the filtrate (i.e. $NaBO_2$ alkaline solution) viscosity within ±0.2 %. The viscometer was filled with the fluid to be characterized and immersed in a water bath maintained at 25°C ± 1°C. As the water bath temperature fluctuation was greater at higher temperatures (50 and 75°C), a silicone based oil of a viscosity of 350 cSt was used. Special care was taken to prevent crystallization from occurring in the viscometer for the high temperature measurements. Since crystallization was associated with an increase in volume, it could have strain the internal wall of the viscometer. Temperature was allowed to stabilize before the first efflux flow time measurement was taken. However, with the set-up used, as shown in Fig. 4.7, it was difficult to precisely reach the desired temperature and maintain it constant throughout the viscosity measurement period.
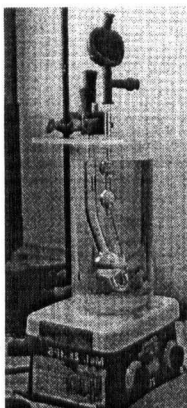
Figure 4.7: Viscometer Experimental Set-up.

The kinematic viscosity was obtained by multiplying the viscometer constant, extrapolated at the measurement temperature, with the efflux time. The dynamic viscosity was calculated by multiplying the experimental kinematic viscosity by the sample density. Between each experiment, the viscometer was rinsed alternately with distilled water and acetone, and dried with Argon to ensure proper drainage and avoid particle accumulation. Calibration runs were performed with distilled water before and after all measurements were taken, and in all cases the viscometer constant did not change significantly (< 2 %) during the course of the experiments. In the case of the alkaline aqueous $NaBO_2$ filtrate at 25°C, three measurements were taken per filling sample while in the case of the dilute aqueous $NaBO_2$ solution and alkaline aqueous $NaBO_2$ filtrate at 50 and 75°C, two measurements were taken per filling samples. The averaged standard deviation on the viscosity measurements on a particular sample were ± 0.007 cP and ± 0.03 cP respectively.

4.5.5 Density

The dilute aqueous $NaBO_2$ solution density was measured by weighting a pycnometer calibrated with de-ionized water and determined to have a volume of 25.034 ml at 25°C. Between measurements, the pycnometer was rinsed, dried in an oven at 70°C and cooled in a desiccator. A standard analytical balance with a precision of ±0.004 g was used for all weight measurements. The average standard deviation for the dilute $NaBO_2$ solution density measurements was ±0.001 g/ml. The average standard deviation for the

density measurements of saturated solutions at 25°C was about ±19 kg/m³. The concentrated alkaline aqueous solution filtrate density was determined by simple weight and volume measurements at room temperature. Volume was determined using graduated cylinders with a readability of ±0.5 ml.

4.6 Precipitate Characterization

The 10 wt% saturated solution wet residue mixtures obtained at 25°C were characterized by X-Ray Diffraction and Scanning Electron Microscopy. The precipitates were decanted and dried in an air oven at 50°C overnight. The dried crystals were crushed and conserved in Petri dishes. Their compositions may quite differ from the pure crystals as they might still contain a significant amount of the mother solution.

4.6.1 X-Ray Diffraction

X-Ray Diffraction (XRD) measurements were taken with a Rigaku Multiflex XRD 2 kW analyzer using Cu radiation. The diffraction patterns were recorded at 40 kV and 20 mA in the angular range of θ=10-65°, with a continuous scan speed of 2 deg./min and a sampling width of 0.05°. The intensities observed were corrected for background noise, and peaks were determined using the MDI Jade 7 software.

4.6.2 Scanning Electron Microscopy

Scanning Electron Microscopy (SEM) images were taken using a Hitachi model S-3500N system. Most precipitate crystallographic morphologies were observed at low scanning speed under low vacuum mode. The vacuum pressure was 20 Pa and the accelerating voltage was 20 kV.

CHAPTER V

RESULTS AND DISCUSSION

5.1 Aqueous NaBO₂ Solutions Physicochemical Properties

In this Section, the experimentally obtained solubility and transport properties of $NaBO_2$ aqueous solutions are analyzed. Tables B.1 to B.4 in Appendix B contain samples of the physicochemical property raw data analysed in the following pages.

5.1.1 Solubility

To test the validity of the experimental method, first the solubility of $NaBO_2$ was measured in water at 25°C by ICP-MS analysis of the filtrate and compared with values reported in the literature. The ICP-MS analysis boron concentration was converted to weight percentage in terms of $NaBO_2.2H_2O$ or $NaBO_2$ for ease of comparison. Table 5.1 compares the experimental solubility value obtained with the literature data.

Table 5.1: Comparison of $NaBO_2$ Solubility wt% in Water at 25°C.

Solubility [wt% as $NaBO_2.2H_2O$]	Solubility [wt% as $NaBO_2$]	Source / Reference
30.45	19.68*	Present work ICP-MS analysis ± 1.28 wt%, ± 3°C.
34.05*	22.00	[Blasdale, W. C. et al., (1938)]
33.43*	21.60	[Nies, N. P. et al., (1967)]
33.40	21.58*	[US Borax]
33.83*	21.86**	[Kojima, Y., et al., 2002 and 2004b]

* Converted based on molecular weight ratio.
** Estimated from visual observation.

An average solubility value of 30.45 ±1.28 wt% of $NaBO_2.2H_2O$ was determined at 25°C ± 3°C. In terms of anhydrous $NaBO_2$ the mean solubility experimental value obtained was 2.32 and 1.92 wt% lower than

the solubility values reported in the literature [Blasdale, W. C. *et al.*, (1938), Nies, N. P. *et al.*, (1967)]. All of these early studies used the methyl red - mannitol titration method to measure solubility. As mentioned in Section 4.5.1, in this analytical method, the boric acid concentration represents the total amount of boron in the sample. It is unknown if measures were taken to repel CO_2 trapped in the solutions. If present, aqueous CO_2 will react with water and form a bicarbonate which dissociates as a carbonic acid. This carbonate acid gets titrated as if it was boric acid, the resulting titration boron concentration values are falsified. Thus, if no special measures are taken to remove CO_2, this analytical boron detection method is not as precise as ICP-MS analysis, which did not exist at that time. Based on these results, the boron determination methodology employed was judged to be adequate for the purposes of this study.

5.1.2 Transport Properties

A) Conductivity

The solution concentrations covered in the conductivity experiments ranged from 0.0033 to 3.3 M. The measured conductivities were corrected for the solvent impurities by subtracting the conductivity of the solvent. As explained in Section 3.1.2 A), the various conductivity models are only valid for a certain concentration range. Hence, the Kohlrausch square root second extension correlation (Eq. 3.4) and the Kohlrausch cubic root correlation (Eq. 3.5) were not valid over the concentration range studied and did not represent the experimental data. To extrapolate at zero concentration, the variation of the molar conductivity as a function of the square root of the concentration for the $NaBO_2$-water system was plotted according to the Kohlrausch correlation and its first extension (Eq. 3.2 and 3.3) in Fig. 5.1. The molar conductivity decreased as the concentration increased. The non-linear model fitting equations obtained from the Sigma Plot accurately represented the experimental data. As seen in Fig. 5.1, the molar conductivity measurements seem to obey the lower orders of the Kohlrausch square root correlation at very dilute concentrations. The empirical value of K in Eq. 3.2 (78.28) is only 0.51 % lower than the value predicted from the Debye-Huckel-Onsager theory as per Eq. 3.9 (78.68). Eq. 3.3 seems to graphically represent the best fit at concentrations lower than 0.65 M. A theoretical limiting molar conductivity of

76.33 S.cm^2/mol was estimated by extrapolation using the Onsager expression (Eq. 3.10). Hence the limiting molar conductivity value obtained from Eq. 3.2 or 3.3 would have a relative error of 5.72 %.
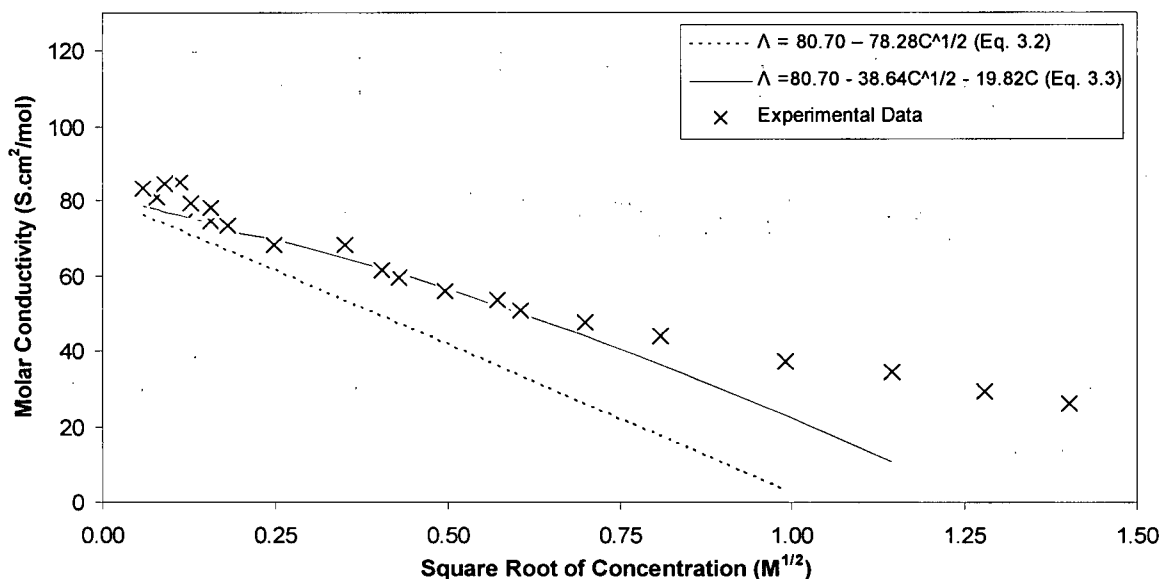
Figure 5.1: Molar Conductivity as a Function of the Square Root of the Concentration at 25°C ± 3°C.

Table 5.2 summarizes and compares the limiting molar conductivity values predicted by fitting the different models. As can be seen, all the values are relatively close. The limiting molar conductivity obtained from Eq. 3.2 and 3.3 is within 3.34 % from the value reported in the literature, which was reported in Table 3.4 [Maksimova, I. N. *et al.*, (1963)].

Table 5.2: Comparison of Limiting Molar Conductivity Predictions at 25°C ± 3°C.

Equation Description	Limiting Molar Conductivity [S.cm^2/mol]
Kohlraush Square Root (Eq. 3.2)	80.70
Kohlraush Square Root Extention 1 (Eq. 3.3)	80.70
Kohlraush Square Root Extention 2 (Eq. 3.4)	84.92
Kohlraush Cubic Root (Eq. 3.5)	91.19
Onsager Limiting Law (Eq. 3.10)	76.33

The limiting ionic transport properties summarized in Table 5.3 were calculated with Eq. 3.7, based on the NaBO$_2$ limiting molar conductivity value obtained from the lower orders of the Kohlrausch square root correlations (Eq. 3.2 and 3.3), i.e. 80.70 S.cm^2/mol.

Table 5.3: Infinite Dilution Transport Properties for Na$^+$BO$_2^-$ at 25°C ± 3°C.

Parameter [Units]	Limiting Molar Conductivity [S.cm^2/mol]	Ionic Mobility [10^{-4} cm^2/s.V]	Diffusion Coefficient [10^{-5} cm^2/s]	Transport Number [Dimensionless]
Na$^+$	50.11 [Dean, J. A., (1999)]	5.19	1.33	0.621
BO$_2^-$	30.59	3.17	0.81	0.379

The calculated BO$_2^-$ limiting molar conductivity is low compared to that of other monovalent ions, which is typically around 75 S.cm^2/mol [Dean, J. A., (1999)]. Yet, it is within 9 % of the value in Table 3.4 which was reported in the literature [Maksimova, I. N. *et al.*, (1963)]. The ionic mobility calculated shows that Na$^+$ moves faster when submitted to a potential gradient. However, the mobility value of BO$_2^-$ is outside of the reported mobility value range for various borate anions [Kesans, A. *et al.*, (1955)]. The calculated BO$_2^-$ diffusion coefficient is more than two times lower than that reported for the NO$_2^-$ ion (1.912x10^{-5} cm^2/s) [Lide, D. R., (2005-6)]. The calculated ionic transport numbers are indicative of the fact that the Na$^+$ ions carry most of the charge when current is applied to the NaBO$_2$ aqueous solution.

B) Viscosity

The upper limit of NaBO$_2$ concentration employed in the viscosity determination experiments was dictated by the solubility limit of NaBO$_2$.2H$_2$O in water at 25°C which ranged from 33.40 to 34.05 wt% as NaBO$_2$.2H$_2$O [Blasdale, W. C. *et al.*, (1938), Nies, N. P. *et al.*, (1967), Kojima, Y., *et al.*, (2002 and 2004b)]. The solution concentrations covered in the viscosity experiments ranged from 0.0025 to 0.5 M. Using the limiting ionic molar conductivities of Table 5.3, the value of coefficient A was estimated to be equal to 0.0099 1/M$^{1/2}$ using Eq. 3.14. This value is comparable to that reported for other electrolytes such as NaCl (0.0062 1/M$^{1/2}$) [Horvath, A. L., (1985)]. The value of coefficient B was estimated by plotting $(\eta/\eta_0 - 1)/C^{1/2}$ as a function of $C^{1/2}$ in accordance with the Jones-Dole and the extended Jones-Dole

correlations, corresponding to Eq. 3.13 and 3.15 respectively. The theoretical value of coefficient A at infinite dilution was used to fit the model. In Fig. 5.2, the best fitting model was plotted along with the experimental data. The $NaBO_2$ concentration increased as the viscosity increased and the equation was found more appropriate for very dilute concentrations.
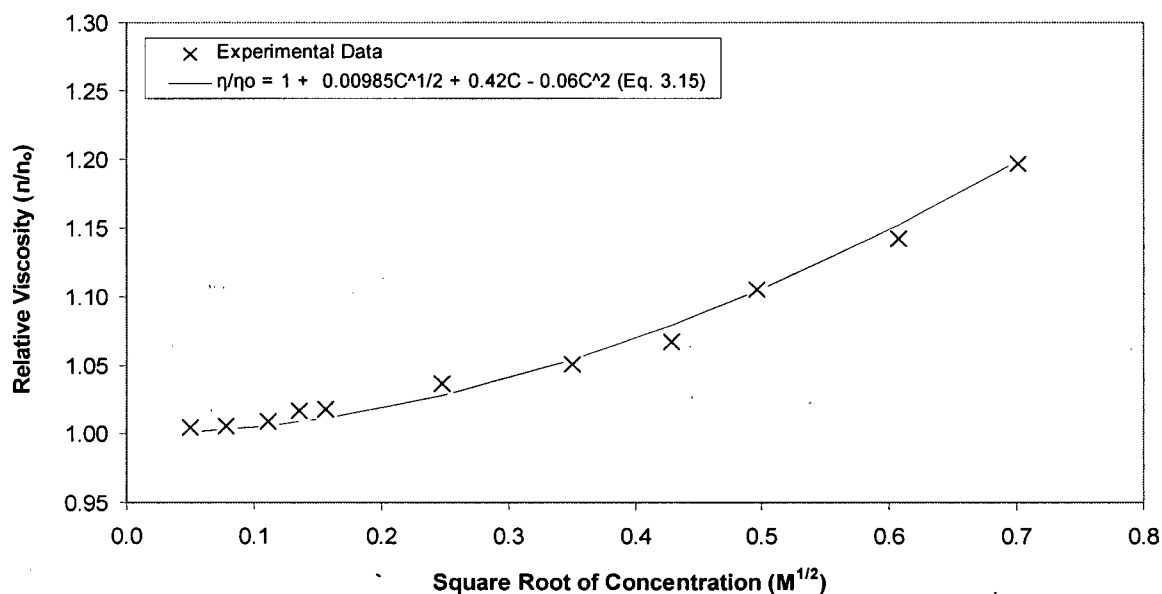
Figure 5.2: Relative Viscosity as a Function of the Square Root of the Concentration at $25°C \pm 3°C$.

Both model fittings were excellent, although Eq. 3.15 resulted in a slightly better fit than Eq. 3.13 as it is valid over a wider concentration range. Both correlations gave a small positive B coefficient value indicating that the association between the ions constituting the electrolyte are weak. The extended Jones-Dole correlation shown in Fig. 5.2 gave a $NaBO_2$ B coefficient of 0.4185 1/M. As the B coefficients are additive between the cation and anion, a B coefficient of -0.4660 1/M was obtained for BO_2^-. This value is one order of magnitude higher than that reported for the NO_3^- ion (-0.0450 1/M) [Horvath, A. L., (1985] but much smaller than the B coefficients of $B(OH)_4^-$ (0.233 1/M) in dilute aqueous solutions at $25°C$ [Corti, H. et al., (1980)]. It is expected that, in a solution of medium size ions (K^+, Cl^-), the different viscous forces tend to cancel each other [Erdey-Gruz, T., (1974)]. It is possible that, due to its size and shape, the BO_2^- ion slightly alters the solvent's viscosity and influences the orientation of the polar water molecules of the

solvent. However, the negative B coefficient values would indicate that, due to polarization effect, the ions have a stronger tendency to disorder the solvent's structure.

5.2 Aqueous NaBO$_2$ Solutions Physicochemical Properties with Alkali Additive

The solubility and physicochemical properties of saturated NaBO$_2$ aqueous solutions are analyzed in this Section. Appendix B contains examples of the raw data gathered in Tables B.5 and B.6. The summary of the averages used to carry out the analysis can be found in Table B.7. Unless indicated otherwise, all properties reported in this Section were measured in the filtrate of NaBO$_2$ saturated alkaline aqueous solutions. The error bars shown on the Figures showing measured values represent the standard deviation values obtained from a minimum of three measurements performed on three different solutions of the same composition. The standard deviations were calculated using the conventional statistical formula with N$\geq$ 3.

5.2.1 Solubility

As seen in Chapter 4, in this study, NaBO$_2$.2H$_2$O is the compound used to prepare the solutions. Hence, in this thesis all solubility values are reported in terms of NaBO$_2$.2H$_2$O. Figure 5.3 illustrates the solubility of NaBO$_2$.2H$_2$O as a function of the saturated solution hydroxide content at 25°C $\pm$ 3°C.
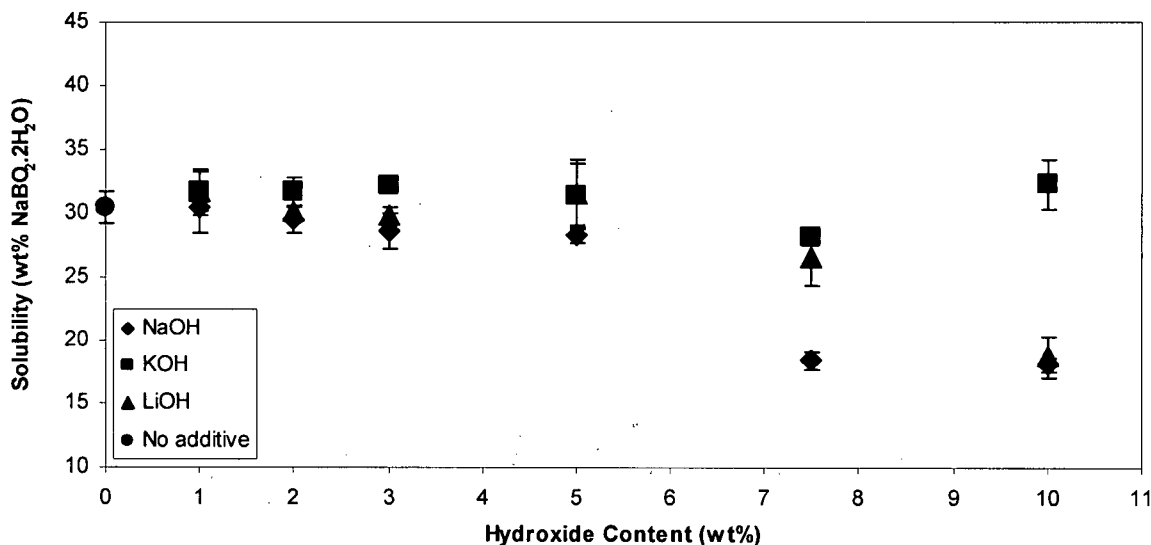
Figure 5.3: $NaBO_2$ Solubility as a Function of Hydroxide Content at 25°C ± 3°C.

The impact of alkali addition on $NaBO_2$ solubility differs greatly depending on the alkali hydroxide used. An addition of 1 wt% hydroxide resulted only in a minor solubility improvement in all cases over the solution containing no hydroxide. The solubility decreased in the cases of NaOH and LiOH, while it increased as the wt% KOH increased. The decrease in $NaBO_2$ solubility with increasing NaOH wt% agrees with the literature [Amendola S. C. et al., (2000a)]. More than 1 wt% of NaOH and LiOH resulted in solute precipitation. The trends observed are in accordance with the solubility of the alkali additive in pure water at 25°C, i.e. KOH is the most soluble, while LiOH is the least. However, the solubility of $NaBO_2.2H_2O$ in NaOH is slightly lower than in LiOH. The low solubility of NaOH can be attributed to the common ion effect, which further reduces the solubility of $NaBO_2$. At 10 wt% NaOH, the solubility was 10.89 wt% in terms of anhydrous $NaBO_2$, which is 4.11 wt% lower than the reported value [Suda, S., (2003b)]. Based on these results, it is not surprising that at room temperature, only a 2 wt% H_2 storage capacity can be achieved with concentrated NaOH solution before the precipitation of the reaction by-product [Hua, D. et al., (2003)]. Moreover, the solubility is linked to the hydration shell of the alkali cation. Small ions bind more solvent molecules and are more hydrated. The effective ionic radii of K^+, Na^+ and Li^+ in pure water are 3 Å, 4 Å and 6 Å respectively [Dean, J. A., (1999)]. Thus, the effective available H_2O content is the lower in the case of Li^+, yielding the lowest solubility for $NaBO_2$. Based on Fig. 5.4, KOH is a better alkali additive to maintain the hydrolysis by-product in solution. It is expected

that the non-monotonic behaviour observed about 7.5 wt% KOH is not due to experimental error but caused by a lost in the crystallization water of the $NaBO_2.2H_2O$ powder used to prepare the solutions. Hence, this measurement should be verified.

5.2.2 pH

Figure 5.4 shows that the filtrate pH increased as the quantity of alkali hydroxide added to the saturated $NaBO_2$ solution increased. As the pH measurements were taken after filtration of the saturated $NaBO_2$ alkaline aqueous solution, the concentration of $NaBO_2$ in the filtrate varied as shown in Fig. 5.3.
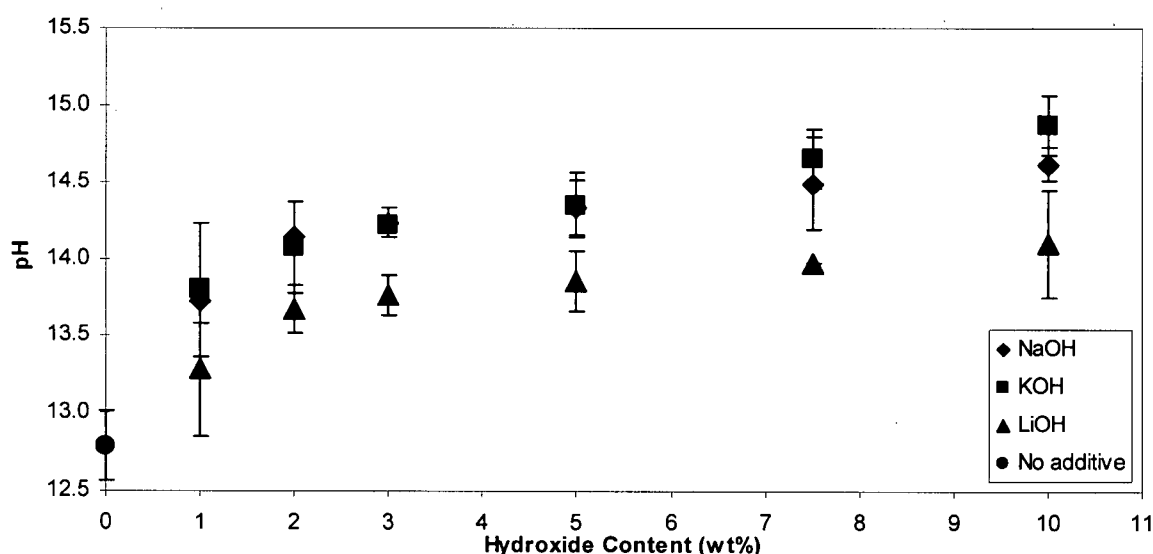
Figure 5.4: Filtrate pH as a Function of Hydroxide Content at $25°C \pm 3°C$.

The filtrate of the KOH- and NaOH-stabilized solutions exhibited a higher pH than the filtrate of the LiOH-stabilized solutions. More precipitation resulted in a filtrate with a lower pH, while less precipitation resulted in a higher pH. The $NaBO_2$ precipitation decreased the total alkali content of the filtrate, which lead to lower pH values. The addition of LiOH resulted in the lowest $NaBO_2$ solubility, and had a lower pH at 10 wt%. In NaOH, increased pH suppressed the solubility of $NaBO_2$ due to the presence of the common Na^+ ion. Hence, the KOH system was more alkaline than the NaOH system at 10 wt% due to the higher $NaBO_2$ solubility.

A) NaBH₄ Solution Half-Life

Although the high pH of the stabilized NaBH₄ solutions prompts safety concerns associated with the handling of caustic solutions, it is not a disadvantage as it significantly extends the life of the NaBH₄ solution by preventing the uncontrolled release of H₂. Employing Eq. 2.68, Fig. 5.5, demonstrates that the stability of NaBH₄ solutions depends on the solution's pH but is only indirectly independent of the cation present, through the resulting pH.
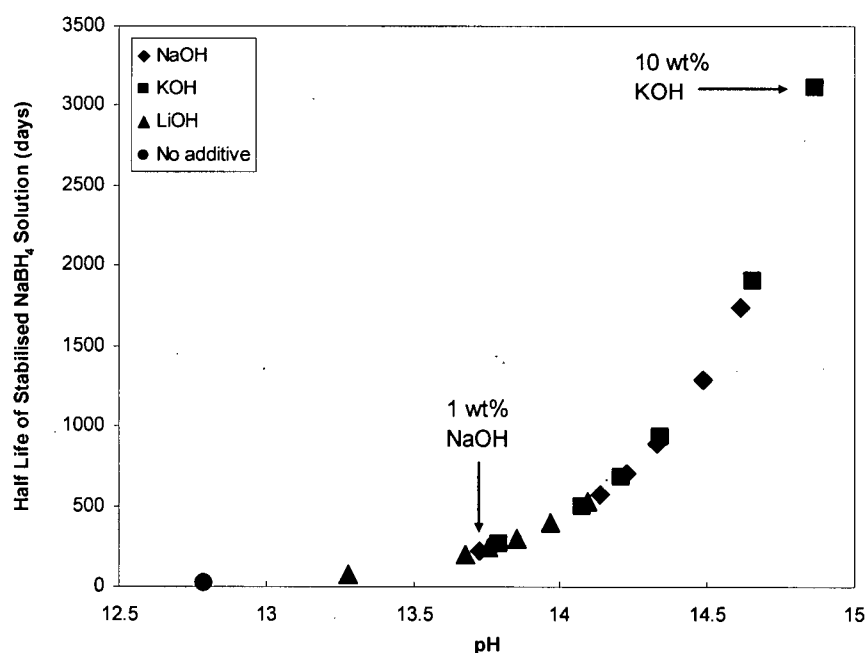
Figure 5.5: Estimated Half-Life of Alkaline Aqueous Solutions of NaBH₄ as a function pH at 25°C ± 3°C using Eq. 2.68.

The addition of 1 wt% NaOH extended the half-life to about 200 days over the NaBO₂ solution containing no hydroxide stabilizer. A NaBH₄ solution lifetime of nine years can be achieved with 10 wt% of KOH, providing hydrolysis catalysts are absent.

5.2.3 Transport Properties

A) Ionic Conductivity

a) Effect of Hydroxide Concentration on the Conductivity of Saturated NaBO₂ Solutions

Figure 5.6 shows the ionic conductivity of the filtrated $NaBO_2$ saturated aqueous solution as a function of alkali concentration.
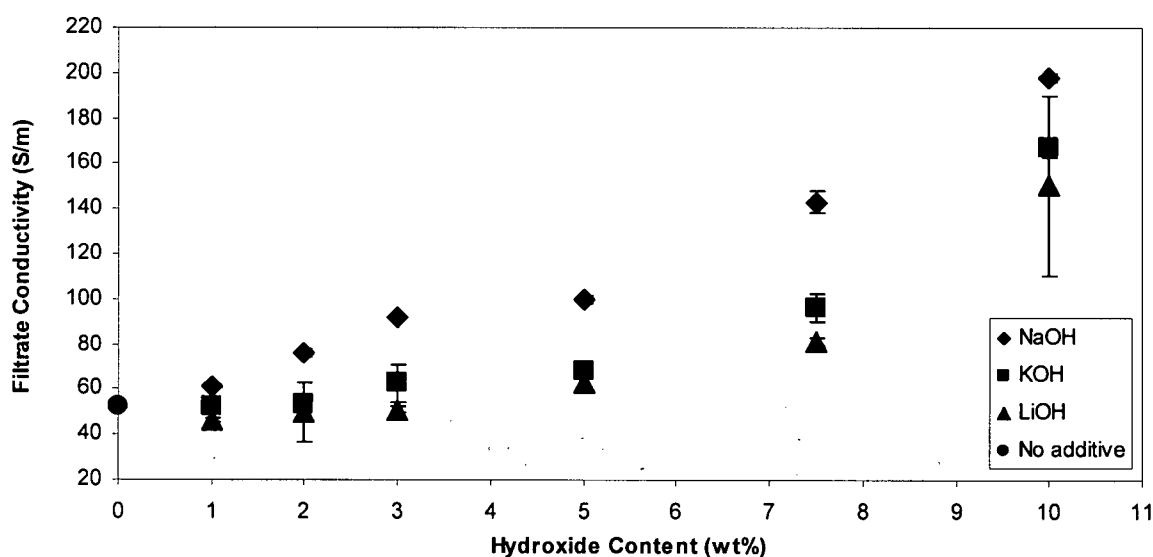
Figure 5.6: $NaBO_2$ Ionic Conductivity in the Filtrate as a Function of Hydroxide Content at 25°C ± 3°C.

The $NaBO_2$ content in the saturated solution was about 32-35 wt%. As seen previously, the extent of precipitation varied depending on the type of hydroxide and its concentration. Hence, the quantity of $NaBO_2$ in the filtrate fluctuated as the saturated solution composition changed. The ionic conductivity was measured after filtration of the saturated solution. Although the filtrate conductivity was proportional to the ion concentration and depended on the type of ion present, the conductivity measurements were difficult to interpret as the weight percentage of solute contained in the filtrate varied slightly with the alkali hydroxide concentration and the type of alkali hydroxide present as previously shown in Fig. 5.3.

113

For example, in the case of the NaOH-stabilized solution, there was a difference of 12.43 wt% between the maximum and minimum $NaBO_2$ content depending on the NaOH concentration used over the concentration range studied.

b) Unsaturated NaBO₂ Alkaline Aqueous Solution

The ionic conductivity was measured at a constant concentration of $NaBO_2$. Unsaturated aqueous solutions containing 5 wt% $NaBO_2.2H_2O$ and varying concentration of alkali additive were prepared. As the conductivity meter limit was reached in solutions containing more than 5 wt% hydroxide, no measurements could be made on solutions containing higher hydroxide concentrations. Figure 5.7 shows the ionic conductivity of the unsaturated solution as a function of the alkali hydroxide content.
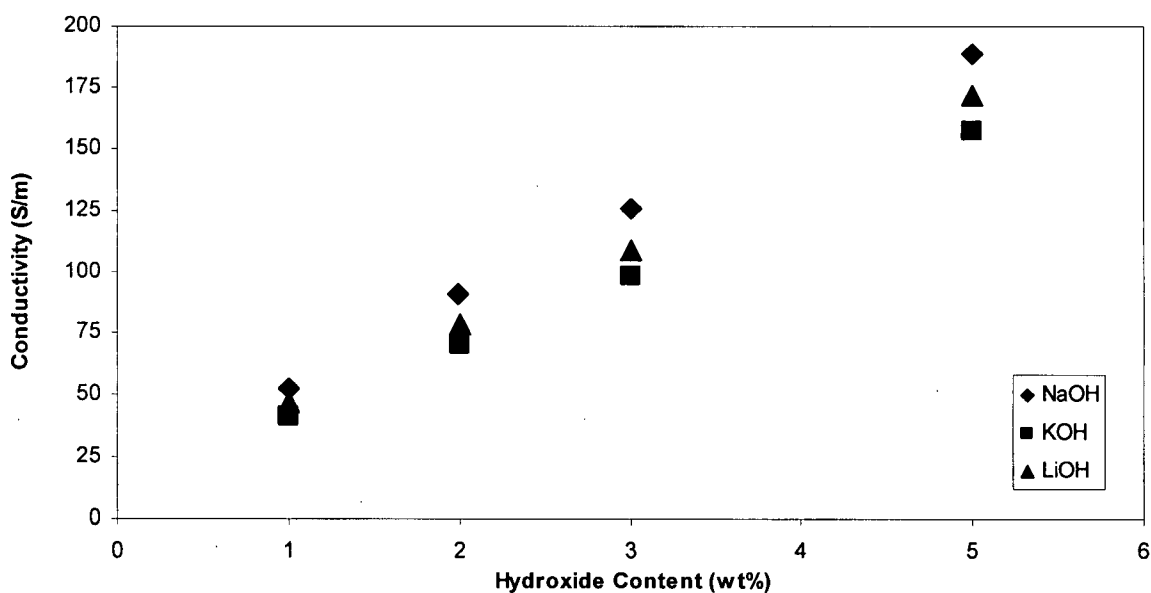
Figure 5.7: Ionic Conductivity as a Function of Hydroxide Content of the Unsaturated 5 wt% $NaBO_2$ Aqueous Solution at 25°C ± 3°C.

As shown in Table 3.3, the reported conductivity of a 5.4 wt% $NaBO_2$ aqueous solution is 39 S/m [Maksimova, I. N. et al., (1963)]. The ionic conductivity of strong electrolyte solutions depended significantly on the hydroxide concentration and almost increased linearly. This confirms that the OH⁻ ion is the most important contributor to the solution conductivity. This behaviour is also interlinked with the

increased in ionic mobility as the concentration increases. It would be expected that conductivity increase as the cation size decrease but this was not the case, when considering the effective ionic radius $(Li^+>Na^+>K^+)$. Similarly to the saturated solution case, the highest ionic conductivity was obtained for the NaOH-stabilized solution. However, in the unsaturated solutions, KOH as the alkali source yielded the lowest ionic conductivities rather than LiOH.

B) Molar Conductivity

a) Unsaturated NaBO₂ Alkaline Aqueous Solution

Figure 5.8 shows the molar conductivity as a function of hydroxide content for the unsaturated $NaBO_2$ solutions.
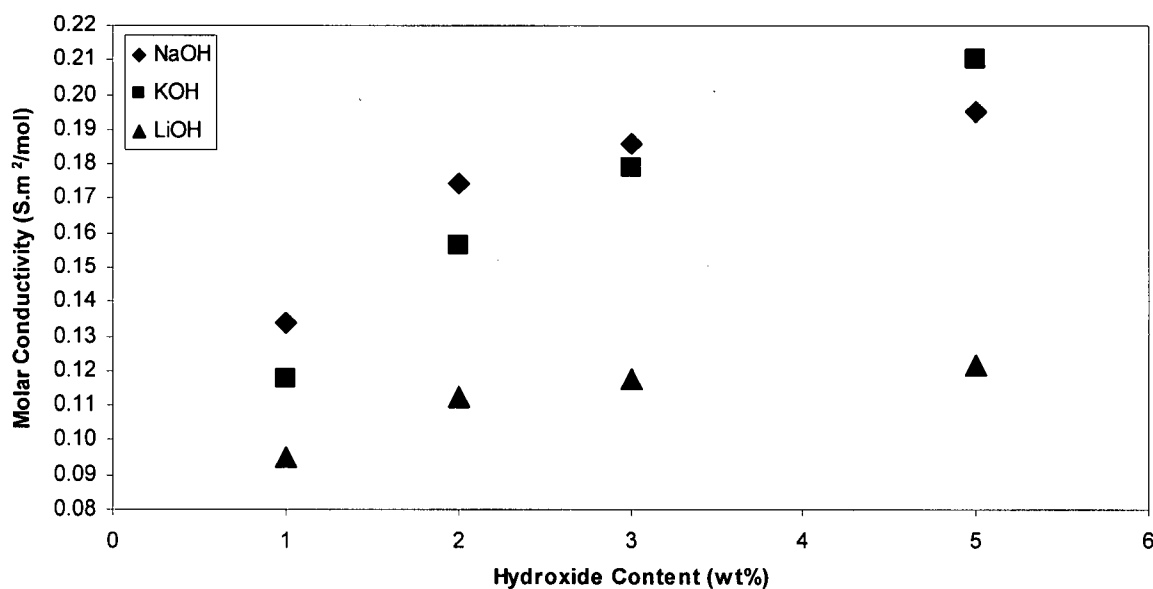
Figure 5.8: Molar Conductivity as a Function of Hydroxide Content of the Unsaturated 5 wt% $NaBO_2$ Aqueous Solution at 25°C ± 3°C.

Unlike the ionic conductivity, the molar conductivity of $NaBO_2$ unsaturated solutions did not increase linearly with the hydroxide concentration. Furthermore, the molar conductivity did not follow the same relative hydroxide order as in Fig. 5.8. As it is inversely proportional to the molecular weight of the alkali hydroxide present, the total solute molar concentration in the solution is mainly impacted by the hydroxide

concentration. Hence, the relative molecular weight of the alkali hydroxide, KOH>NaOH>LiOH, will have a direct impact on the molar conductivity. This explains why, at all hydroxide concentrations, the molar conductivity was the lowest for the LiOH-stabilized solution. However, the conductivity of the NaOH-stabilized solutions did not agree with this trend, probably due to the common ion effect. The molar conductivity of the NaOH- and LiOH-stabilized solutions seems to even out as the hydroxide content increases pass 3 wt%, while the KOH-stabilized solution molar conductivity seams to get steady at hydroxide concentrations greater than 5 wt%. It would be interesting to extend the concentration range studied to see if a maximum is reached in the molar conductivity at a certain hydroxide concentration. It appears that the molar conductivity of the KOH-stabilized solution crossed the NaOH-stabilized solution molar conductivity around 4 wt% hydroxide addition. At low wt%, the molar conductivity was the highest for the NaOH-stabilized solution, while at 5 wt% hydroxide, it is the highest for the KOH-stabilized solution. The reasons behind this behaviour are not clear at this point and require further investigations.

b) Effect of Hydroxide Concentration on the Molar Conductivity of Saturated NaBO$_2$ Solutions

Figure 5.9 shows the molar conductivity as a function of hydroxide content for the saturated NaBO$_2$ solutions.
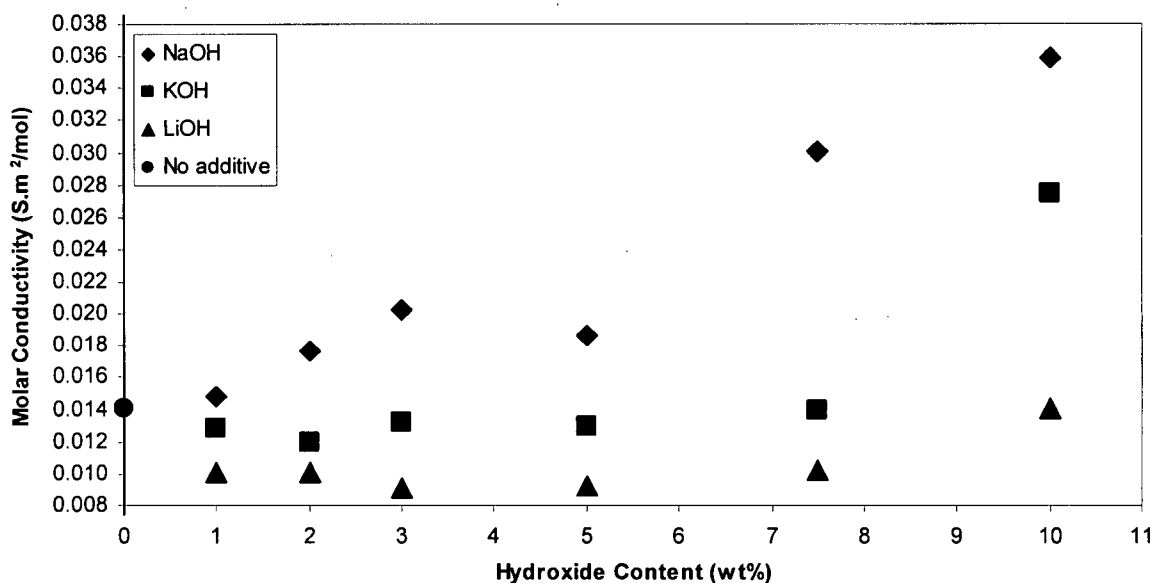
Figure 5.9: Molar Conductivity in the Filtrate as a Function of Hydroxide Content at $25^{\circ}C \pm 3^{\circ}C$.

As can be seen, the filtrate molar conductivity value obtained at 5 wt% NaOH seems to be about 21 % lower than the value which would be expected from the linear data trend. This error might be because the ionic conductivity measure is too low. For this solution composition, the filtrate ionic conductivity measurement was verified, and, as can be seen in Fig. 5.7, although it appears to be slightly low, it is within the experimental data trend. Hence, the error was attributed to a too high concentration of $NaBO_2$, probably caused by $NaBO_2.2H_2O$ hydration losses.

C) Dynamic Viscosity

The deionized water viscosity was 0.86 cP, while the filtrated $NaBO_2$ saturated aqueous solution viscosity was 5.31 cP. Figure 5.10 shows dynamic viscosity as a function of hydroxide content in the $NaBO_2$ saturated solution.

117
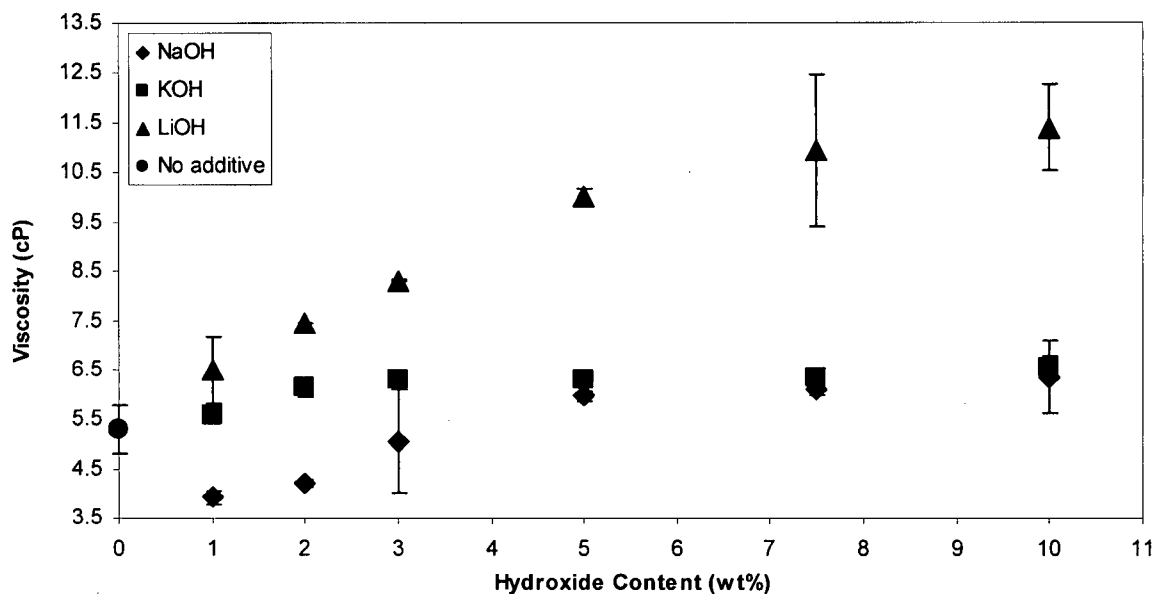
Figure 5.10: Filtrate Dynamic Viscosity as a Function of Hydroxide Content at 25°C ± 3°C.

At 25°C, the filtrate dynamic viscosity increased with increasing hydroxide content in the saturated solution, but not in a linear way. In pure water and at 25°C, the viscosity of a LiOH solution exceeds that of a NaOH solution, which in turns exceeds that of a KOH solution. However, in saturated $NaBO_2$ solutions, the filtrate dynamic viscosity of the saturated solutions containing LiOH or KOH exceeded the filtrate dynamic viscosity of the saturated solution containing NaOH. Furthermore, the addition of LiOH or KOH both resulted in higher dynamic viscosities than that of the $NaBO_2$ aqueous solution. Additions of NaOH resulted in a dynamic viscosity lower then that of the saturated $NaBO_2$ aqueous solution filtrate. As the addition of NaOH significantly decreased the solubility of $NaBO_2$, the resulting filtrate contained fewer Na^+ ions. Hence, the filtrate resistance to flow was lower and its resulting dynamic viscosity was closer to that of water. It is possible that precipitation of $NaBO_2$ in NaOH solution resulted in structural changes in the solvent, due to the common ion effect, and that significantly decreased the filtrate dynamic viscosity. In general, the larger the effective ionic radii of the cation ($Li^+>Na^+>K^+$), the sharper was the extent of the dynamic viscosity increase. The filtrate dynamic viscosity increased more sharply with increasing concentration of LiOH than with increasing concentrations of NaOH and KOH. While additions of LiOH also resulted in low $NaBO_2$ solubility, the large hydration shell of Li^+ significantly restrained the movement

118

of ions in the filtrate. It seems that the ion hydration effect raised the dynamic viscosity of the filtrate. The large hydrated Li^+ ion created more and more friction as the LiOH concentration increased in the saturated solution filtrate and the ion mobility decreased sharply. This ionic electric field reduces the mobility of the molecules and increases the dynamic viscosity of the solution. Hence, on a dynamic viscosity basis, KOH or NaOH seem to be better electrolytes than LiOH for the system under consideration.

D) Walden Product

From the experimentally determined viscosity and molar conductance values, it is possible to verify if the Walden's rule holds for the solutions studied. The filtrate Walden products for the saturated $NaBO_2$ aqueous solution as well as for the saturated $NaBO_2$ alkaline aqueous solutions were calculated and plotted as a function of the saturated $NaBO_2$ solution hydroxide content in Fig. 5.11. It was found that Eq. 3.21 was mostly applicable to the solutions at low hydroxide concentrations as the magnitude of the Walden product was significantly different at higher hydroxide concentrations. More specifically, the Wladen product remained constant for concentrations up to 3 wt% for NaOH and LiOH, and for concentrations up to 7.5 wt% for KOH.

At 1 wt% hydroxide, the Walden product of the filtrate containing hydroxide matched that of the filtrate of the aqueous $NaBO_2$ saturated solution to within ±4 to 22 %, while at 3 wt% hydroxide, it matched the filtrate of the aqueous $NaBO_2$ saturated solution within ±0.8 to 37 %. The best match was obtained at 2 wt% hydroxide content, as the Walden product of the filtrate containing hydroxide matched that of the filtrate of the aqueous $NaBO_2$ saturated solution within ±1.8 %. At this hydroxide concentration, the Walden product was independent of the solvent as the hydroxide cations were not significantly hydrated and their concentration had a similar effect on the filtrate transport properties, i.e. molar conductivity and dynamic viscosity.
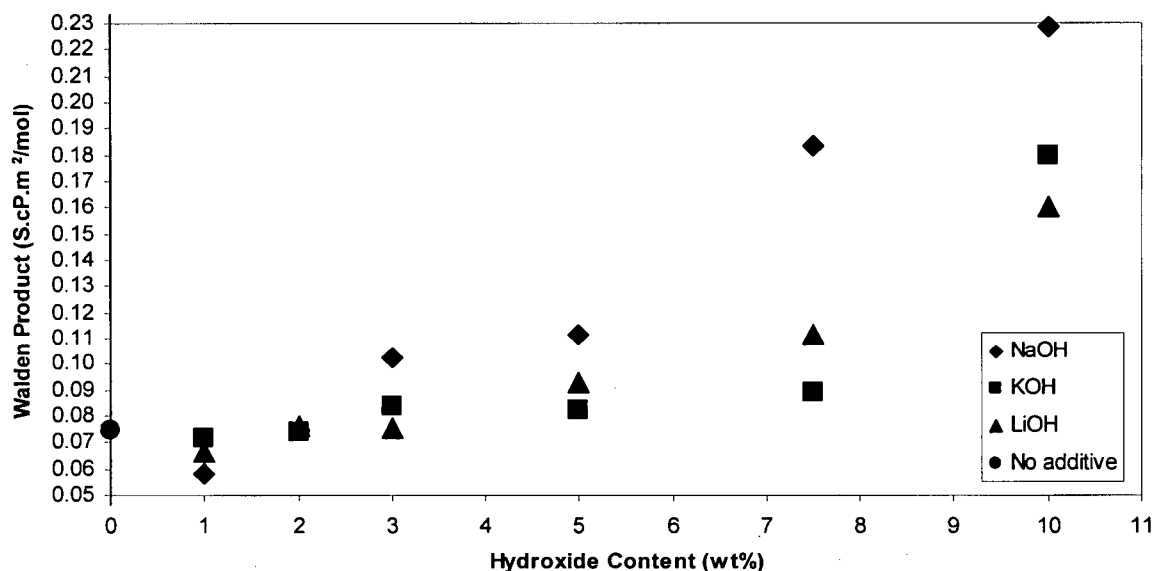
Figure 5.11: Filtrate Walden Product as a Function of Hydroxide Content at 25°C ± 3°C.

At high alkali hydroxide content, however, the right part of Eq. 3.22 yielded values over two orders of magnitude greater than the left part of Eq. 3.22. Therefore, it can be concluded that those solutions are outside of the applicability limit of the Walden rule as other ionic interactions were significant and had to be taken into account. At 10 wt% hydroxide, the structure of the filtrate of the saturated salt solution more closely resembles that of a molten salt than that of water. It is worth noting that the solute-solvent interactions in the filtrates were appreciably greater when the solution was stabilized with NaOH rather than KOH and LiOH.

5.2.4 Specific Gravity

The filtrate specific gravity as a function of hydroxide concentration is shown in Fig. 5.12. The filtrate specific gravity corresponds to the ratio of the solution density and the density of the deionized distilled water used to make the solutions at the same temperature. The filtrate specific gravity increased proportionally with the hydroxide content in the saturated solution. Similarly, for a fixed $NaBH_4$ concentration at 20°C, the specific gravity of alkaline aqueous $NaBH_4$ solution increases as the wt% NaOH increases [Li, Z. P., (2004)]. A solution containing 25 wt% $NaBH_4$ and 10 wt% NaOH had a specific

120

gravity of 1.9 at 20°C, this is higher than the specific gravity of the filtrate of a saturated $NaBO_2$ solution containing 10 wt% NaOH at 25°C which is about 1.34. In pure water, the density of KOH is greater than that of NaOH, which exceeds the density of LiOH, and parallels the order of magnitude of the molecular weight of the three alkali additive. Accordingly, the KOH-stabilized filtrate had the highest specific gravity, which exceeded the specific gravity of the LiOH-stabilized filtrate. However, the specific gravity of the NaOH-stabilized filtrate was the lowest, probably due to the low $NaBO_2$ solubility and the common ion effect.
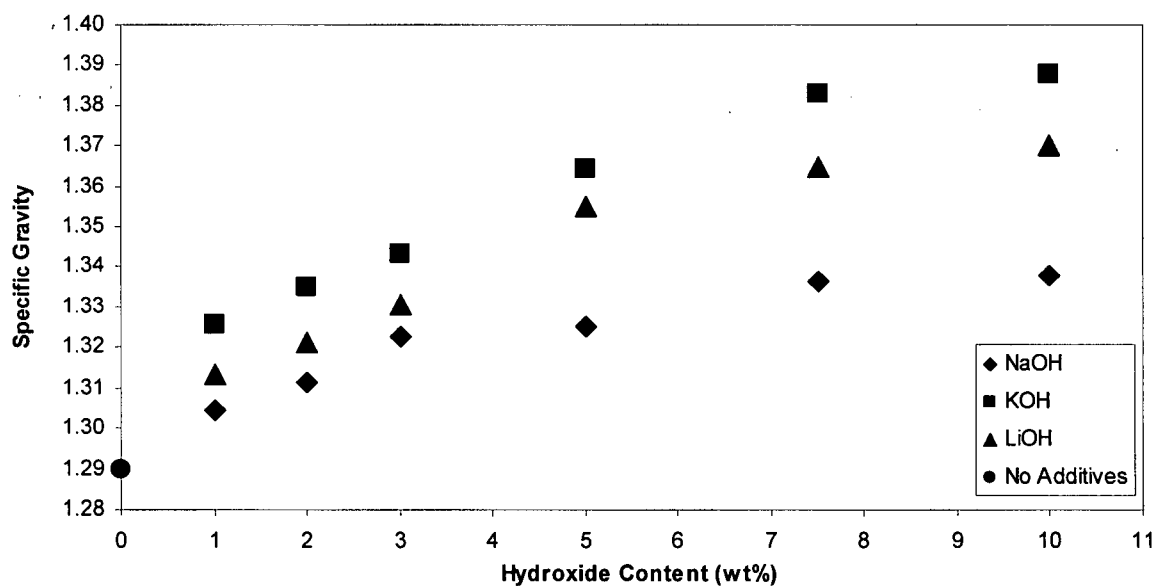
Figure 5.12: Filtrate Specific Gravity as a Function of Hydroxide Content at 25°C ± 3°C.

5.3 Effect of Temperature

The temperature effect was investigated by carrying out experiments on saturated $NaBO_2$ aqueous solutions containing 0, 1, 5 and 10 wt% NaOH and KOH at 50 and 75°C. Only two trials were conducted per solution. Due to experimental difficulties in retrieving a representative sample and in filtrating the gel-like solutions, some experimental results obtained did not represent the solution content and had to be discarded. At 50 and 75°C, the solutions were very viscous and sticky. It appears that equilibrium was not easily achieved within 5 hours of stirring as liquid and solid phase separation was not achieved, even after

an hour of settling. Hence, the retrieval of representative filtrate samples for solubility and physicochemical parameter measurements was nearly impossible. Table B.8 in Appendix 2 is a summary of the averaged physicochemical properties for the solution studied at 25, 50 and 75°C.

5.3.1 Solubility

At 50 and 75°C, the filtrate samples sent for ICP-MS analysis were completely solidified since, as soon as the filtrate temperature decreased to room temperature, significant crystallization occurred in the super-saturated solutions. Even though digesting of the sample was carried out prior to ICP-MS analysis, it is suspected that the element concentration values obtained are not representative of the expected sample content.

Figure 5.13 shows the experimentally measured $NaBO_2.2H_2O$ solubilities. As expected, the solubility increased as temperature increased. At 50 and 75°C, increasing hydroxide concentration reduced the solubility of $NaBO_2$ in all cases. However, it can be seen that $NaBO_2.2H_2O$ solubility values in excess of 100 wt% were obtained, which is not mathematically possible. The $NaBO_2.2H_2O$ solubility values obtained in aqueous solution at 50 and 75°C were much greater than the ones reported in the literature. At 50 and 75°C, average solubility values of 92.22 and 113.56 wt% $NaBO_2.2H_2O$ were obtained, respectively. According to the values listed in Table 3.9, the reported average solubility for each temperature should be around 49.92 and 66.13 wt% $NaBO_2.2H_2O$ respectively. Hence, the experimentally determined solubility values are almost twice as large as the ones reported in the literature when compared on the same $NaBO_2.2H_2O$ solubility basis. This excess solubility can be partly attributed to $NaBO_2.2H_2O$ hydration water lost during the solution preparation at 50 and 75°C. For example, based on $NaBO_2$, average solubility values of 59.59 and 73.38 wt% would be obtained at 50 and 75°C, respectively. However, even when no hydration water is taken into account, the solubility values are about 10 % higher than the ones reported in the literature. Similarly, at 75°C, solubility values in excess of 100 wt% were obtained for saturated $NaBO_2$ alkaline aqueous solutions stabilized with 1 and 5 wt% hydroxide. The experimental causes of the error in the measurement are not clear at this time and require further investigations. Hence,

the values shown in Fig. 5.14 should be used with caution. A suitable and reliable methodology to determine the solubility of NaBO2.2H$_2$O at 50 and 75°C needs to be developed.
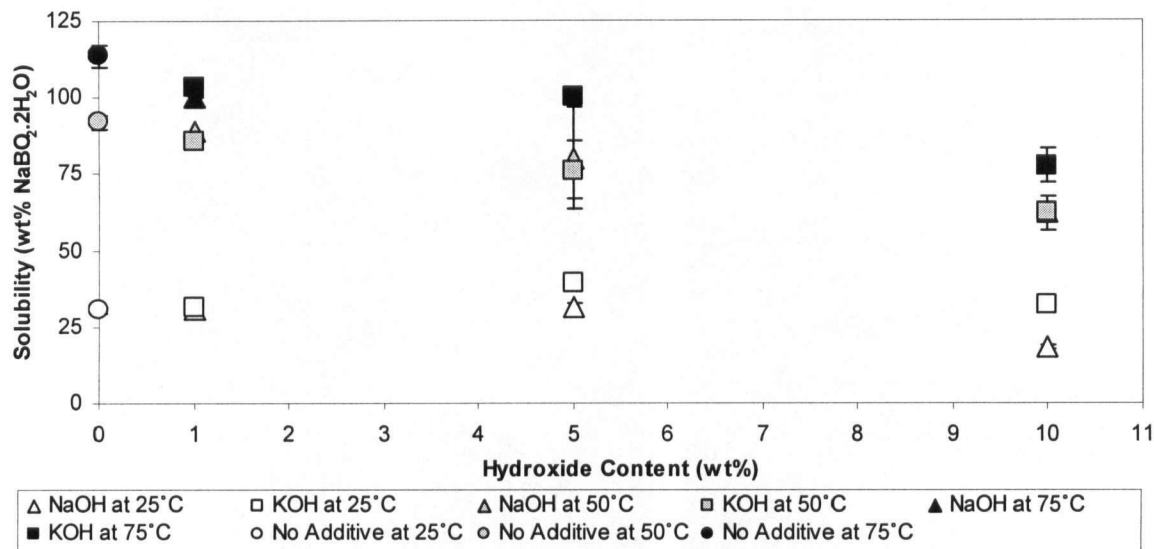
Figure 5.13: NaBO$_2$ Solubility as a Function of Hydroxide Content at 25, 50 and 75°C.

5.3.2 Transport Properties

A) Ionic Conductivity

a) Effect of Hydroxide Concentration on the Conductivity of Saturated NaBO$_2$ Solutions

Figure 5.14 illustrates the ionic conductivity measurements as a function of NaOH and KOH content at 25, 50 and 75°C in the filtrate of saturated NaBO$_2$ solutions. As expected, conductivity increased with the hydroxide concentration and with temperature. However, it was not the case at 75°C at hydroxide content greater than 1 wt%. Hence, at this temperature, the composition of the filtrate sample characterized did not represent the content of the solution and the data were not included in Fig. 5.14.
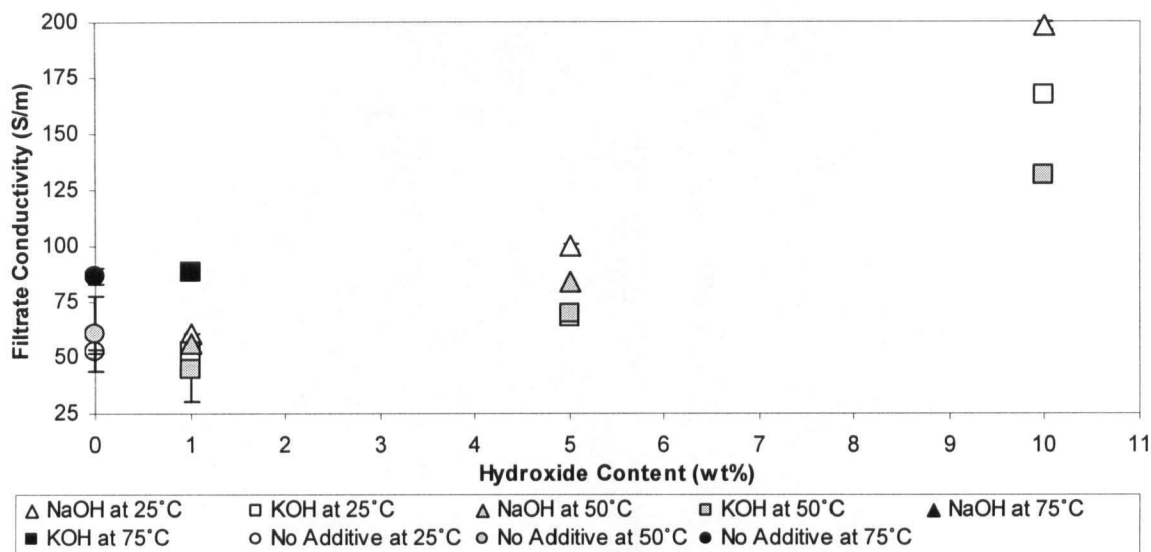
Figure 5.14: NaBO$_2$ Ionic Conductivity in the Filtrate as a Function of Hydroxide Content at 25, 50 and 75°C.

For a more meaningful analysis, conductivity measurements on saturated NaBO$_2$ alkaline aqueous solutions should be performed without filtration. To verify the conductivity trends, conductivity measurements were performed in unsaturated NaBO$_2$ alkaline aqueous solutions.

b) Unsaturated NaBO$_2$ Alkaline Aqueous Solution

Conductivity measurements were performed on unsaturated 5 wt% NaBO$_2$ solutions as a function of hydroxide content at 50 and 75°C. When no alkali additives were present, conductivity values of 36.25 and 59.40 S/m were obtained at 50 and 75°C respectively. When using Eq. 3.24 and 3.25 with the conductivity measured at 25°C, predicted conductivity values of 42.33 and 57.42 S/m were calculated at 50 and 75°C respectively. According to this, in solutions containing no alkali, the conductivity values measured would be about 14% too low at 50°C and about 3% too high at 75°C. The conductivity values measured were plotted along with the conductivity measurements at 25°C in Fig. 5.15 and 5.16, for NaOH and KOH, respectively.

124
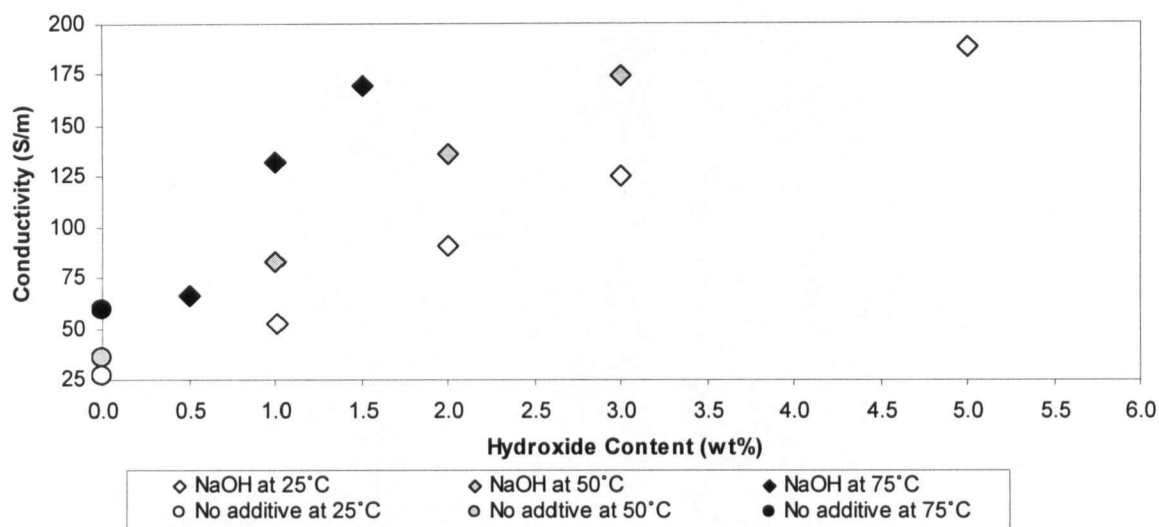
Figure 5.15: Ionic Conductivity as a Function of NaOH of the Unsaturated 5 wt% NaBO$_2$ Aqueous Solution at 25, 50 and 75°C.
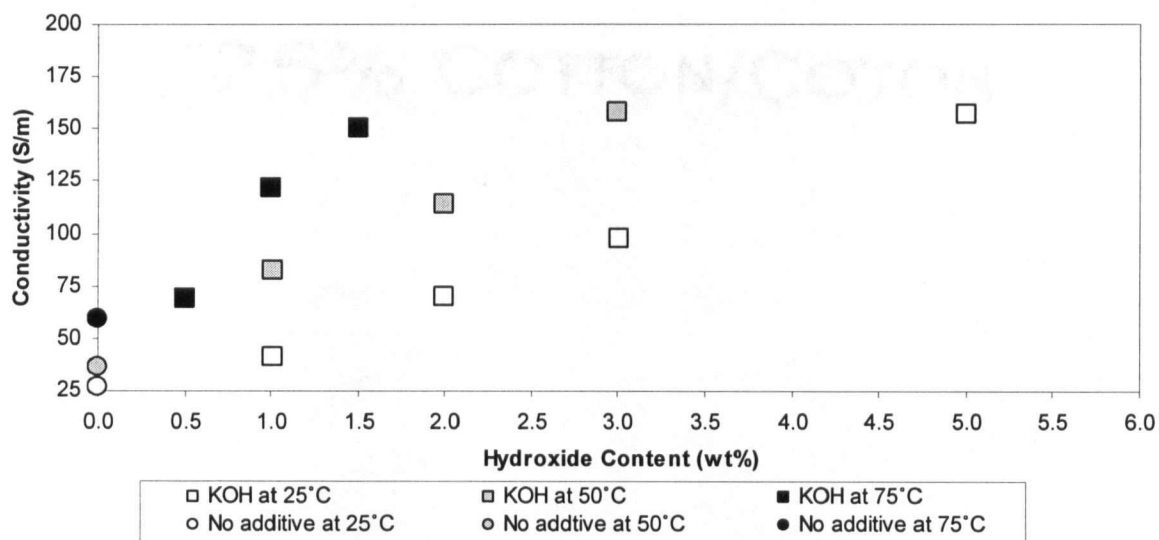
Figure 5.16: Ionic Conductivity as a Function of KOH of the Unsaturated 5 wt% NaBO$_2$ Aqueous Solution at 25, 50 and 75°C.

Lower hydroxide weight percentages were used as the conductivity meter limit of 200 S/m was easily reached at high temperatures. It seems that, at 75°C and 0.5 wt% hydroxide, the conductivity measurements are slightly lower than expected, based on the conductivity values obtained for the solution containing no alkali additive. These measurements should be verified.

125

B) Molar Conductivity

a) Unsaturated NaBO₂ Alkaline Aqueous Solution

The unsaturated conductivity values of Fig. 5.15 and 5.16 were used to construct the graph shown in Fig. 5.17. The molar conductivity increased as temperature increased. At 50°C, the molar conductivity of the solutions stabilized with NaOH exceeded the ones with KOH. However, at 75°C, the molar conductivity of solutions containing either stabilizer was the same.
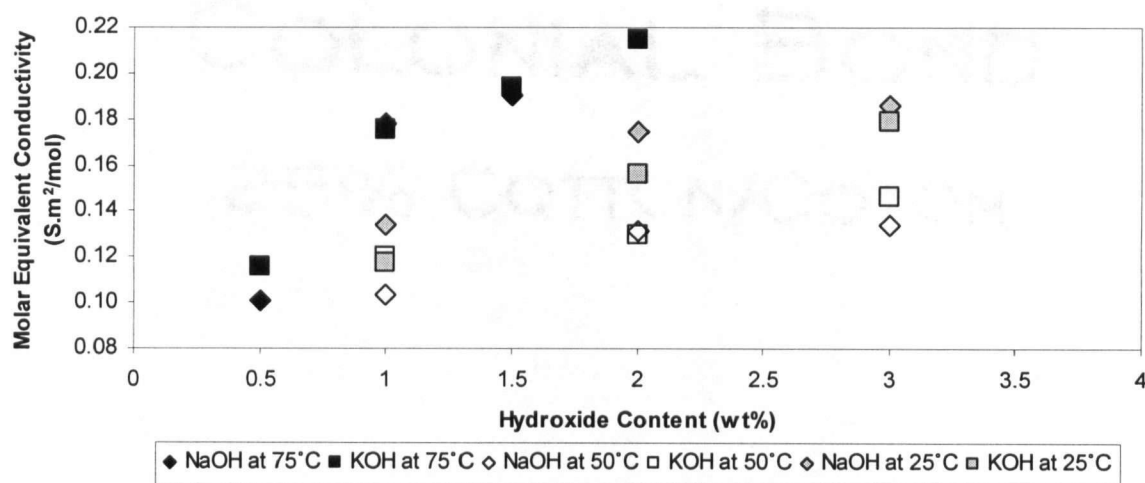
Figure 5.17: Molar Conductivity as a Function of Hydroxide Content of the Unsaturated 5 wt% NaBO₂ Aqueous Solution at 25, 50 and 75°C.

5.4 Effect of Glycine Additions

In Section 3.1.4 D), it was reported that glycine improved the aqueous solubility of the sodium tetra- and pentaborates, as well as $LiBO_2$, while it decreased the solubility of $NaBO_2$ and KBO_2. To see if the addition of LiOH would have a positive impact on the $NaBO_2$ solubility results, preliminary experiments were conducted to investigate the effect of the addition of 10 wt% glycine, on the solubility and physicochemical properties of saturated aqueous solutions of $NaBO_2$ containing 0 and 5 wt% alkali hydroxide at 25°C ± 3°C. Two trials were conducted per solution composition. The summary of the averaged physicochemical parameters measured can be found in Table B.9 in Appendix B.

5.4.1 Solubility

The addition of 10 wt% glycine significantly decreased the solubility of $NaBO_2$ in water. The solubility of $NaBO_2$ in 10 wt% glycine in water was found to be equal to 0.68 wt% at 25°C, which is 3.6 times lower than the value listed in Table 3.9. As shown in Table 5.4, the use of 5 wt% alkali stabilizers had little improvement effect on the resulting solubility. The observed solubility decrease in the presence of glycine confirms that, even in aqueous solutions stabilized with LiOH, $NaBO_2$ is the main solute formed. If $LiBO_2$ would be formed, the solubility would be expected to increase in the presence of glycine in aqueous solution as discussed in Section 3.1.4 D) [Skvortsov, V. G. et al., (1988)].

Table 5.4: Effect of Glycine on the Filtrate Solubility as a Function of Hydroxide Content at 25°C ± 3°C.

Glycine Content [wt%]	Alkali Content [wt%]	$NaBO_2 \cdot 2H_2O$ Solubility [wt%]	Standard Deviation [± wt%]
0	0	30.45	1.28
0	5, NaOH	29.83	2.83
0	5, KOH	31.46	2.27
0	5, LiOH	31.51	0.00
10	0	0.68	0.01
10	5, NaOH	0.78	0.02
10	5, KOH	1.06	0.06
10	5, LiOH	1.17	0.02

Further tests should be performed to investigate the effect of lower glycine concentrations and higher alkali additive concentrations on the solubility of $NaBO_2$ in water. Also, solubility measurements should be made to investigate the solubility of glycine in alkaline aqueous $NaBO_2$ solutions.

5.4.2 pH

The addition of glycine decreased the pH of the deionised distilled water. The addition of hydroxide increased the filtrate pH, but the resulting pH was still lower than that of the filtrate containing no glycine. When comparing Fig. 5.5 to Table 5.5, it is clear that the extent of the pH increase resulting from the

addition of 5 wt% alkali hydroxide is significantly lower when 10 wt% glycine is present in the alkaline aqueous saturated $NaBO_2$ solution filtrate.

Table 5.5: Effect of Glycine on the Filtrate pH as a Function of Hydroxide Content at $25^{\circ}C \pm 3^{\circ}C$.

Glycine Content [wt%]	Alkali Content [wt%]	Filtrate pH	Standard Deviation [± pH unit]
0	0	12.79	0.22
0	5, NaOH	14.33	0.17
0	5, KOH	14.34	0.22
0	5, LiOH	13.85	0.19
10	0	11.8	0.01
10	5, NaOH	11.86	0.02
10	. 5, KOH	12.55	0.23
10	5, LiOH	12.03	0.25

A) NaBH₄ Solution Half-Life

Figure 5.18 presents the $NaBH_4$ solution half-life estimates based on the filtrate pH values displayed in Table 5.5. As can be anticipated, the addition of glycine decreased the expected half-life of the solution. The decrease in half-life due to glycine addition is not as significant as that caused by a rise in temperature.
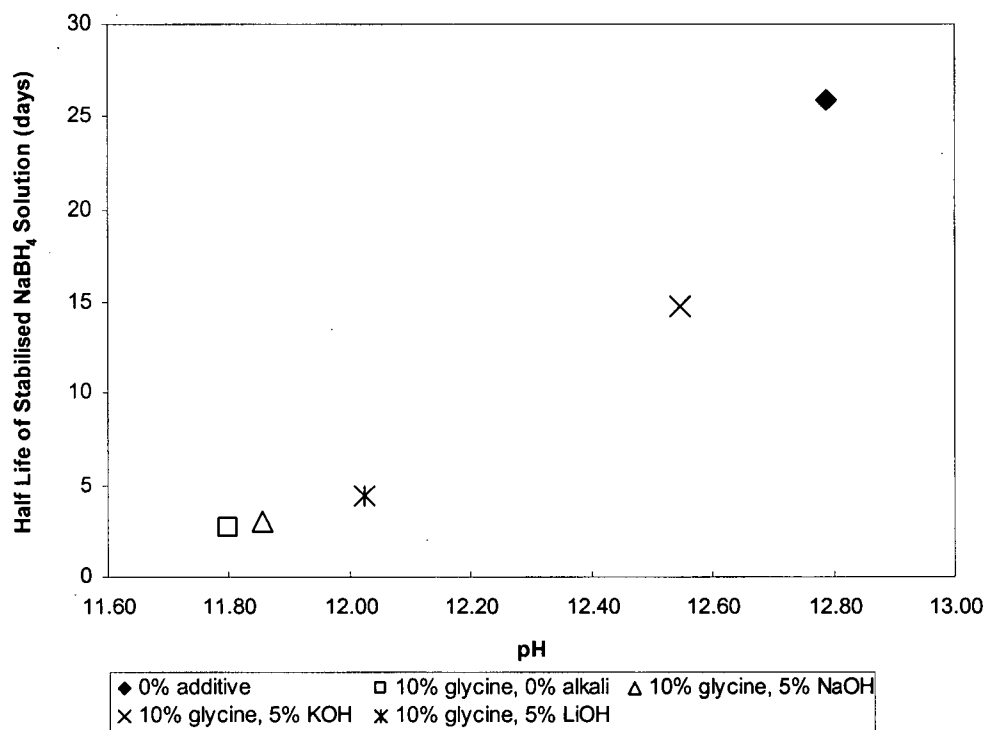
Figure 5.18: Effect of Glycine on the Estimated Half-Life of Alkaline Aqueous Solutions as a function pH at $25^\circ C \pm 3^\circ C$ using Eq. 2.68.

5.4.3 Transport Properties

A) Ionic Conductivity

Table 5.6 reveals that the 10 wt% glycine $NaBO_2$ alkaline aqueous solution conductivity decreased when NaOH and LiOH were used as the stabilizers, but increased when stabilized with KOH. However at 5 wt% KOH, the extent of the 10 wt% glycine conductivity improvement was not as significant as when no glycine was present in the solution. Nevertheless, more measurements should be taken to further investigate the conductivity improvement resulting from the combination of KOH and glycine at lower glycine concentrations.

Table 5.6: Effect of Glycine on the Filtrate Ionic Conductivity as a Function of Hydroxide Content at 25°C ± 3°C.

Glycine Content [wt%]	Alkali Content [wt%]	Ionic Conductivity [S/m]	Standard Deviation [± S/m]
0	0	52.67	0.86
0	5, NaOH	99.77	1.40
0	5, KOH	68.18	3.50
0	5, LiOH	62.76	2.04
10	0	48.75	0.64
10	5, NaOH	50.75	1.34
10	5, KOH	56.55	0.21
10	5, LiOH	36.40	0.14

B) Molar Conductivity

The molar conductivity was calculated based on the total solute concentration in the solution, i.e. glycine, hydroxide and $NaBO_2$. Table 5.7 shows that the molar conductivity was the greatest when only glycine was present in the saturated aqueous solution of $NaBO_2$. The addition of 5 wt% hydroxide decreased the molar conductivity of the saturated $NaBO_2$ aqueous solution filtrate containing 10 wt% glycine. The extent of the molar conductivity decrease was the greatest in the case of 5 wt% LiOH addition.

Table 5.7: Effect of Glycine on the Filtrate Molar Conductivity as a Function of Hydroxide Content at 25°C ± 3°C.

Glycine Content [wt%]	Alkali Content [wt%]	Molar Conductivity [S.m^2/mol]
0	0	0.0141
0	5, NaOH	0.0186
0	5, KOH	0.0130
0	5, LiOH	0.0092
10	0	0.0275
10	5, NaOH	0.0153
10	5, KOH	0.0189
10	5, LiOH	0.0080

C) Dynamic Viscosity

As seen in Table 5.8, the dynamic viscosity of the filtrate of the saturated $NaBO_2$ aqueous solutions containing glycine was significantly lower than in the absence of glycine. Like for the filtrate containing no glycine, at 5 wt% hydroxide, the viscosity was the greatest when LiOH was used as the stabilizer.

Table 5.8: Effect of Glycine on the Filtrate Dynamic Viscosity as a Function of Hydroxide Content at 25°C ± 3°C.

Glycine Content [wt%]	Alkali Content [wt%]	Dynamic Viscosity [cP]	Standard Deviation [± cP]
0	0	5.31	0.49
0	5, NaOH	31.90	0.10
0	5, KOH	34.53	0.08
0	5, LiOH	39.40	0.17
10	0	2.18	0.09
10	5, NaOH	1.77	0.21
10	5, KOH	1.97	0.20
10	5, LiOH	3.14	0.00

5.4.4 Specific Gravity

Glycine has a molecular weight of 75.07 g/mol, which is greater than that of the three alkali hydroxide additives used in this study. Table 5.9 proves that, as expected, the addition of glycine increases the specific gravity of the filtrate. Even though at 5 wt% alkali additive, the filtrate specific gravities increased, the extent of the increase was not as pronounced as for solutions containing no glycine as shown in Fig. 5.13. This is mainly because the glycine addition significantly decreased the solubility of $NaBO_2$.

Table 5.9: Effect of Glycine on the Filtrate Specific Gravity as a Function of Hydroxide Content at 25°C ± 3°C.

Glycine Content [wt%]	Alkali Content [wt%]	Specific Gravity
0	0	1.2896
0	5, NaOH	1.3248
0	5, KOH	1.3644
0	5, LiOH	1.3600
10	0	1.3097
10	5, NaOH	1.2914
10	5, KOH	1.3304
10	5, LiOH	1.3272

5.5 Precipitate Characteristics

X-Ray Diffraction and Scanning Electron Microscopic characterization was carried on the composition of the precipitates formed from the saturated aqueous solutions of $NaBO_2$ stabilized with 10 wt% hydroxide. At high pH, replacement of one solute by another could to take place. In the case of the solutions stabilized with KOH and LiOH, KBO_2 and $LiBO_2$ could be formed as the precipitate. The hydration level of the precipitate could also be affected by the type of alkali additive present. Information on the precipitates formed is reviewed in this Section.

5.5.1 X-Ray Diffraction

The precipitates formed from supersaturated $NaBO_2$ solutions containing 10 wt% alkali additive samples were examined by X-Ray Diffraction. Although there were analogies between most XRD patterns, there was a broad variety in the nature of the precipitates formed. Since this work did not intend to be a detailed crystallographic study, the drying process conditions were not strictly controlled and varied from one sample to another. Consequently, precipitate crystals formed from the same solution composition could vary. The molar ratio of Na_2O, B_2O_3 and H_2O, solution pH and chemical composition, heat treatment, hydration level, recrystallization or decomposition conditions and pressure are all factors affecting the precipitate crystal formation. Hence, depending on the hydroxide used, hydrated $NaBO_2$ might not be the only precipitate formed and hydrated borates of KBO_2 and $LiBO_2$ could also be present.

Figure 5.20 shows selected XRD patterns obtained for each solution type and compares them to the peaks obtained from pure $NaBO_2.2H_2O$. The most important peaks of other precipitate XRD patterns obtained can be found in Appendix C. The XRD patterns shown in Fig. 5.19 are considered to be the most relevant as they were performed a shorter time period after the precipitate preparation. The XRD scans obtained for the precipitates formed from KOH and LiOH solutions seem to indicate that hydrated $NaBO_2$ is the predominant species in all cases. The most prominent diffraction peak of the NaOH-stabilized precipitate was recorded at a 2θ of $16.786°$ and corresponded to that of pure $NaBO_2.2H_2O$. The most important peak of the KOH- and LiOH-stabilized precipitates occurred at a two-theta of 31.2. It was at a higher two-theta value than the most important $NaBO_2.2H_2O$ peak. According to the MDI Jade 7 software database, this peak is a characteristic of $NaBO_2.4H_2O$.
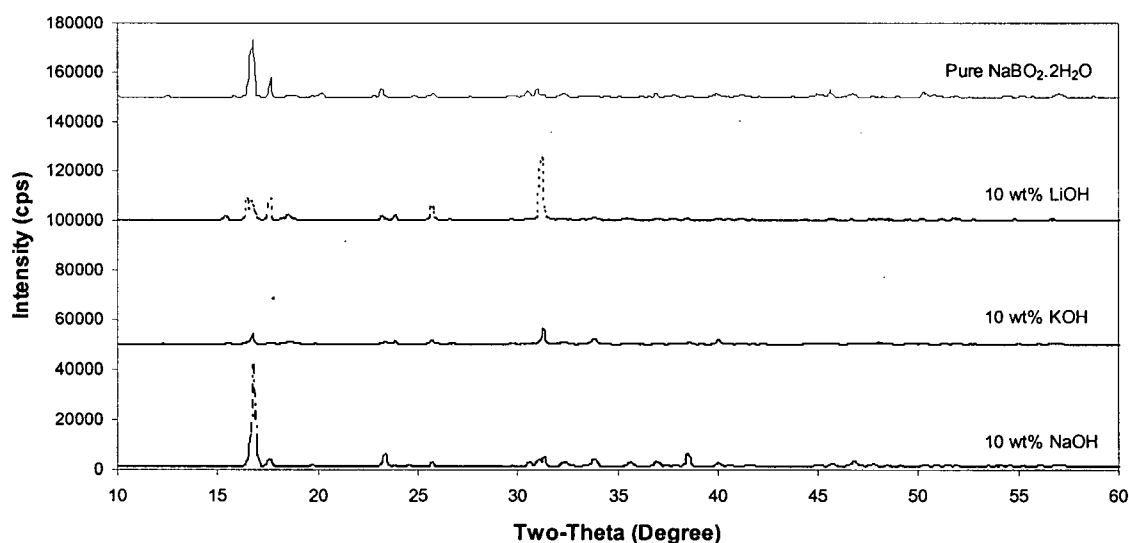
Figure 5.19: Intensity as a Function of Diffraction Angle for Pure $NaBO_2.2H_2O$ and Precipitates of 10 wt% Hydroxide $NaBO_2.2H_2O$ Supersaturated Aqueous Solutions.

It is likely that the NaOH-stabilized precipitate lost some of its hydration water while drying since the transition to the lower hydration level occurs at about $54°C$ [Blasdale, W. C. *et al.*, (1938), Nies, N. P. *et al.*, (1967)] and at $25°C$, the stable hydrate is $NaBO_2.4H_2O$ [Blasdale, W. C. *et al.*, (1938), Nies, N. P. *et al.*, (1967), Kocher, J. *et al.*, (1970), Menzel, H. *et al.*, (1943)]. It is not easy to remove $NaBO_2.2H_2O$ crystals from the alkaline solution in which they are grown [Menzel, H. *et al.*, (1943)]. Due to their

physical and chemical instability, they immediately transform to $NaBO_2.4H_2O$ when in contact with water. Hydrolysis leads to the formation of a hydrated solid phase, but depending on the conditions under which the H_2 generation system operates, the hydration level of the by-product generated will vary.

5.5.2 Scanning Electron Microscopy

Figure 5.20 shows selected SEM images of pure $NaBO_2.2H_2O$ and of the various precipitates obtained. Additional SEM precipitate images can be found in Appendix D. The pure $NaBO_2.2H_2O$ flakes shown in Fig. 5.20 (a) are a few mm long and have a porous surface.
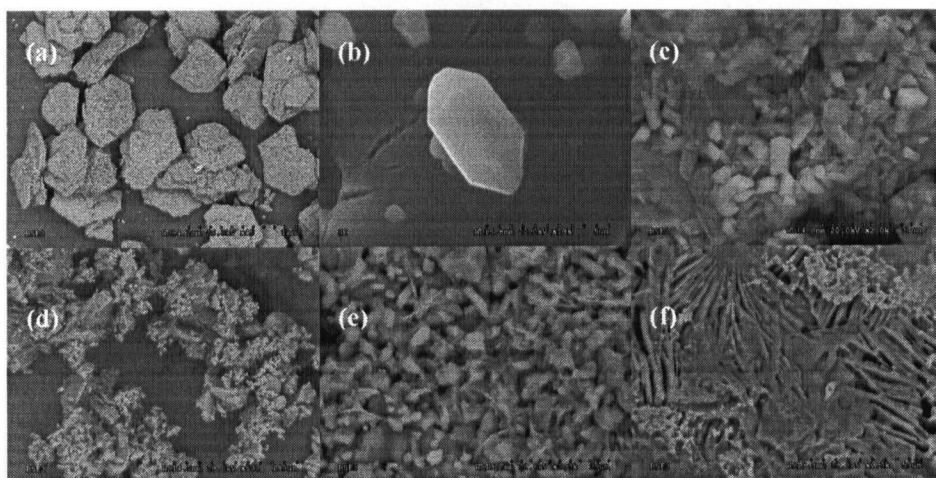
Figure 5.20: Scanning Electron Microscope Precipitate Crystal Images. (a) Pure $NaBO_2.2H_2O$ Flakes (SE, WD14.1mm, x45, 1mm), (b) $NaBO_2.2H_2O$ Crystal (SE, WD15.8mm, x10.0k, 5um), (c) 10 wt% NaOH, Saturated $NaBO_2.2H_2O$ Aqueous Solution Precipitate (BSE2, WD14mm, x2.0k, 20um), (d) 10 wt% KOH, Saturated $NaBO_2.2H_2O$ Aqueous Solution Precipitate (BSE2, WD14mm, x500, 100um), (e) 10 wt% LiOH, Saturated $NaBO_2.2H_2O$ Aqueous Solution Precipitate (BSE2, WD13.4mm, x1.0k, 50um), (f) 10 wt% LiOH Saturated $NaBO_2.2H_2O$ Aqueous Solution Precipitate (BSE2, WD13.3mm, x1.0k, 50um).

Freshly decanted crystals contained in alkaline solutions are clear, but as soon as the alkaline solution diffuses out of the crystals, they become opaque. The $NaBO_2.2H_2O$ crystals have the distinctive columnar lozenge shape seen in Fig. 5.20 (b). The precipitate formed from saturated $NaBO_2$ solution stabilized with NaOH shown in Fig. 5.20 (c) resembles a dispersion of small individual eroded and crumbled crystals. The KOH-stabilized aqueous $NaBO_2$ solution precipitate of Fig. 5.201 (d) was similarly constituted. The precipitate of the LiOH-stabilized $NaBO_2$ saturated solutions was a thick suspension, which, once dried

overnight, had the aspect of slush. The scattered group of small individual crystals, shown in Fig. 5.20 (e), was formed. To investigate how heat treatment affects the crystal surface morphology, this precipitate was dried for a longer period of time. This gave the crystals the intricate microstructure revealed in Fig. 5.20 (f), likely caused by the evaporation of the alkaline solution it contained.

CHAPTER VI

CONCLUSIONS

6.1 Conclusions

In this thesis, the effect of three alkali additives on the solubility and physicochemical properties of diluted and saturated aqueous $NaBO_2$ solutions was investigated. The present study was designed to determine which of these alkali additives was the most suitable and which concentration of alkali additive was optimal for the electrochemical reduction of $NaBO_2$ in aqueous media. The most obvious finding emerging from the experimental measurements is that all solution characteristics cannot be optimized at once. In fact, from the background information reviewed, it is clear that various parameters have different impact on the $NaBH_4$ H_2 generation and storage system properties. Table 6.1 summarizes the interactions between the variables affecting the system.

Table 6.1: Variable Effect on Various Parameters of the $NaBH_4$ H_2 Generation and Storage System (+ increase, - decrease, op=optimum point, n=none).

Variable Effect Vs Parameter	H_2 gen. rate	Solubility	$t_{1/2}$	pH	Viscosity	Conductivity	Weight Density	Volume Density
Catalyst loading +	+	n	n	n	n	+	n	n
T +	+	+	-	n	-	+	+	+
$[NaBH_4]$ +	op	n	n	n	-	+	+	+
$[MOH]$ +	-	-	+	+	+	-	-	-
Closed P	+	n	n	n	n	n	-	n

The findings of this thesis further confirm that compromises are required to create either a viable H_2 generation and storage system or a favourable electrolyte media for the electrochemical recycling of the hydrolysis waste solutions. This illustrates the complexity of the system being investigated given the number of variables and the interrelationships. The physicochemical property data obtained enhanced the general understanding of the effect of alkali additives on the solution properties and their impact on the H_2 storage and generation system. It revealed that, based on conductivity and viscosity, NaOH is a more

suitable additive for the electrochemical recycling of the spent $NaBO_2$ solution, while KOH addition favours the H_2 generation and storage system, based solubility and pH. A number of recommendations were made to address the shortcomings of the present study and suggestions for future work directions are given. Finally, the significance of the knowledge acquire through this thesis is placed in perspective.

6.1.1 System Considerations

Table 6.2 synthesizes the major findings of this study having a significant influence over future development and application.

Table 6.2: Summary of Alkali Hydroxide Additive Effect on the H_2 Storage and Generation System and Electrochemical Recycling.

Additive	Property	Consequence
NaOH	- Highest ionic conductivity	- Lowers Ohmic drop
	- Lowest viscosity	- Reduces mass transport losses
KOH	- Improved $NaBO_2$ solubility	- Improves hydrolysis conversion efficiency
		- Permits the use of a more concentrated solution
		- Reduces spent tank emptying frequency
	- Highest pH	- Extends $NaBH_4$ solution half-life
		- Prevents unsafe H_2 release
	- Highest specific gravity	- Lowers system gravimetric density
LiOH	- All properties	- Not favourable

Although all the filtrate ionic conductivities were high, the ionic conductivity of unsaturated $NaBO_2$ solutions containing NaOH was the highest, while the ionic conductivity of unsaturated $NaBO_2$ solutions containing KOH was the lowest. This high conductivity enhances the current carrying capacity of the solution and would stimulate the electrochemical reaction of the species it contains. The addition of NaOH resulted in the lowest dynamic viscosity and the addition of KOH resulted in a lower filtrate dynamic viscosity than the addition of LiOH. The low viscosity resulting from the addition of NaOH would reduce the mass transport losses and would allow more $NaBH_4$ and H_2O to contact the catalyst surface, and thereby potentially increase the H_2 generation. It would also result in superior electrochemical cell performance as Ohmic losses would be reduced.

137

The results obtained reveal that the most important factors affecting the improvement of the solubility of $NaBO_2$ are the type of hydroxide present in the solution and its concentration. The optimal alkali additive concentration under which the $NaBO_2$ precipitate's interference with H_2 generation will be minimized is 10 wt% KOH. Only the addition of KOH was able to maintain and improve the solubility of $NaBO_2$ in alkaline aqueous solution and could possibly improve the hydrolysis reaction conversion efficiency. Raising the $NaBO_2$ solubility permits the use of more concentrated $NaBH_4$ solution which increases the H_2 storage and generation capacity of the system, and reduces the frequency at which a spent solution tank would require emptying. The electrochemical recycling favors a reactant solution with a high concentration as it minimizes the volume of $NaBO_2$ solution required per unit of $NaBH_4$ produced. High H_2 evolution overpotentials are more likely to be achieved in highly concentrated alkaline aqueous solutions. Since the KOH-stabilized filtrate had the highest pH, KOH additions would extend the half-life of the $NaBH_4$ solution and prevent the unsafe non-catalytic release of H_2. Filtrate solutions containing KOH had the highest specific gravity, and the weight of the storage system would be higher with KOH as the stabilizer. Another practical implication is that the system weight increases as the hydroxide content increases. To some extent, a 10 wt% KOH addition would reduce the acceleration capabilities of the FCV.

The addition of LiOH did not affect the solution properties in a way that was beneficial to either the $NaBH_4$ H_2 generation or storage system or to the electroreduction of $NaBO_2$. From the XRD data and SEM pictures, it was not possible to confirm the hydration level of $NaBO_2$ precipitate from the various alkaline solutions. However, it is clear that the hydration level of the $NaBO_2$ by-product not only affects the mass and heat transport properties of the solution, but also lessens the theoretical gravimetric density of the H_2 storage and generation system. Hence, it is recommended to operate the H_2 generation system at a temperature favouring the formation of a less hydrated form of $NaBO_2$.

6.1.2 Future Research and Recommendations

In the current work, it was assumed that $NaBO_2$ is the main $NaBH_4$ hydrolysis by-product in alkaline aqueous media. However, the exact composition of the $NaBH_4$ hydrolysis alkaline aqueous waste solution as a function of pH and temperature should be verified to confirm that $NaBO_2.2H_2O$ is the primary

138

hydrolysis borate formed and that the alkali additives do not react with NaBH₄ to form other complex polyborates. Among other things, the pH and temperature of $NaBH_4$ alkaline aqueous solutions should be measured before and after hydrolysis. The difference between the $NaBH_4$ dissolution rate and the hydrolysis reaction rate should be compared as a function of pH and temperature.

It would be useful to determine if other potassium-containing compounds than KOH would be suitable additives to enhance the solubility of $NaBO_2$. Solubility measurements should be carried out with $NaBO_2$ and $NaBH_4$ combined in the alkaline aqueous solution to further investigate the common ion effect on the boron-containing anion solubility. Mixtures of KOH and NaOH should also be investigated to potentially optimize the $NaBO_2$ alkaline aqueous solution conductivity and solubility. The solubility measurements obtained at 5 and 7.5 wt% hydroxide require verification and special care should be taken to avoid $NaBO_2.2H_2O$ dehydration during the course of the experiments. Other methodologies, such as atomic absorption (AA), should be used to verify the ICP-MS solubility measurements. The use of ammonia as a co-solvent should be investigated even though it is expected that low solubility ammonia borate compounds will be formed in the saturated aqueous $NaBO_2$ solutions. Conductivity and pH measurements should be taken prior to the solution filtration. To ensure the validity of the pH measurements in concentrated sodium solutions, a low sodium error electrode should be used instead of a general purpose glass electrode.

A suitable procedure has to be developed to determine the solubility of $NaBO_2.2H_2O$ at 50-75°C as the solubility values measured were too high. A water bath capable of maintaining temperatures less than 5°C above ambient should be used. Experiments should be carried-out at temperatures close to PEMFC operating conditions and the freezing point of the various solutions should also be determined. Also, the effect of NaOH and KOH on the electroreduction of $NaBO_2$ to $NaBH_4$ in water should be investigated. However, it has been reported that if the $NaBO_2$ electroreduction is not carried-out in an environment free of water, the production of $NaBH_4$ will be limited. Consequently, efforts should be focused on the use of dry or water free media such as organic solvents, ionic liquids, or molten salts, which are likely to be more favourable to successfully electroreduce $NaBO_2$. It is important to note that in an organic solvent, the conductivity is likely to be lower than in the aqueous solution, and that a suitable supporting electrolyte, like the ones studied in this thesis, would still be needed.

Future work should include electrochemical measurements in aqueous alkaline solutions of $NaBO_2$ to investigate the feasibility of the direct electroreduction of $NaBO_2$ to $NaBH_4$ at various electrode materials. Organic additives should be used to increase the H_2 evolution reaction overpotential and thereby favor the reduction of $NaBO_2$ to $NaBH_4$. In addition, the catalytic hydrolysis and electrooxidation of $NaBH_4$ on a variety of electrode materials possessing catalytic affinities for the hydrolysis of $NaBH_4$, such as Pt, Ru, Ni and Ag, should be looked at. The hydrolysis reaction rate should be studied by measuring the H_2 evolution rate using a specially designed set-up. Voltammetry at rotating disk electrodes and chronoamperometry at microdisk electrodes are among the techniques that could be used. Electrochemical quartz crystal microbalance and cyclic voltammetry measurements could be combined to identify potential unstable electro-oxidation reaction intermediates and rapid chemical reaction stages.

6.2 Summary of Contributions

This thesis has gone some way towards enhancing the understanding of the effect of hydroxides on the solubility and physicochemical properties of $NaBO_2$ aqueous solutions. The physicochemical parameters determined in this study will form the basis upon which electrochemical recycling investigations $NaBO_2$ to $NaBH_4$ in aqueous media will be pursued. The current findings add to a continuously growing body of literature on the use of $NaBH_4$ as a H_2 carrier in emerging fuel cell power generation technologies, such as B-PEMFCs and DBFCs.

It is believed that the low electrochemical activity of the $NaBO_2$ alkaline aqueous solutions could be alleviated by the development of an appropriate electrolyte media to carry the electroreduction. It was demonstrated that a practical electrochemical recycling procedure could open a wide range of commercial possibilities for $NaBH_4$ and that a sustainable electrochemical method to recycle $NaBO_2$ to $NaBH_4$ would remove one of the most important obstacles to the adoption of $NaBH_4$ as the H_2 carrier of choice for automotive H_2 fuel cell applications. The success of this H_2 storage system clearly lies in the development of a sustainable and efficient electrochemical method to convert $NaBO_2$ to $NaBH_4$, which would lead to major cost reductions.

REFERENCES

A

Afzal, M., Iqbal, M. J., and, Ahmad, H., (1994), Collect. Czech. Chem. Commun., 59, pp. 1296-1300.

Aiello, R., Sharp, J. H., and Matthews, M. A., (1999), Int. J. Hydrogen Energy, 24, pp. 1123-1130.

Amendola, S. C., (2002), US Patent 6497973.

Amendola, S. C., Kelly, M.T., and Wu, Y., (2003), US Patent 6524542.

Amendola, S. C., Onnerud, P., Kelly, M. T., Petillo, P. J., Sharp-Goldman, S. L and Binder, M. J., (1999), Journal of Power Sources, 84, pp. 130-133.

Amendola, S. C., Sharp-Goldman, S. L., Saleem Janjua, M., Spencer, N. C., Kelly, M. T., Petillo, P. J., and Binder, M., (2000a), Int. J. Hydrogen Energy, 25, pp. 969-975.

Amendola, S. C., Sharp-Goldman, S. L., Saleem Janjua, M., Spencer, N. C., Kelly, M. T., Petillo, P. J., and Binder, M., (2000b), Journal of Power Sources, 85, pp. 186-189.

Andrew, H. E., (1976), Ceramic Bulletin, 55 (6), pp. 583-584.

Antropov, L. I., (1972), *Theoretical electrochemistry*, Mir, Moscow, 567 p.

Ay, M., Midilli, A., and Dincer, I., (2006), Journal of Power Sources, In Press.

B

Basson, W. D., Bohmer, R. G. and, Stanton, D. A., (1969), The Analyst, 94, pp. 1135-1141.

BCS Inc., (2002), Energy and Environmental Profile of the US Mining Industry, Chapter 3, Potash, Soda, Ash and Borates, pp. 3-1.

Belcher, B., Tully, S. W., and, Svehla, G., (1970), Anal. Chim. Acta, 50, pp. 261-267.

Bettera, J., (2003), *PSA Peugeot Citroën Fuel Cell Activities*, Business Briefing: Global Automotive Manufacturing & Technology, pp. 1-5.

Betty, K. R., and Day, G. T., (1986), The Analyst, 111 (3), pp. 455-457.

Bingham, D., Wendt, K., and Wilding, B., (2004), Idaho National Engineering and Environmental Laboratory, US Department of Energy, Energy Efficiency and Renewable Energy, Presentation, http://www1.eere.energy.gov/hydrogenandfuelcells/pdfs/review04/st_4_wilding.pdf.

Bingham, D. N., Wilding, B. M., Klinger, K. M., Zollinger, W. T., and Wendt, K. M., (2005), US Patent Application 20050077170 A1.

Blasdale, W. C., and Slansky, C. M., (1938), Journal of the American Chemical Society, 61, pp. 917-920.

Blumenthal, H., (1951), Analytical Chemistry, 23 (7), pp. 992-994.

Bonhoff, K., Gronich, S., Garbak, J., and Hooker, D., (2005), *DOE Hydrogen Program, FY 2005 Progress Report, VIII.A Vehicle Demonstrations*, pp. 1143-1146.

Botello, J. C., Morales-Dominguez, E., Domingeuez, J. M., Gutierrez, A., Rojas-Hernandez, A., and Ramirez, M. T. (2003), Spectrochimica Acta Part A, 59, pp. 1477-1486.

Bouaziz, R., (1962), Bulletin de la Société Chimique de France, 5, pp. 1451-1459.

Breslau, B. R., and Miller, I. F., (1970), Journal of Physical Chemistry, 74 (5), pp. 1056-1061.

Brown, B. B., (1957), Journal of the American Chemical Society, 79, pp. 4241-4242.

Brown, H. C., (1955), Analytical Chemistry, 27, pp. 156-158.

Brown, H. C., Mead, E. J., and Subba Rao, B.C., (1955), Journal of the American Chemical Society, 77, pp. 6209-6213.

Buckingham, D. A., and Lyday, P. A., (2002), *Historical Statistics for Boron*, US Geological Survey, Open File Report 01-006, pp. 1-6.

C

Celikkan, H., Aydin, H., and, Aksu, M. L., (2005), Turkish Journal of Chemistry, 29, pp. 519-524.

Chaikin, S. W., (1953), Analytical Chemistry, 25 (5), pp. 831-832.

Chandra, D., Reilley, J. J., and Chellappa, R., (2006), Journal of Materials, 58 (2), pp. 26-32.

Chaurasia, S. C., (2004), National Center for Compositional Characterisation of Materials, 502 (2), pp. 265-270.

Chowdoji Rao, K, Subha, M. C. S., and, Brahmaji Rao, S., (1999), Indian Journal of Chemistry, 28a, pp. 102-105.

Cloutier, C. R., Alfantazi, A., and Gyenge, E., (2006), Materials Science Forum/Advanced Materials Research, Trans Tech Publications, In Press.

Cloutier, C. R., Alfantazi, A., and Gyenge, E., (2007), Journal of Fuel Cell Science and Technology, In Press.

Constable, F. H., and Isnel, A. H., (1953), Reviews of Faculty of Science, University of Istanbul, Series C, 18a, pp. 166-177.

Cooper, H. B. H., (1973), US Patent 3734842.

Corti, H., Crovetto, R., and Fernandez-Prini, R., (1980), Journal of the Chemical Society, Faraday Transactions, 76 (10), pp. 2179-2186.

Covington, A. K., and Newman, K. E., (1973), J. Inorg. Nucl. Chem., 35, pp. 3257-3262.

D

Daimler Chrysler, Press Release, (2002), New York.

Davis B., Lo, F., Calabretta, D., and Abdul, M., (2005), 44th Annual Conference of Metallurgists of CIM, Calgary, Alberta, Canada, pp. 595-605.

Davis, E. R., Bromels, E., and Kibby, C. L., (1962), Journal of the American Chemical Society, 84 (6), pp. 885-892.

Dawidowicz, A. L., Matuzewitz, J., and Wysocka-Lisek, J., (1989), Talanta, 5, pp. 581-584.

Dean, J. A., (1999), *Lange's Handbook of Chemistry*, 15th Edition, McGraw-Hill, USA.

Department of Energy, (2003), Controlled H_2 Fleet and Infrastructure Demonstration and Validation Project, Draft Revision 3, Appendix A, pp. A1-A25.

Department of Energy, (2004), *Hydrogen Storage "Think Tank" Report*, Office of Hydrogen, Fuel Cells and Infrastructure Technologies, Washington, DC., p. 6.

Dhanesh, C., James, J. R., and Raja, C., (2006), Journal of Materials, 58(2), pp. 26-32.

Drescher, A., (1989), Analytica Chemica Acta, 219, pp. 273-279.

Drescher, A., and Kucharkowski, R., (1998), Wissenschaftliche Berichte, 38, pp. 8-19.

Dodd, S., (1929), The Analyst, 54, pp. 282-285.

Druzhinin, G. and Skvortsov, V.G., (1968), Russian Journal of Inorganic Chemistry, 13 (5), pp. 754-756.

E

Erdey-Gruz, T., (1974), *Transport Phenomena in Aqueous Solutions*, Adam Hilger Ltd., England.

Eysseltova, J., and Dosoudilova, Jana, (1994), Collection Czech. Chem. Commun., 59, pp. 1337-1341.

F

Filby, E. E., (1976), US Patent 3993732.

Frei, V., and Ustianovicova, A., (1963), Russian Journal of Physical Chemistry, 37 (5), pp. 612-613.

G

Garret, D. E., (1998), *Borates, Handbook of Deposits, Processing, Properties and Use*, Academic Press, London, UK, pp. 23-49.

Gervasio, D., Xu, M. and Thomas, E., (2005), *Properties of Aqueous Alkaline Sodium Borohydride Solutions and By-products Formed During Hydrolysis*, Presentation, Fuel Cell Design, Fabrication and Materials Selection Workshop.

Gouper, A. M., Pletcher, D., and Walsh, F. C., (1990), Chem. Rev., 90, pp. 837-865.

Gyenge, E. L., and Oloman, C. W., (1998), Journal of Applied Electrochemistry, 28, pp. 1147-1151.

H

Hale, C. H. and Sharifian, H., (1990), US Patent 4931154.

Hampton, D. S. Jr., and Wiersena, R. J., (1972), Inorganic Chemistry, 11 5, pp. 1152-1154.

Hart, D., (2003), Frontiers in the Ecology and the Environment, 1(3), pp. 138-145.

Hayes, M. R., and Metcalfe, J., (1962), The Analyst, 87, pp. 956-969.

Helmy, F. M., Shebi, F. A., Sartori, P. and Solimam, A. D., (1987), Chemiker-Zeitung, 111 (12), p. 367.

Horvath, A. L., (1985), *Handbook of Aqueous Electrolyte Solutions*, Ellis Horwood Ltd., England.

Hua, D., Hanxi, Y., Xinping, A., and Chuansin, C., (2003), Int. J. Hydrogen Energy, 28, pp. 1095-1100.

Huff, G. F., Chapel, F., McElroy, A. D., City, E. and Adams, R. M., (1958), US Patent 2855353.

J

Jacques S., Berthet, M. P. and Bonnetot, B., (1970), Prog. Inorg. Chem., 11, pp. 99-231.

Jacques, S., Berthet, M. P., and Bonnetot, B., (2004), Chemical Engineering Transactions, 4, pp. 331-336.

Jenkins, H. D. B., Roobottom, H. K., Passmore, J., and, Glasser, L., (1999), Inorganic Chemistry, 38, pp. 3609-3620.

Jeong, S. U., Kim, R. K., Cho, E.A., Kim, H.-J., Nam, S.-W., Oh, I.-H., Hong, S.-A. and Kim, S.H., (2005), Journal of Power Sources, 144 (1), pp. 129-134.

Jigong, L., Foutch, G. L., and Na, J. W., (1999), Separation Science and Technology, 34 (15), pp. 2923-2941.

John, K. R. C., Jr., (1951), Analytical Chemistry, 24, p. 806.

Johnson, E. A., and Toogood, M. J., (1954), The Analyst, 79, pp. 493-496.

K

Kaufman, C. M., and Sen, B., (1985), J. Chem. Soc., Dalton Trans., pp. 307-312.

Kesans, A., Vimba, S., and Svarcs, E., (1955), Latvijas PSR Zinatnu Akad. Vestis, 8, pp. 127-134.

Kim, J.-H., Lee, H., Han, S.-C., Kim, H.-S., Song, M.-S., and Lee, J.-Y., (2004a), Int. J. Hydrogen Energy, 29, pp. 263-267.

Kim, J.-H., Kim, K.-T., Kang, Y.-M., Kim, H.-S., Song, M.-S., Lee, Y.-J. Lee, P. S., and Lee, J.-Y., (2004b), J. Alloys and Compounds, 379, pp. 222-227.

Kirk, R. E., Othmer, D. F., Kroschwitz, J. I., and Howe-Grant, M., (1992), Kirk-Othmer Encyclopedia of Chemical Technology.

Knorre, H., Main, H.A., Kloepfer, H, Main, F. A., and Bretschneider, G., (1968), US Patent 3379511.

Kocher, J., and Lahlou, A., (1970), Bulletin de la société chimique de France, 6, pp. 2083-2089.

Kojima, Y., and Haga, T., (2003), Int. J. Hydrogen Energy, 28, pp. 989-993.

Kojima, Y., Kawai, Y., Nakanishi, H., and Matsumoto, S., (2004a), J. Power Sources, 135, pp. 36-41.

Kojima, Y., Suzuki, K.-I., and Kawai, Y., (2006), Journal of Power Sources, 155, pp. 325-328.

Kojima, Y., Suzuki, K.-I., Fukumoto, K., Sakai, M., Yamamoto, T., Kawai, Y., and Hayashi, H., (2002), Int. J. Hydrogen Energy, 27, pp. 1029-1034.

Kojima, Y., Suzuki, K.-I., Fukumoto, K., Kawai, Y., Kimbara, M., Nakanishi, H., and Matsumoto, S., (2004b), Journal of Power Sources, 125, pp. 22-26.

Kong, V. C. Y., Foulkes, F. R., Kirk, D. W., and Hinatsu, J.T., (1999), Int. J. Hydrogen Energy, 24, pp. 665-675.

Konoplev, V. N., (1988), Russian Journal of Inorganic Chemistry, 33, pp. 433-434.

Kreevoy, M. M., and Jacobson, R.W., (1979), Ventron Alembic, 15, pp. 2-3.

Krishnan, P., Yang, T.-H., Lee, W.-Y., and Kim, C.-S., (2005), Journal of Power Sources, 143, pp. 17-23.

Kuleshova, O. D., (1985), Journal of analytical chemistry of the USSR, 40 (1), pp. 151-153.

L

Larminie, J., and Dicks, A., 2003, *Fuel Cell Systems Explained*, Second Edition, John Wiley and Sons Ltd., West Sussex, England, pp. 297-301.

Lencka, M. M., Anderko, A., Sanders, S. J., and Young, R. D., (1998), International Journal of Thermophysics, 19 (2), pp. 367-378.

Levy, A., Brown J. B., and Lyons, C.J., (1960), Industrial and Engineering Chemistry, 52, pp. 211-214.

Li, J., Li, B., and Gao, S., (2000), Xi-an Branch, Phys. Chem. Minerals, 27, pp. 342-346.

Li, Z. P., Liu, B. H., Arai K., and Suda, S., J., (2003b), Electrochemical Soc., 150 (7), pp. 868-872.

Li, Z. P., Morigazaki, N., Liu, B. H., and Suda, S., (2003a), J. Alloys and Compounds, 349, pp. 232-236.

Li, Z. P., Liu, B. H., Arai, K., Asaba, K., and Suda, S., (2004), Journal of Power Sources, 126, pp. 28-33.

Lide, D. R., (2005-6), *CRC Handbook of Chemistry and Physics*, 86th Edition, CRC Press, USA.

Linden, D., (1984), *Handbook of Batteries and Fuel Cells*, McGraw Hill Inc., pp. 42-48.

Linkous, C. A., (2003-4), Florida Solar Energy Center, Task Number III-C, http://www.fsec.ucf.edu/hydrogen/reports/taskiiic-linkous-fsec.pdf.

Linkous, C. A., Bhuller, S. K. and Slattery, D. K., (2004), *A H2 Storage Cycle Based on Alkali Metal Borohydrides*, Conference Abstract, 206th Meeting of the Electrochemical Society, p. 550.

Lopez Garcia, I., Hernandez Cordoba, M., and, Sanchez-Pedreno, C., (1985), The Analyst, 100 (10), pp. 1259-1262.

Lyday, P. A., (2000), Boron, U.S. Geological Survey Minerals Yearbook, pp.14.1-14.8.

Lyday, P. A., (2005), *Boron Statistics*, US Geological Survey, Mineral Commodity Summaries, Annual Publication, pp. 36-37.

Lyttle, D. A., (1963), Journal of analytical chemistry, 24 (11), pp. 1843-1844.

M

Maksimova, I. N., and Yushkevich, V. F., (1963), Russian Journal of Physical Chemistry, 37 (8), pp. 1005-1007.

Mal'tseva, N. N., Kedrova, N. S., Sizareva, A. S., and Konoplev, (1991), Russian Journal of Inorganic Chemistry, 36 (1), pp. 37-38.

Martin, D. R., (1961), *Borax to Boranes*, Advances in Chemistry Series, American Chemical Society Applied Publications, pp. 1-4.

Martinus, N., Crawford, D., Sinclair, D., and Vincent, C. A., (1977), Electrochimica Acta, 22 (10), pp. 1183-1187.

Mattson, B., (2005), Educacion Quimica, 16 (4), pp. 114-127.

Mellor, J. W., (1980), *Supplement to Mellor's Comprehensive Treatise on Inorganic and Theoretical Chemistry*, Longman Group Ltd., N.Y., USA.

Menzel, H., and Schulz, H., (1943), Zeitschrift fur Anorganische und Allgemeine Chemie, 251, pp. 167-200.

MERIT (Materials & Energy Research Institute Tokyo), Ltd., (1986), Nagano-Ken, Japan, http://merit.hydrogen.co.jp/Why_BH4/WhyBH4.html.

Mesmer, R. E., (1972), Inorganic Chemistry, 11 (3), pp. 537-544.

Midgley, D., (1992), The Analyst, 117, pp. 199-202.

Mikio, K., and Hitoshi, I., (2003), Japanese Patent Application JP 2003247088.

Mirkin, M. V., (1991), Anal. Chem., 63, pp. 532-533.

Mirkin, M. V., and Bard, A. J., (1991), Anal. Chem., 63, pp. 532-533.

Mohring, R. M., and Wu, Y., (2003), American Institute of Physics Conference Proceedings, 671, pp. 90-100.

Momii, R. K., and Nachtrieb, N. H., (1967), Inorganic Chemistry, 6 (6), pp. 1189-1192.

N

Nies, N. P., and Hulbert, R. W., (1967), Journal of Chemical and Engineering Data, 12 (3), pp. 303-313.

Norkus, P. K., (1968), Journal of Analytical Chemistry of the URSS, 23 (4), pp. 558-562.

O

Out, D. J. P., and Los, J. M., (1980), J. Solut. Chem., 9 (1), pp. 19-35.

P

Pinto, A. M. F. R., Falcao, D. S., Silva, R. A., and Rangel, C. M., (2006), Int. J. of Hydrogen Energy, In Press.

R

Richardson, B. S., Birdwell, J. F., Pin, F. G., Janson, J. F., and Lind, R. F., (2005), Journal of Power Sources, 145, pp. 21-29.

Roobottom, H. K., Jenkins, H. D. B., Passmore, J., and, Glasser, L., (1999), Journal of Chemical Education, 76 (11), pp. 1570-1573.

Ross, W. J., and, White, J. C., (1960), Talanta, 3, pp. 311-317.

Rothbaum, H. P., Tood, H. J. and Walker, I. K., (1936), Chemical Engineering Data, 1 (1), pp. 95-99.
Sadetdinov, Sh. V., (1985), Russian Journal of Inorganic Chemistry, 30, pp. 1913-1915.

Roy, M. A., (1964), *Boron, Metallo-Boron Compounds and Boranes*, John Wiley & Sons, pp. 390.

Rudie, C. N., (1979), Journal of the American Chemical Society, 56 (4), pp. 520-521.

S

Sadetdinov, Sh. V., (1985), Russian Journal of Inorganic Chemistry, 30, pp. 1913-1915.

Salentine, C. G., (1983), Ignore. Chem., 32, pp. 3920-3924.

Sagrado, S., (1998), Talanta, 45, pp. 835-842.

Sah, R. N., (1997), Plant and Soil, 193, pp. 15-33.

Schlesinger, H. I., Brown, H. C., Finholt, A. E., Gilbreath, J. R., Hoekstra, H. R. and Hyde, E. K., (1953), J. Am. Chem. Soc., 75, pp. 215-219.

Seijiro, S., (2004), Patent JP2004-010446.

Sharifian, H., and Dutcher, J. S., (1990), US Patent 4904357.

Shedlovsky, T., (1938), J. Franklin Institute, 225, p. 739-743.

Skvortsov, V. G., (1974), Russian Journal of Inorganic Chemistry, 19 (7), pp. 1088-1089.

Skvortsov, V. G., Molodkin, A. K., Rodionov, N. S. and, Tsekhanskii, R. S., (1986a), Russian Journal of Inorganic Chemistry, 31 (6), pp. 934-935.

Skvortsov, V. G., Molodkin, A. K., Rodionov, N. S. and Tsekhanskii, R. S., (1986b), Russian Journal of Inorganic Chemistry, 31, pp. 911-913.

Skvortsov, V. G., Petrova, O. V., Belova, V. F., Sadetdinov, Sh. V., (1992), Russian Journal of Inorganic Chemistry, 37 (4), pp. 475-475.

Skvortosov, V. G., Tsekhanskii, R. S., Molodkin, A. K., Petrova, O. V. and Akimov, V. M., (1988), Russian Journal of Inorganic Chemistry, 33 (6), pp. 921-923.

Snover J., and Wu, Y., (2004), US Patent 6706909 B1.

Snyder, K. A., (2005), Cement and Concrete Research, 35, pp. 421-422.

Staden, J. F., (2000), S. Afr. J. Chem., 53 (2), pp. 77-85.

Stockmayer, W. H., Rice, D. W., and Stephenson, C. C., (1955), J. Am. Chem. Soc., 77, pp. 1980-1983.

Suda, S., (2003), *The Sodium Borohydride Hydrogen Energy Systems,* R&D Policies, KUCEL-MERIT Group, pp. 1-11.

Suda, S., Sun, Y. M., Liu, B.-H., Zhou, Y., Morimitsu, S., Arai, K., Tsukamoto, N., Uchida, M., Candra, Y., and Li, Z.-P., (2001), Applied Physics A, Materials Science and Processing, 725, pp. 209-212.

Sun, Y., and Liang, Z., (2003), Patent CN1396307.

Szklarska-Smialowska, S., and Smialowski, M., (1963), J. of the Electrochemical Society, 110, pp. 444-448.

U

Uddin, F., and Saeed, R., (2001), Acta Cientifica Venezolana, 52, pp. 186-191.

Ullmann, F., (2000), *Ullmann's Encyclopedia of Industrial Chemistry*.

Urusova, M. A., and Valyashko, V. M., (1993), Institute of General and Inorganic Chemistry, Academy of Sciences of the URSS Journal of Inorganic Chemistry, 38 (4), pp. 662-664.

US Borax, $NaBO_2.2H_2O$ product data sheet.

V

Van Staden, J. F., and Van Der Merwe, T. A., (2000), The Analyst, 125, pp. 2094-2099.

W

Wee, J.-H., (2006), Journal of Power Sources, 155, pp. 329-339.

Wei, W. C., Chen, C.-J., and, Yang, M.-H., (1995), Journal of Analytical Atomic Spectrometry, 10, pp. 955-961.

Wei, X.-Y., Zhang, L.-J., Liang, J.-J., Wei, Z.-M., and Weng, D.-H., (2003), Huagong Jishu Yu Kaifa, 32 (3), pp. 1-3.

Weiren, R., and Deren, Q., (1998), Journal of Fudan University, 37 (3), pp. 276-278.

Wilding, B., Bingham, D., Wendt, K., and Klingler, K., (2004), *Hydrogen Storage: Radiolysis for Borate Regeneration*, DOE Hydrogen Program, Progress Report, pp. 200-204.

Wipke, K., Welch, C., Thomas, H., Sprik, S., Gronich, S., Garbak, J., Hooker, D., (2006), Controlled Hydrogen Fleet and Infrastructure Demonstration and Validation Project, Progress Update, National Hydrogen Association Conference, Long Beach, California, pp. 1-21.

Wu, C., Zhang, H., and Yi, B., (2004), Catalysis Today, 93-95, pp. 477-483.

Wu, Y., (2003a), *Hydrogen Storage via Sodium Borohydride, Presentation*, GCEP Hydrogen Workshop, Stanford University, CA, USA, http://gcep.stanford.edu/pdfs/hydrogen_workshop/Wu.pdf.

Wu, Y., (2003b), *Process for the Regeneration of Sodium Borate to Sodium Borohydride for Use as Hydrogen Storage Source*, Fuel Cells and Infrastructure Technologies Program Review, DOE Hydrogen Program, Progress Report, pp. 1-2.

Wu, Y., (2004), *Low-Cost, Off-Board Regeneration of Sodium Borohydride*, Fuel Cells and Infrastructure Technologies Program Review, DOE Hydrogen Program, Presentation, http://www1.eere.energy.gov/hydrogenandfuelcells/pdfs/review04/st_5p_wu.pdf.

Wu, Y., Kelly, M. T., and Ortega, J. V., (2004a), *Low-Cost, Off-Board Regeneration of Sodium Borohydride*, DOE Hydrogen Program, Progress Report, pp. 195-199.

Wu, Y., Kelly, M. T., and Ortega, J. V., (2004b), *Review of Chemical Processes for the Synthesis of Sodium Borohydride*, DOE Cooperative Agreement DE-FC36-04GO14008, pp. 1-24.

X

Xia, Z. T., and Chan, S. H., (2005), Journal of Power Sources, 152, pp. 46-49.

Xu, J., Kelly, M., Pez, G., Wu, Y. and Sharp-Goldman, S., (2004), US Patent 20040011662.

Y

Yu, Z., (2002), Patent WO 02062701.

Z

Zhang Q., Smith, G., Wu, Y. and Mohring, R., (2006), Int. J. of Hydrogen Energy, In Press.

APPENDIX

Appendix A: Comparison to DOE Range, Storage Cost, Energy Density and Specific Energy Targets.

Table A.1: Fuel Cost for Target Range and Storage Cost Estimation.

Fuel Cost for Range Target

1 [mol $NaBH_4$] produces 4 [moles of H_2]	$NaBH_4$ Cost (Specialty Chemical) = $80-100US/kg
37.83 [g $NaBH_4$] produces 4*(2.0158) [g of H_2]	$NaBH_4$ Cost (Industry) = $50US/kg

[g $NaBH_4$] needed to produce 8000 [g of H_2]:
  37533.49 [g]
    37.53 [kg]
	[g $NaBH_4$] needed to produce 1000 [g of H_2]:
	  4691.69 [g]
	    4.69 [kg]

[US$] for 8 kg H_2:	[US$] for 1 kg H_2:

Specialty Chemical		Industry	Specialty Chemical		Industry
$3,002.68	$3,753.35	$1,876.67	$375.33	$469.17	$234.58
(min.)	(max.)	(average)	(min.)	(max.)	(average)

DOE 2015 Target for Range is: 8 [kg H_2] for 400 [km]

Storage Cost Estimation [$/kWh]

0.07	[Wh/molH_2]
0.03	[kWh/gH_2]
261.65	[kWh] for 8000g H_2
565.15	[$] for 8 kg H_2 (Specialty Chemical)
$NaBH_4$ cost is: **5.31**	times too high

DOE 2015 Storage Cost Target is: 2.16 [$US/kWh]

Complete hydrolysis of $NaBH_4$ produces 2.37 [l] H_2 at STP per gram of $NaBH_4$

37.83 [g $NaBH_4$] produces 4*(2.0158) [g of H_2]	
1 [g $NaBH_4$] needed to produce x[g of H_2]: 0.21 [g H_2 produced]	
1 [mol H_2] = 2.0158 [g H_2 produced]	
? [mol] = 0.106571504 [g H_2]	
0.11	[mol H_2 produced]
22.4	[l H_2 per mol] at STP
2.37	[l H_2 per g $NaBH_4$] at STP

Table A.2: Volumetric and Gravimetric Energy Density Comparison.

Volumetric Energy Density [KWh/l]

For PEMFC:	$H_2 \rightarrow 2H^+ + 2e^-$		-1.23 [V]
	2F per 1 mol H_2 consumed		
	= 2*96485C = [A.s]		
	= 2*26.8 [A.h]		
Theoretical Energy Density	65.93	[Wh/molH_2]	
	0.07	[kWh/molH_2]	

PEMFC Feed with H_2:

Ideal Gas Law		200	[atm]
PV = nRT		25	[°C]
V = nRT/P		298.15	[°K]
	0.12 [l]		
Theoretical Energy Density	0.54	[kWh/lH_2]	

PEMFC Feed with NaBH$_4$ fuel:

1 [mol NaBH$_4$] forms 4 [moles H_2]		
Theoretical Energy Density	0.26	[kWh/molNaBH$_4$]
Assuming 20 wt % NaBH$_4$ in 2M NaOH in water		
200 [g NaBH$_4$] per 1000 [g solution]		
5.29	[mol NaBH$_4$/l or kg solution]	
Theoretical Energy Density	1.39	[kWh/l solution]

DOE 2015 Target is: 2.69 [kWh/l]

Gravimetric Energy Density [kWh/kg]

4 [moles H_2] =	8.63	[g H_2]		
200 [g NaBH$_4$] =	5.29	[mol NaBH$_4$]		
1 [mol NaBH$_4$] = 4 [moles H_2]				
5.29	[mol NaBH$_4$] =		21.15	[mol H_2]
21.15	[mol H_2] =		45.63	[g H_2]
			0.05	[kg H_2]
0.26	[kWh/molNaBH$_4$]			
1.39	[kWh/0.05 kgH_2]			
27.5	[kWh/kg]			

DOE 2015 Target is: 3.00 [kWh/kg]

Appendix B: Filtrate Characterization Data

Table B.1: Physicochemical Properties Raw Data, Unsaturated Diluted Aqueous Solutions of $NaBO_2$ at $25°C \pm 3°C$, Trial 1.

Concentration [M]	Density [g/ml]	Conductivity [S/m]	Dynamic Viscosity [cP]
0.4910	1.0329	2.35	1.0916
0.3683	1.0251	1.86	1.0590
0.2455	1.0145	1.40	1.0135
0.1841	1.0094	1.08	0.9701
0.1228	1.0087	0.98	0.9677
0.0614	1.0008	0.42	0.9403
0.0246	0.9983	0.19	0.9432
0.0184	0.9968	0.14	0.9252
0.0123	0.9977	0.10	0.9169
0.0061	0.9964	0.04	0.9161
0.0025	0.9971	0.02	0.9159

Table B.2: Physicochemical Properties Raw Data, Unsaturated Diluted Aqueous Solutions of $NaBO_2$ at $25°C \pm 3°C$, Trial 2.

Concentration [M]	Density [g/ml]	Conductivity [S/m]	Dynamic Viscosity [cP]
0.4910	1.0334	2.29	1.0861
0.3683	1.0235	1.87	1.0356
0.2455	1.0156	1.34	0.9972
0.1841	1.0111	1.09	0.9762
0.1228	1.0043	0.78	0.9506
0.0614	1.0005	0.42	0.9424
0.0246	0.9975	0.18	0.9201
0.0184	0.9986	0.15	0.9182
0.0123	0.9982	0.11	0.9162
0.0061	0.9972	0.05	0.9124
0.0025	0.9965	0.02	0.9043

Table B.3: Physicochemical Properties Raw Data, Unsaturated Diluted Aqueous Solutions of $NaBO_2$ at $25°C \pm 3°C$, Trial 3.

Concentration [M]	Density [g/ml]	Conductivity [S/m]	Dynamic Viscosity [cP]
0.4910	1.0352	2.35	1.0890
0.3683	1.0230	1.89	1.0233
0.2455	1.0159	1.38	1.0030
0.1841	1.0110	1.12	0.9657
0.1228	1.0063	0.75	0.9487
0.0614	0.9987	0.42	0.9442
0.0246	0.9987	0.18	0.9293
0.0184	0.9975	0.14	0.9302
0.0123	0.9959	0.10	0.9189
0.0061	0.9967	0.05	0.9165
0.0025	0.9974	0.03	0.9082

Table B.4: Summary of Averages, Conductivity of Unsaturated $NaBO_2$ Aqueous Alkaline Solutions Filtrate at 25, 50 and 75°C.

Solution Composition	Alkali [wt %]	T [°C]	Conductivity [S/m]
No additive	0	25.00	27.25
	0	50.00	36.25
	0	75.00	59.40
NaOH	1	25.00	52.30
	2	25.00	91.00
	3	25.00	125.30
	5	25.00	188.50
	10	25.00	-
	1	50.00	82.55
	2	50.00	136.30
	3	50.00	174.27
	5	50.00	-
	10	50.00	-
	0.5	75.00	65.85
	1	75.00	132.10
	1.5	75.00	169.50
	2	75.00	-
	3	75.00	-
	5	75.00	-
	10	75.00	-
KOH	1	25.00	41.20
	2	25.00	70.33
	3	25.00	98.15
	5	25.00	156.95
	10	25.00	-
	1	50.00	82.25
	2	50.00	114.10
	3	50.00	157.80
	5	50.00	-
	10	50.00	-
	0.5	75.00	68.90
	1	75.00	121.50
	1.5	75.00	150.30
	2	75.00	193.30
	3	75.00	-
	5	75.00	-
	10	75.00	-
LiOH	1	25.00	47.20
	2	25.00	78.07
	3	25.00	108.60
	5	25.00	171.90
	10	25.00	-

Table B.5: Filtrate Physicochemical Properties Raw Data, Saturated Aqueous Solutions of $NaBO_2$ at 25°C ± 3°C.

Solution ID Code	pH	Density [kg/m³]	Conductivity [S/m]	$NaBO_2.2H_2O$ [wt %]	Viscosity [cP]
22				31.46	
24				32.40	
26				30.80	
53				28.54	
54				28.83	
55				30.14	
82				30.61	
83				30.84	
94	12.77			~~39.21~~	
95	12.61			30.31	
96	12.59		·	29.77	
97	12.55	1207.34		30.50	
98	12.53	1232.22		28.65	
119	12.77	1249.87		~~24.35~~	
144 A	13.13	1219.90	~~53.70~~		
144 B	13.11	1233.82	53.60		
188	12.95	1286.92	51.90		5.66
190	12.87	1299.00	52.50		4.97
viscometer test					~~6.84~~
# of Observations	10	7	3	8	2
Arithmetic Mean	12.79	1247.01	52.67	30.45	5.31
Standard Deviation	0.22	34.17	0.86	1.28	0.49
Standard Error	4.26	509.25	37.24	11.52	5.32

Table B.6: Filtrate Physicochemical Properties Raw Data, Saturated Aqueous Solutions of $NaBO_2$ stabilized with 7.5 wt% KOH at 25°C ± 3°C.

Solution ID Code	pH	Density [kg/m³]	Conductivity [S/m]	$NaBO_2.2H_2O$ [wt %]	Viscosity [cP]
268	~~14.49~~	1300.09	98.40	27.85	6.14
271	14.91	1359.02	96.90	28.20	6.52
274	~~14.35~~	1310.97	108.00	28.1271	~~6.1075~~
293	14.70	1382.09	92.30		6.38
294	14.51	1325.61	91.90	~~38.4335~~	6.31
295	14.50	1345.96	91.60		6.45
# of Observations	4	6	6	3	5
Arithmetic Mean	14.66	1337.29	96.52	28.06	6.36
Standard Deviation	0.19	30.88	6.31	0.19	0.14
Standard Error	8.46	598.19	43.24	19.84	3.18

Table B.7: Summary of Averages, Effect of Alkali Hydroxide Addition on the Physicochemical Properties of Saturated $NaBO_2$ Aqueous Solutions Filtrate at $25°C \pm 3°C$.

Solution Composition	Alkali [wt%]	pH	Density [kg/m³]	Conductivity [S/m]	Viscosity [cP]	Solubility [wt %]
Water	0	6.14	967.00	1.5 uS/m	0.86	-
No alkali	0	12.79	1247.01	52.67	5.31	30.45
NaOH	1	13.73	1261.54	60.85	3.93	30.52
NaOH	2	14.14	1267.94	75.93	4.23	29.50
NaOH	3	14.23	1279.05	92.00	5.08	28.60
NaOH	5	14.33	1281.11	99.77	5.99	29.83
NaOH	7.5	14.49	1292.09	142.97	6.11	18.38
NaOH	10	14.62	1293.57	198.27	6.37	18.09
KOH	1	13.79	1281.60	.52.30	5.58	31.67
KOH	2	14.07	1290.98	53.70	6.14	31.72
KOH	3	14.21	1298.71	62.85	6.30	32.11
KOH	5	14.34	1319.37	68.18	6.32	31.46
KOH	7.5	14.66	1337.29	96.52	6.36	28.06
KOH	10	14.87	1341.81	·167.05 ··	6.54	32.27
LiOH	1	13.28	1269.87	46.30	6.51	31.72
LiOH	2	13.68	1277.63	49.60	7.49	30.23
LiOH	3	13.76	1286.65	51.05	8.32	29.92
LiOH	5	13.85	1310.34	62.76	10.01	31.51
LiOH	7.5	13.97	1319.50	81.50	10.92	26.57
LiOH	10	14.10	1324.74	150.28	11.38	18.68

Table B.8: Summary of Averages, Effect of Temperature on the Physicochemical Properties of Saturated $NaBO_2$ Aqueous Alkaline Solutions Filtrate at 25, 50 and 75°C.

Solution Composition	Alkali [wt%]	T [°C]	pH	Density [kg/m³]	Conductivity [S/m]	Viscosity [cP]	Solubility [wt %]
No alkali	0	25	12.79	1247.01	52.67	5.31	30.45
No alkali	0	50	13.74	1554.50	60.74	23.88	92.22
No alkali	0	75	10.52	1583.00	86.89	2.51	113.56
NaOH	1	25	13.73	1261.54	60.85	3.93	30.52
NaOH	5	25	14.33	1285.99	99.77	5.99	31.09
NaOH	10	25	14.62	1293.57	198.27	6.37	18.09
NaOH	1	50	12.33	1623.50	56.51	30.46	89.24
NaOH	5	50	12.98	1479.20	83.61	11.84	80.09
NaOH	10	50	12.10	1514.59	-	-	62.01
NaOH	1	75	10.65	1568.86	-	2.17	100.32
NaOH	5	75	10.09	-	-	-	-
NaOH	10	75	-	-	-	-	-
KOH	1	25	13.79	1281.60	52.30	5.58	31.67
KOH	5	25	14.34	1319.37	68.18	6.32	38.96
KOH	10	25	14.87	1341.81	167.05	6.54	32.27
KOH	1	50	12.17	1577.29	44.20	28.89	85.76
KOH	5	50	13.57	1549.26	69.85	83.16	76.14
KOH	10	50	11.66	1532.97	131.43	8.70	62.05
KOH	1	75	10.63	1593.64	88.55	2.85	103.68
KOH	5	75	-	-	-	-	100.15
KOH	10	75	-	1380.25	-	-	77.51

Table B.9: Summary of Averages, Effect of Glycine on the Physicochemical Properties of Saturated $NaBO_2$ Aqueous Alkaline Solutions Filtrate at 25°C ± 3°C.

Solution Composition	Alkali [wt%]	Glycine [wt%]	pH	Density [kg/m³]	Conductivity [S/m]	Viscosity [cP]	$NaBO_2.2H_2O$ [wt %]
No additive	0	0	12.79	1247.01	52.67	5.31	30.45
Glycine	0	10	11.80	1266.48	48.75	2.18	0.68
NaOH	5	0	14.33	1281.11	99.77	31.90	29.83
Glycine and NaOH	5	10	11.86	1248.81	50.75	1.77	0.78
KOH	5	0	14.34	1319.37	68.18	34.53	31.46
Glycine and KOH	5	10	12.55	1286.48	56.55	1.97	1.06
LiOH	5	0	13.85	1310.34	62.76	39.40	31.51
Glycine and LiOH	5	10	12.03	1283.41	36.40	3.14	1.17

Appendix C: Precipitate XRD Data

Table C.1: Summary of Three Most Important XRD Peaks for Various Boron Compounds from Different Sources.

Chemical Formula	PDF Source	Reference ID Code	1st Max Peak 2-theta	1st Max Peak A%/Int	2nd Max Peak 2-theta	2nd Max Peak A%/Int	3rd Max Peak 2-theta	3rd Max Peak A%/Int
$NaBO_2.2H_2O$	JCPDS	06-0122	16.745	100	23.39	65	31.137	30
$NaBO_2.2H_2O$	Jade	081-1512	16.768	100	23.385	50.9	17.631	46.5
$NaBH_4.2H_2O$	JCPDS	26-1233	15.491	100	33.18	30	-	-
$NaBO_2(OH)_2$	JCPDS	27-1222	6.866	100	9.994	100	15.919	100
$Na_2B_2O_5.4H_2O$	JCPDS	24-1054	18.163	100	36.803	60	30.44	50
$NaBO_2$	JCPDS	32-1046	29.131	100	32.853	75	34.277	75
$NaBO_2$	JCPDS	37-0115	33.903	100	38.382	60	40.033	60
B_2O_3	JCPDS	44-1085	32.054	100	26.002	51	43.08	40
B_2O_3	JCPDS	24-0160	32.042	100	32.136	67	26.002	56
B_2O_3	JCPDS	13-0570	27.768	100	14.556	35	23.389	25
B_2O_3	JCPDS	06-0634	43.16	100	32.199	90	40.448	70
B_2O_3	JCPDS	06-0297	27.768	100	14.556	35	39.854	14
Na_2O	JCPDS	23-0528	46.133	100	32.172	41	27.769	33
Na_2O	JCPDS	03-1074	46.534	100	32.411	40	27.946	40
$Na_2B_2O_4.H_2O$	JCPDS	20-1078	18.641	100	24.87	95	31.274	80
$Na_2B_2O_4.H_2O$	JCPDS	16-0242	16.713	100	18.625	100	25.062	100
$Na_2B_2O_4.2H_2O$	JCPDS	14-0678	22.375	100	25.575	100	30.697	100
$Na_2B_2O_5.4H_2O$	Jade	076-0756	31.28	100	33.819	78.9	25.722	71.7
$Na_2B_2O_4.8H_2O$	JCPDS	14-0677	18.625	100	25.801	100	31.36	100
$Na_2B_2O_4.8H_2O$	JCPDS	09-0011	31.274	100	33.563	90	18.8	80
$LiBO_2$	JCPDS	18-0738	25.228	100	41.201	100	50.686	80
$LiBO_2$	JCPDS	20-0619	35.553	100	17.632	60	13.096	60
$LiOH.H_2O$	Jade	025-0486	33.73	100	30.064	66	36.962	45
$LiOH.H_2O$	Jade	076-1074	33.562	100	30.055	62.6	36.932	48.8
$LiOH.H_2O$	Jade	075-0883	33.79	100	30.116	62.6	37.075	48.4
KBO_2	JCPDS	19-0979	31.73	100	29.281	100	-	-
KBO_2	JCPDS	03-0729	14.443	100	13.393	83	17.969	33

Table C.2: Summary of Three Most Important XRD Peaks for the Precipitates of Saturates Alkaline Aqueous Solutions of $NaBO_2$ at 25°C ± 3°C.

Additive	Additive [wt %]	Max Peak 2-theta	A%	2nd Max Peak 2-theta	A%	3rd Max Peak 2-theta	A%	4th Max Peak 2-theta	A%	5th Max Peak 2-theta	A%	MDI Jade 7 Sample ID
None	-	41.444	100	30.698	70	26.922	63	20.403	62.2	16.734	61.4	unknown
None	-	16.762	100	17.633	18.1	30.952	12	23.188	10.1	30.49	9	$NaBO_2.2H_2O$
None	-	16.753	100	23.352	18.5	31.053	8.3	45.753	8.2	46.666	7.9	$NaBO_2.2H_2O$
None	-	16.809	100	31.169	6.5	34.003	5.9	45.295	2.5	-	-	unknown
NaOH	10.00	16.683	100	31.214	24.4	33.896	14.9	23.874	13.9	-	-	$NaBO_2.2H_2O$
NaOH	10.00	16.786	100	23.355	14.4	38.503	14.4	31.053	11.8	-	-	$NaBO_2.2H_2O$
NaOH	10.00	17.086	100	37.359	13.9	46.022	13.7	31.361	8.3	23.679	8.2	unknown
KOH	10.00	31.26	100	33.755	63.6	16.736	58.1	25.701	34.1	-	-	$NaBO_2.4H_2O$
KOH	10.00	17.128	100	18.944	14.3	32.56	11.1	31.337	10	41.511	8.5	$NaBO_2.2H_2O$
KOH	10.00	16.889	100	38.608	14.3	34.046	6	23.483	5.7	31.156	5.4	$NaBO_2.2H_2O$
KOH	10.00	16.952	100	31.228	9.9	23.502	4.3	34.048	3.1	-	-	$NaBO_2.2H_2O$
KOH	10.00	16.793	100	16.948	15.8	16.665	15	31.143	11.1	23.406	11	$NaBO_2.2H_2O$
KOH	10.00	54.97	100	23.424	77.6	31.255	68.1	16.511	56.2	54.935	50.1	unknown
LiOH	10.00	31.154	100	16.462	35.8	17.585	25.6	25.684	21.2	-	-	$NaBO_2.4H_2O$
LiOH	1.00	30.436	100	20.146	87	35.708	52.9	29.652	39	18.762	37.5	tincalconite
LiOH	10.00	33.654	100	33.654	78.7	29.957	54.8	39.75	44.4	18.462	43.8	unknown
LiOH	10.00	22.946	100	16.745	64	30.548	49.7	33.598	32.8	17.558	32.4	unknown

Appendix D: Precipitate SEM Pictures
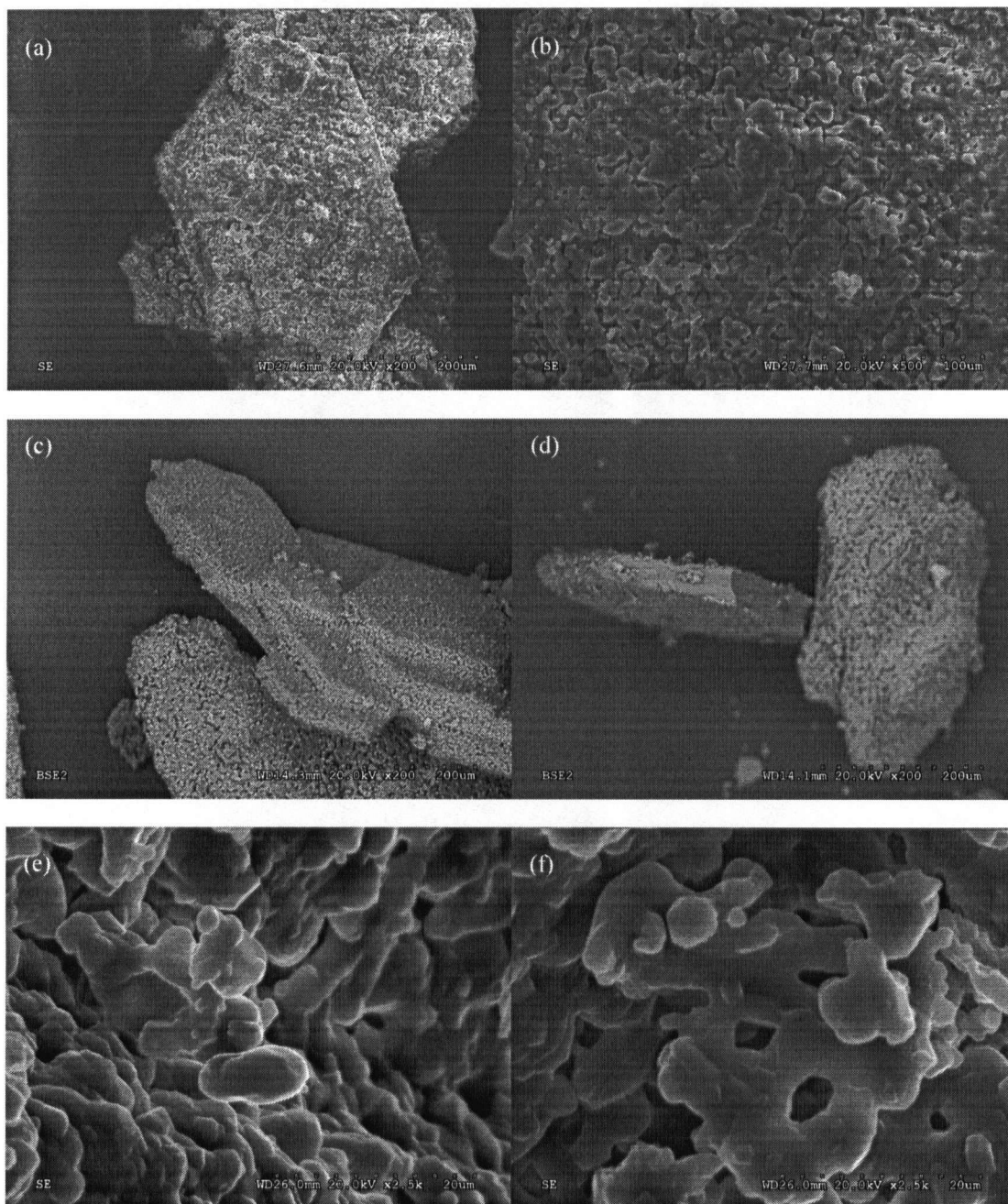

Fig. D.1: Scanning Electron Microscope Precipitate Crystal Images of Pure $NaBO_2 \cdot 2H_2O$ (a) SE, WD27.6mm, x200, 200um, (b) SE, WD25.5mm, x700, 50um, (c) BSE2, WD14.3mm, x200, 200um, (d) BSE2, WD14.1 mm, x200, 200um, (e) SE, WD26.0mm, x2.5k, 20um, (f) SE, WD26.0mm, x2.5k, 20um.
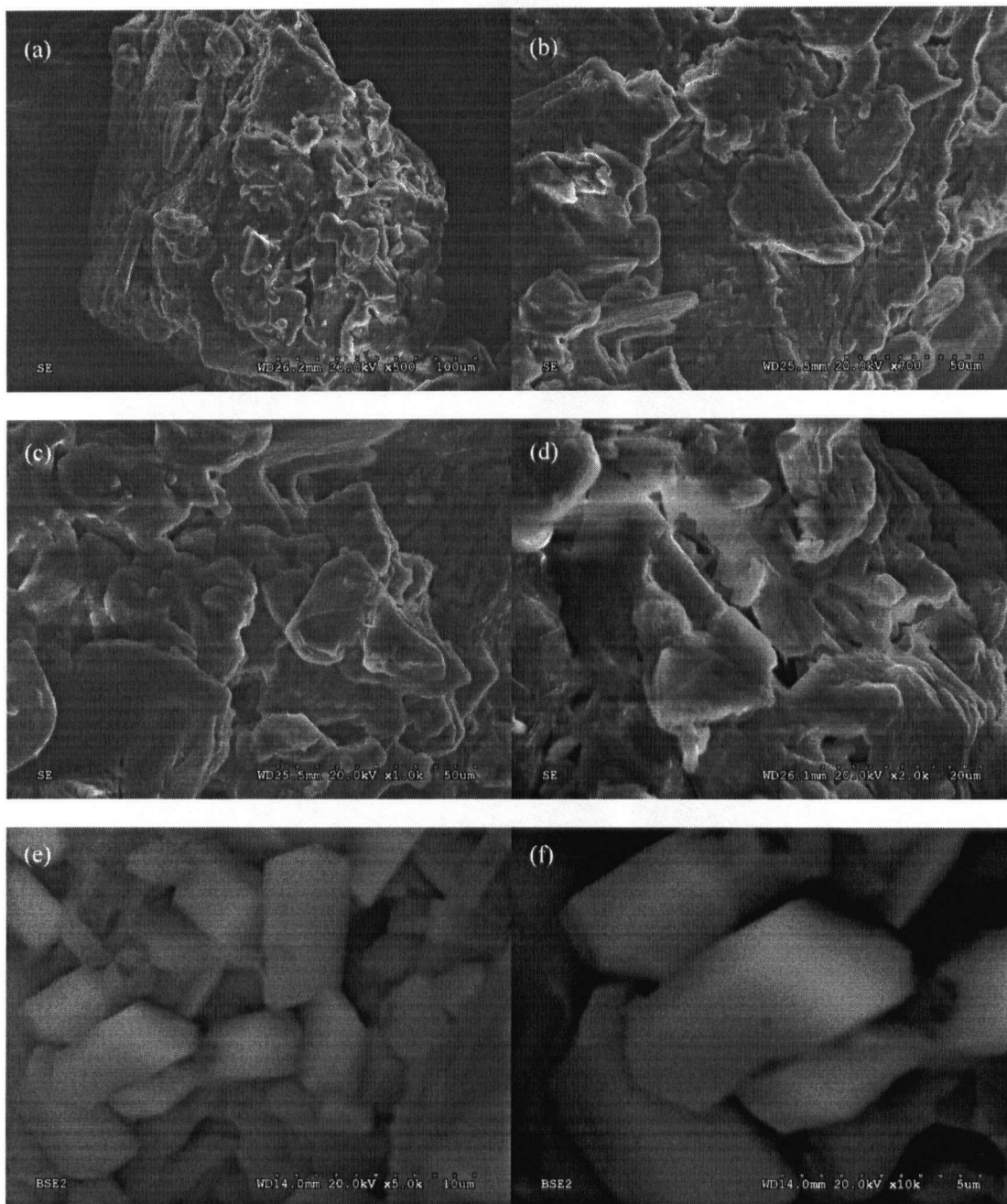
Fig. D.2: Scanning Electron Microscope Precipitate Crystal Images of Precipitates formed from Saturated Aqueous Solutions of NaBO$_2$ stabilized with 10 wt% NaOH (a) SE, WD26.2mm, x500, 100um, (b) SE, WD25.5mm, x700, 50um, (c) SE, WD25.5mm, x1.0k, 50um, (d) SE, WD26.1mm, x2.0k, 20um, (e) BSE2, WD14.0mm, x5.0k, 10um, (f) BSE2, WD14.0mm, x10k, 5um.
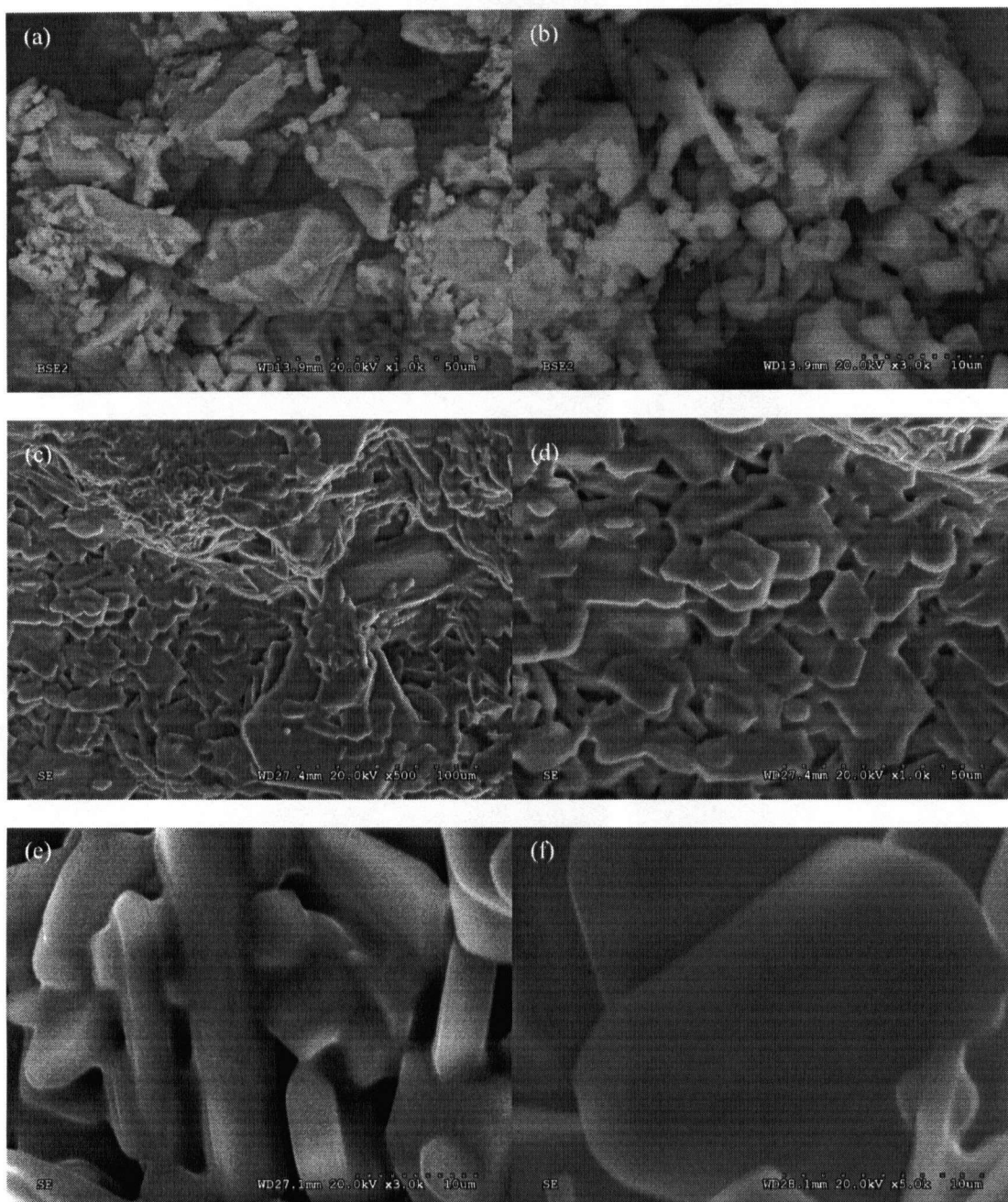
Fig. D.3: Scanning Electron Microscope Precipitate Crystal Images of Precipitates formed from Saturated Aqueous Solutions of NaBO$_2$ stabilized with 10 wt% KOH (a) BSE2, WD13.9mm, x1.0k, 50um, (b) BSE2, WD13.9mm, x3.0K, 10um, (c) SE, WD27.4mm, x500, 100um, (d) SE, WD27.4mm, x1.0k, 50um, (e) SE, WD27.1mm, x3.0k, 10um, (f) SE, WD28.1mm, x5.0k, 10um.
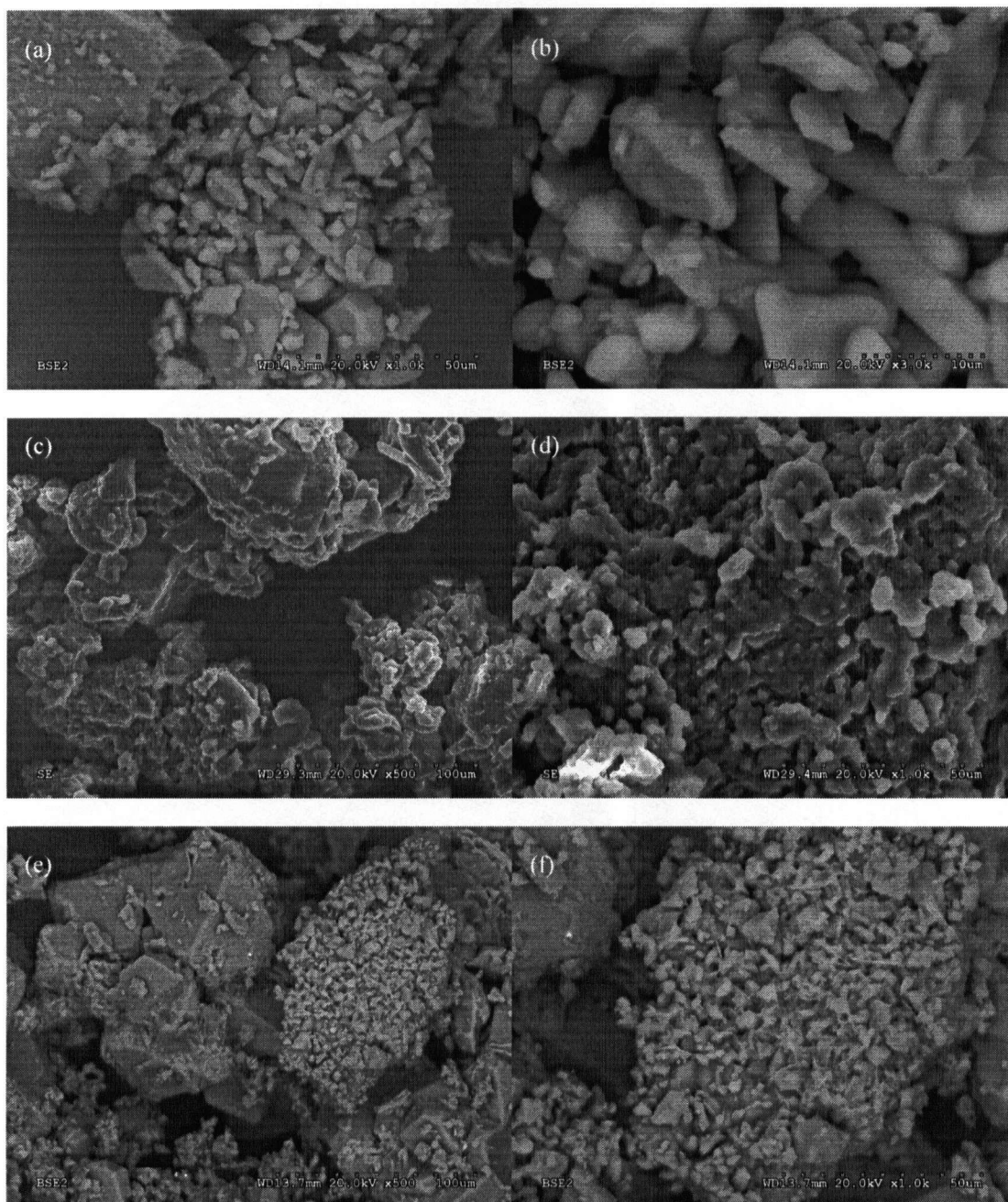
Fig. D.4: Scanning Electron Microscope Precipitate Crystal Images of Precipitates formed from Saturated Aqueous Solutions of NaBO$_2$ stabilized with 10 wt% LiOH (a) BSE2, WD14.1mm, x1.0K, 50um, (b) BSE2, WD14.1mm, x3.0k, 10um, (c) SE, WD29.3mm, x500, 100um, (d) SE, WD29.4mm, x1.0k, 50um, (e) BSE2, WD13.7mm, x500, 100um, (f) BSE2, WD13.7mm, x1.0k, 50um.
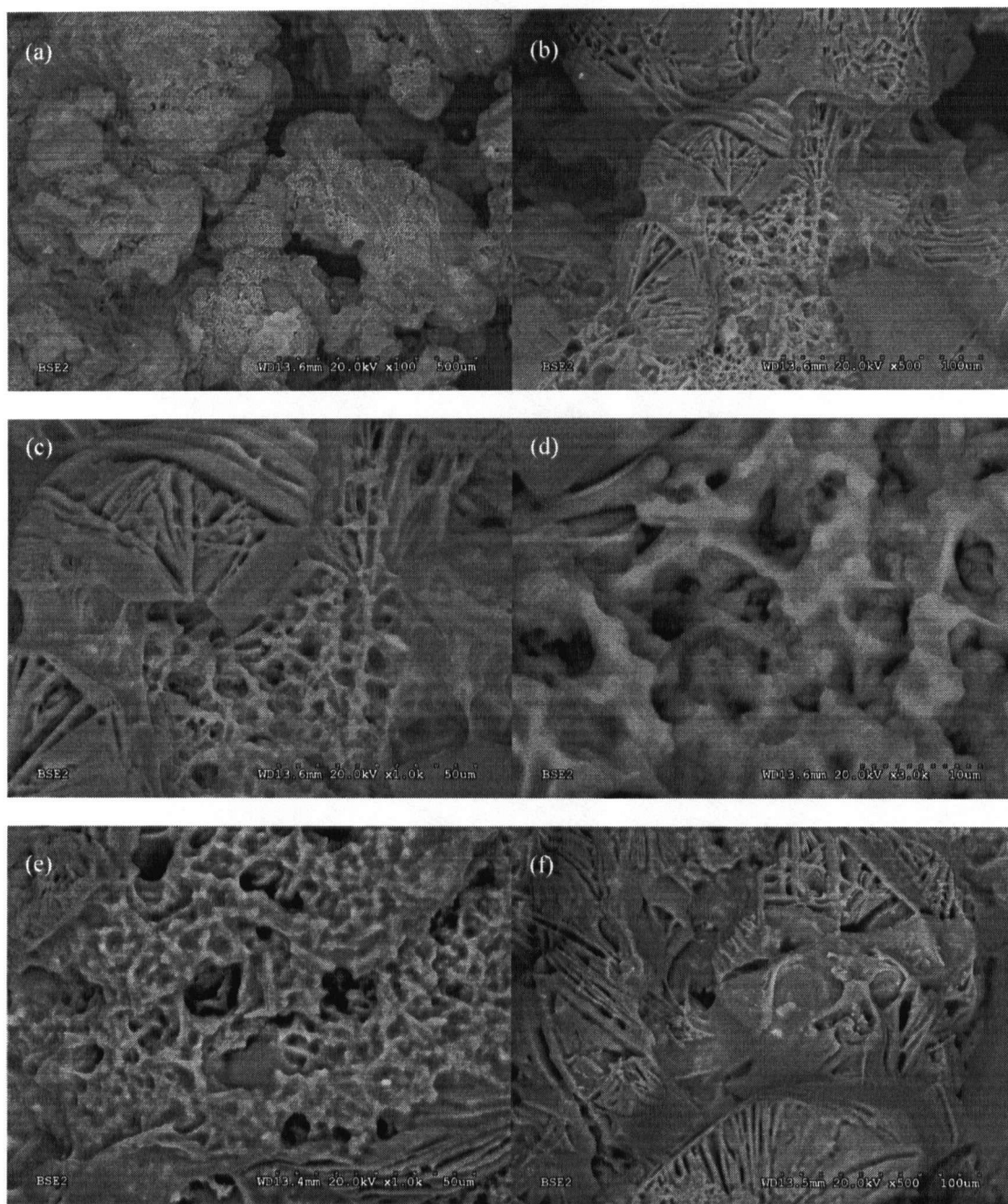
Fig. D.5: Scanning Electron Microscope Precipitate Crystal Images of Over dried Precipitates formed from Saturated Aqueous Solutions of $NaBO_2$ stabilized with 10 wt% LiOH (a) BSE2, WD13.6mm, x100, 500um, (b) BSE2, WD13.6mm, x500, 100um, (c) BSE2, WD13.6mm, x1.0k, 50um, (d) BSE2, WD13.6mm, x3.0k, 10um, (e) BSE2, WD13.4mm, x1.0k, 50um, (f) BSE2, WD13.5mm, x500, 100um.